Faculty of Engineering and Information Technology
University of Technology Sydney

Research into Target Recognition Techniques based on Device-Free Sensing Approach

A thesis submitted in partial fulfillment of
the requirements for the degree of
Doctor of Philosophy

by

Yi Zhong

March 2019

CERTIFICATE OF AUTHORSHIP/ORIGINALITY

I, Yi Zhong declares that this thesis, is submitted in fulfilment of the requirements for the award of Doctoral degree, in the School of Electrical and Data Engineering, Faculty of Engineering and Information Technology at the University of Technology Sydney.

This thesis is wholly my own work unless otherwise reference or acknowledged. In addition, I certify that all information sources and literature used are indicated in the thesis.

I certify that the work in this thesis has not previously been submitted for a degree nor has it been submitted as part of the requirements for a degree at any other academic institution except as fully acknowledged within the text. This thesis is the result of a Collaborative Doctoral Research Degree program with Beijing University of Posts and Telecommunications.

This research is supported by the Australian Government Research Training Program.

Signature of Candidate

Production Note:
Signature removed
prior to publication.

11/03/2019

Acknowledgments

Foremost, I would like to express my sincere gratitude to my supervisor Prof. Eryk Dutkiewicz for the continuous support of my Ph.D. study and research, for his patience, motivation, enthusiasm, and immense knowledge. His guidance helped me in all the time of research and writing of this thesis. I could not have imagined having a better advisor and mentor for my Ph.D. study.

I also would like to appreciate my co-supervisors Dr. Xi Zhu, Dr. Yang Yang, and Dr. Gengfa Fang for providing me with continuous support throughout my Ph.D. study and research. Without their professional guidance and persistent help, this thesis would not have been possible.

Furthermore, many thanks to the team members and other staff who have provided me with warm help and support. I would like to thank the University of Technology Sydney, Macquarie University and Beijing University of Posts and Telecommunications for offering me all the opportunities to explore the world and myself. I would like to thank all my friends for their company and support.

Last but not least, I would like to thank my parents, for their unconditional support, encouragement, and love throughout the whole Ph.D. studying.

Yi Zhong
November 2018 @ UTS

Contents

List of Figures

List of Tables

List of Publications

Papers Published

- Yan Huang, **Yi Zhong**, Qiang Wu and Eryk Dutkiewicz (2018), Cost-Effective Foliage Penetration Human Detection under Severe Weather Conditions based on Auto-Encoder/Decoder Neuron Network, IEEE Internet of Things Journal. (Early Access)

- **Yi Zhong**, Eryk Dutkiewicz, Yang Yang, Xi Zhu, Zheng Zhou and Ting Jiang (2018), Internet of Mission-Critical Things: Human and Animal Classification—A Device-Free Sensing Approach, IEEE Internet of Things Journal. (Early Access)

- **Yi Zhong**, Yang Yang, Xi Zhu, Eryk Dutkiewicz, Zheng Zhou and Ting Jiang (2018), Impact of Seasonal Variations on Foliage Penetration Experiment: A WSN-Based Device-Free Sensing Approach, IEEE Transactions on Geoscience and Remote Sensing, Volumn 56, Issue 9, pp.5035 - 5045.

- **Yi Zhong**, Yang Yang, Xi Zhu, Eryk Dutkiewicz, Zheng Zhou and Ting Jiang (2017), Device-Free Sensing for Personnel Detection in a Foliage Environment, IEEE Geoscience and Remote Sensing Letters, Volumn 14, Issue 6, pp.921 - 925.

- Xunqian Tong, Yanju Ji, Jun Lin, Jinbao Zhu, Feng Sun, **Yi Zhong**, Yang Yang, and Xi Zhu (2017), Cooperative spectrum sensing based

on a modified shuffled frog leaping algorithm in 5G network, Physical Communication, Volumn 23, Issue 2, pp.438-444.

- **Yi Zhong**, Jinbao Zhu, Eryk Dutkiewicz, Zheng Zhou and Ting Jiang (2017), Device-free sensing for classification of human activities using high-order cumulant algorithm, in 17th International Symposium on Communications and Information Technologies (ISCIT).

- **Yi Zhong**, Zheng Zhou, Ting Jiang, Michael Heimlich, Eryk Dutkiewicz, and Gengfa Fang (2016), Classification of animals and people based on radio-sensor network, in 16th International Symposium on Communications and Information Technologies (ISCIT).

Abstract

Using wireless communication signals, also known as radio-frequency (RF) signals, for not only data communication but also target detection and classification, is an emerging device-free sensing (DFS) technology that has a great potential in our daily life. In particular, this technology can be used for target detection in foliage environments. In this thesis, the target recognition techniques based on RF signals have been extensively investigated. The following outcomes have been achieved.

In order to tackle the issues related to target detection in foliage environments, a novel detection method based on DFS is proposed. Firstly, compared with several different types of RF signals, it has been found that the ultra-wideband (UWB) signal is the most appropriate one. Secondly, the statistical properties of UWB signal are selected as the extracted features. Finally, based on the collected data, the performance of the proposed methods has been extensively verified with different classification algorithms. To minimize the impact on detection accuracy due to unwanted clutters, a high-order cumulants (HOC) algorithm is proposed for feature extraction, which has a good immunity against background noise. First of all, 1-D diagonal slices of fourth-order cumulants are used to extract useful information from the received UWB signals. Then, different classification algorithms are used to demonstrate superior performance of this approach.

Another critical issue related to the proposed method is the potential impact on detection accuracy due to weather variations. Thus, a novel method for recognition based on a hybrid differential evolution and flower pollina-

tion algorithm (DEFPA) is proposed. Using the collected data that has been gained from different weather conditions, the proposed DEFPA approach has not only improved the efficiency of the support vector machine (SVM) classifier, but also classification accuracy as multi-weather conditions are considered.

Although the feasibility of using this technology in different weather conditions has been explored to some extent, we observe that it still cannot perform promisingly under severe weather conditions such as rain, fog, and snow. To address this problem, an Auto-Encoder/Decoder (Auto-ED) deep neural network is proposed. Experimental results demonstrate that the proposed approach can best tackle the challenge of target detection under severe weather condition in the foliage environment.

At the end of this thesis, the summary of the overall work is presented and some possible future work is given.

Chapter 1

Introduction

This chapter provides an overview of this thesis. Section 1.1 states the background of the thesis. Section 1.2 presents the motivation behind the thesis work. Section 1.3 describes the key contributions of the thesis. Section 1.4 introduces the organization of the thesis.

1.1 Background

Internet of Things (IoT) represents the most exciting technological revolution since the last century which has the greatest potential to improve quality of life in several meaningful ways, ranging from smart buildings to smart cities (Kortuem, Kawsar, Sundramoorthy & Fitton 2010) (Fan, Yin, Da Xu, Zeng & Wu 2014) (Zanella, Bui, Castellani, Vangelista & Zorzi 2014) (Lin, Chen, Deng, Hassan & Fortino 2016) (Centenaro, Vangelista, Zanella & Zorzi 2016). Recently, IoT is being considered for critical missions, known as the Internet of Mission-Critical Things (IoMCT), such as surveillance, search & rescue and border patrol (Sun, Wang, Vuran, Al-Rodhaan, Al-Dhelaan & Akyildiz 2011) (Domingo 2012) (Minaeian, Liu & Son 2016). For all of these applications, the detection of human targets in an outdoor environment is essentially required. Currently, human targets, at best, are monitored at just a few locations, with expensive equipment. A low-cost monitoring

system with high reliability is urgently required. The availability of this kind of system will open up a huge potential for not only increasing situational awareness and strategic effectiveness in military and surveillance events but also reducing potential casualties during search-and-rescue operations.

As far as target detection in an outdoor environment is concerned, three approaches have been widely used in the literature. Perhaps the most well-known approaches are the image- (Sakaino 2013) (Liu, Liu, Blasch, Shen, Wang, Ling & Chen 2015) (Chen, Zhao, Sun & Tan 2017) and synthetic-aperture radar (SAR)-based systems (Howard, Roberts & Brankin 1999) (Dias & Marques 2003) (Yu, Wang, Liu & He 2016). However, the cost of using either system is relatively high which completely disables the possibility of deploying them for low-cost sensing. The final approach is to use hybrid sensors such as acoustic, seismic, passive infrared, magnetic and electrostatic sensors for target classification which leads to a dramatically reduced cost compared to the other two approaches. However, the classification accuracy of this approach needs to be further improved.

Wireless technology has advanced by leaps and bounds over the last half-century. Although this technology was originally invented for military and defense, it was actually well known due to the revolution of data communication. As predicted, by 2020, there will be more than 50-billion devices connected through wireless links to enable the IoT. As each of them must have a capability to transmit and receive radio-frequency (RF) signals, it would be a natural choice to fully utilize these signals for not only data communication but also sensing, such as target detection and classification. Consequently, other than an RF transceiver, it requires no additional hardware for sensing. This idea is known as IoT-inspired device-free sensing (DFS) and is getting more and more popular in recent years.

Among different sensing technologies, this approach is perhaps the most promising one that has the potential to dramatically reduce the overall system cost. However, until a few years ago, there were few attempts to use this approach for target detection and classification, although this technology has

been proposed since World War II. The idea was picked up for radar-based applications, but never saw much acceptance beyond that. It would be obvious to ask why, if this technology was developed in the 1930s, it never caught on. One might even suspect that some flaw might have been uncovered that kept such approach out of the mainstream. Although there is no fatal flaw, the transition from radar to IoT-inspired sensing still faces many challenges.

1.2 Motivation

In the thesis, we focus on the research of detection and classification of targets that are obscured in a foliage environment. Currently, it is still a challenging issue due to the low detection and high false alarm rate. This is mainly due to the following facts:

1. Given multipath propagation effects of rough surfaces, scattering from vegetations and ground tend to overwhelm the weak backscattering of targets.

2. When humans and animals appear to have a similar size, it is hard to make a clear distinction between them.

3. Due to the changes in atmosphere and ground conditions, foliage is more likely to be a time variant channel environment, for example, wind results in moving branches and leaves; therefore the foliage clutter is quite impulsive in nature.

Motivated by the recently proposed DFS technologies, we would like to present an effective and robust solution to tackle this issue in a cost-effective way. In this thesis, we aim to investigate and tackle the following four challenges to obtain good performance for target detection and classification in foliage environment.

1.2.1 Humans and Animals Classification in Outdoor Cluttered Environments

As far as cost reduction is concerned, it would be a natural choice to utilize DFS for target detection and classification since it only uses RF signals as a sensing medium without the need for additional equipment. Unfortunately, the performance of DFS-based approaches has mostly been verified only in indoor environments. However, the case of the real world often refers to environmental variations, which is much more complicated than the indoor one. In an outdoor environment, since the time-varying clutters could significantly affect the prorogation of an RF signal in a non-predictable way, the selection of the most appropriate RF signals plays a critical role. In addition, animals may have similar dielectric properties as human beings that could also adversely affect the detection accuracy. To reduce the number of false alarms, it is important to select the distinct features of similar targets. Until now, very few articles discuss this issue in the literature. It is still unknown how to effectively distinguish humans and animals in an outdoor cluttered environment.

1.2.2 Target Recognition in High-clutter Environment

For the case study in the real world, it is much important to deploy DFS technology for target detection and classification in high-clutter environments, such as a foliage environment. In theory, since each target would result in signals to have different patterns, it is possible to detect and classify the types of targets by identifying and interpreting these patterns. However, it would be quite difficult to ensure good detection accuracy in high-clutter scenarios. For example, in a foliage environment, not only the strength of the RF signal tends to be rapidly attenuated due to the severe multipath effects, but also the strong clutters can generate additional noise that would adversely affect the RF signal. In order to correctly classify different targets, the key features of the targets must be extensively analyzed. Previous DFS-based

systems mostly use received signal strength (RSS)-based features for target detection and classification. However, these features may be very similar and can be adversely affected by time-varying noise and clutters. Therefore, a more sophisticated feature extraction method needs to be adopted in a high-clutter foliage environment.

1.2.3 Target Recognition with Seasonal Variations

As far as foliage penetration is concerned, how to ensure the feasibility of using DFS-based approaches with seasonal variations is becoming a critical mission. Since seasonal variations will result in different weather conditions and foliage density, if we only use the datasets obtained in a specific situation to train the classifier, the detection accuracy will be severely affected. To overcome this issue, it is desirable to collect more and more datasets under all seasons. The classical support vector machine (SVM) classifier has been successfully applied to target classification. However, its performance highly relies on the selection of SVM parameters. Although it is possible to obtain the best-optimized parameters for SVM by using an enormous amount of training datasets, the computational cost has significantly risen. Thus, how to determine the optimal parameters for a classifier in a simple but effective way also needs to be investigated in detail.

1.2.4 Target Recognition under Severe Weather Conditions

Weather conditions play a significant role in the fading phenomena in wireless communications. Many studies have intensively investigated weather-induced effects on radio-wave propagation in foliage environments (Lee & Meng 2007). These weather effects will naturally change the property of the propagation channel such as the foliage channel. For example, after heavy rainfall, the tree trunks are often wet and more conductive, which might result in a variation in path attenuation of radio propagation. Since the

changes in temperature, humidity and winds may have significant effects on the radio propagation, the strength of RF signals may reduce in such adverse weather conditions as rain, snow, or fog. Consequently, the classification accuracy can be dramatically degraded. While severe weather conditions are inevitable, it is much important to make the DFS-based approaches appropriately used for target detection and classification in the real world scenarios of foliage environments.

1.3 Contributions

The objectives of this thesis are to tackle the challenges stated in Section 1.2. The contributions of this thesis are stated as follows.

1.3.1 DFS-based Approach for Human and Animal Classification

To distinguish between human and animal targets in a cost-effective way, we utilize a combination of DFS and machine learning technologies to tackle this issue. We collect the datasets of three types of samples, including no target, human target and animal target in a cornfield using impulse-radio ultra-wideband (IR-UWB) transceivers. Here, we select IR-UWB signals because the impulse-shaped signal is relatively immune from multi-path effects or fading problems. Then, we use the statistical properties of the RF signals to describe target features and apply the probability density function (PDF) to select distinct features. The performance of the selected features for target classification is verified by different classical classifiers. The experimental results indicate that the proposed method can provide good access to achieve the aim of low-cost but robust classification of human and animal in a cluttered outdoor environment.

1.3.2 HOC-based Feature Extraction in High Clutter Environment

To improve the detection accuracy of DFS-based approach in a high-clutter environment, we propose a higher-order cumulants (HOC)-based feature extraction algorithm for target recognition. We utilize IR-UWB transceivers to collect the datasets of three types of samples, including no target, human target and animal target in a medium-sized forest, which is dominated by a mixture of small- and medium-sized trees with varying amounts of brush and shrubs. Furthermore, we apply HOC to analyze the received target signals because it can provide high noise immunity and contain both amplitude and phase information of a signal. Finally, we use 1-D slices of fourth-order cumulants to extract useful information. The performance of the HOC-based features for target classification is verified by different classical classifiers. The experimental results show that the performance has been improved of using the HOC-based algorithm over the conventional RSS-based one.

1.3.3 Target Detection with Seasonal Variations based on DEFPA-SVM

To ensure reasonable detection accuracy with seasonal variations, we propose a new recognition method using an optimization-based support vector machine (SVM) to recognize targets obscured by foliage in different seasons. In a medium-sized forest, we use IR-UWB transceivers to collect the datasets of four types of samples under four weather conditions in different seasons. From these real received RF signals, we apply the HOC-based algorithm to extract the target features. Then, we propose a new hybrid differential evolution and flower pollination optimization algorithm (DEFPA) to optimize the SVM parameters accommodated to datasets of all seasons. Finally, the extracted features are input into the proposed DEFPA-SVM to automatically classify the types of targets. Experimental results demonstrate the effectiveness and robustness of the proposed method for target recognition

with seasonal variations in foliage environments.

1.3.4 Target Detection under Severe Weather Conditions based on Auto-ED Deep Neural Network

To improve the performance under adverse weather conditions such as rain, fog, and snow, we present an Auto-Encoder/Decoder (Auto-ED) deep neural network for target recognition in foliage environment. In the encoder process, we utilize fractionally-strided convolution operation to encode signal-based inputs into higher dimensional tensors. Here, We use the HOC as the input vector to the encoder in our proposed Auto-ED neural network. In the decoder process, we apply convolution operations to extract deep representations and learn the classifier simultaneously. The effectiveness of the proposed approach is verified by datasets introduced in Section 1.3.3. The experimental results indicate that the proposed method can best tackle the challenge of target detection under severe weather conditions in foliage environments,

1.4 Organization of the Thesis

The thesis is structured as follow:

Chapter 1 is the introduction of the thesis. Section 1.2 states the motivation of this thesis, i.e., the main challenges we aim to tackle. Section 1.3 describes the main contributions of this thesis. Section 1.4 introduces the organization of this thesis.

Chapter 2 comprehensively reviews the different research fields that are related to this thesis. We first present the current studies of target detection and classification in foliage environments. i.e., WSN-based approach and Radar-based approach in Section 2.1. Then, in Section 2.2, we introduce the existing DFS-based approaches for device-free localization, device-free intrusion detection and device-free activity recognition.

Chapter 3 presents a DFS-based approach for human and animal clas-

sification in a cluttered outdoor environment. We point out the challenges in Section 3.1 and then introduce the data measurement and collection in Section 3.2. In Section 3.3, we describe the details of our proposed feature extraction and selection method. Section 3.4 provides the experimental results and analysis. Finally, We summarize this chapter in Section 3.5.

Chapter 4 extends the work in Chapter 3, which focuses on the target detection and classification in a high-clutter environment. Section 4.1 first introduces the problems and then Section 4.2 provides the data measurement and collection taken in a foliage environment. In Section 4.3, we propose the HOC-based feature extraction method. Simulation results are analyzed in Section 4.4 and this chapter is summarized in Section 4.5.

Chapter 5 further investigates the impact of seasonal variations on detection accuracy in foliage environment. Section 5.2 presents the data measurement and collection taken in a foliage environment under four different weather conditions. In Section 5.3, we briefly introduce the basic idea of SVM. Then in Section 5.4, we propose a new DEFPA algorithm to determine the optimal parameters for SVM. The experimental results are given in Section 5.5. Finally, the summary is shown in Section 5.6.

Chapter 6 extends the work in Chapter 5, which centers on addressing performance under severe weather conditions. We first review related works in Section 6.2 and then propose Auto-ED neural network approach in Section 6.3. Section 6.4 provides the experimental dataset and simulation results. We summarize this chapter in Section 6.5.

Finally, Chapter 7 concludes the work in this thesis and gives the outlook for future work.

Chapter 2

Literature Review

This chapter reviews the related work, in regarding with all the important fields related to this thesis. The studies of target detection and classification in foliage environments are introduced in Section 2.1. The literature related to DFS technology and its applications is listed in Section 2.2.

2.1 Target Detection and Classification in Foliage Environments

Detection and classification of targets that are embedded in foliage environments is of interest to both military and civilian research. The accurate and effective detection can provide a broad range of applications, such as detecting weapon caches during military operations and detecting intrusion for security systems. However, detecting and classifying targets, such as human, vehicles, and weapons that are hidden in foliage is still a challenging issue. The conventional manual monitoring for target detection in foliage environments suffers from intensive human involvement. Due to the harsh and complex conditions of the extreme environment, huge amounts of manpower, material and financial resources are required. In addition, this manual-based approach can neither allow real-time monitoring nor ensure a good detection accuracy. In order to dramatically reduce the implementation cost and

improve the performance, a cost-effective monitoring system with a high reliability is urgently required for target detection in foliage environments. In the literature, there have been two classical methods, one is the wireless sensor network (WSN) -based approach, and the other is the radar-based approach.

2.1.1 WSN-based Target Detection Approach

The WSN-based target detection approach utilizes a large number of sensors spatially deployed over a wide area for detecting and classifying the presence of the targets. Target detection can be accomplished by making use of multiple sensing modalities, such as acoustic, seismic, ultrasonic, passive infrared (PIR), magnetic, electrostatic and video. The description of these sensors is given below (Damarla & Ufford 2007):

- **Acoustic** sensors use piezoelectric materials to detect acoustic waves, such as hoof sounds of animals and human footstep sounds.
- **Seismic** sensors capture the vibrations in the ground caused by the motion of the targets or ground coupling of acoustic waves.
- **Ultrasonic** sensors also known as acoustic Doppler sensors, emit acoustic waves toward objects and receive reflected responses from objects.
- **Passive infrared** devices are very inexpensive sensors, which can be used to detect the nearby presence of a warm body within a cone-shaped field of view.
- **Magnetic** sensors can be used to detect ferromagnetic materials carried by people, such as keys, firearms, and knives.
- **Electrostatic** sensors can be used to detect the built-up electric charge on personnel.
- **Video** sensors can capture color or grayscale video for human gait detection and object recognition

Target detection in foliage environments, particularly in terms of human and animal classification is a challenging problem. For example, acoustic sensors may analyze sounds and determine if there is any target present. However, in an outdoor scene, the signals are contaminated by wind sounds, human voices, or unexpected airplane engine sounds. Although computer vision is the most widely used technique for detecting humans, video sensors are not preferred in long-lasting missions because they consume high amounts of power and require a large memory size. Moreover, the imaging sensors usually suffer from the problem of line-of-sight (LOS) constraints, e.g., branches and leaves of trees in foliage environment. Therefore, it is preferable to use non-imaging sensors, since they tend to be low power and long-lasting. However, non-imaging sensors are adversely affected by the ambiguity among the footsteps of animals alone, humans alone, and of animals traveling together with humans (Huang, Damarla & Hasegawa-Johnson 2011). In addition, discriminating footstep signals from noise sources is also a challenging task, because the signal-to-noise ratio (SNR) of footsteps decreases rapidly with the distance between the sensor and the targets. Furthermore, the footstep signals may vary significantly due to the environmental variations (Jin, Sarkar, Ray, Gupta & Damarla 2012).

Traditionally, seismic sensors are widely used for target detection. Previous research has focused on footstep detection by means of estimating gait frequency (Sabatier & Ekimov 2008) (Houston & McGaffigan 2003). (Park, Dibazar & Berger 2009) proposed an algorithm that extracts temporal gait patterns to provide information on the temporal distribution of gait beats. In general, a person walks with a rhythm and has a gait frequency of approximately 1.5 Hz. However, if multiple people are walking out of sync, it is difficult to estimate the cadence of an individual person. Moreover, if there are animals, people walking can be mistaken for their seismic signatures. In order to reduce false alarm triggering, high-fidelity sensors that capture the phenomenology associated with people and animals walking are urgently required. Ultrasonic methods were proposed for the detection of moving

targets by means of micro-Doppler gait signatures. In (Zhang, Pouliquen, Waxman & Andreou 2007), Gaussian mixture models (GMM) are used to classify human and four-legged animals. In (Kalgaonkar & Raj 2007), the cepstral coefficients are used as features to identify human walking.

As shown in the above literature review, no single sensor can discriminate between human and four-legged animals in different situations and circumstances. Therefore, some researchers proposed to use hybrid sensors to identify targets. (Damarla, Mehmood & Sabatier 2011) and (Damarla & Ufford 2007) used multi-modal sensors, namely, acoustic, seismic, PIR, magnetic and electrostatic to detect people. (Iyengar, Varshney & Damarla 2007), (Iyengar, Varshney & Damarla 2011) and (Sundaresan, Subramanian, Varshney & Damarla 2010) utilized both the acoustic and seismic sensors and developed joint probability distributions based on Copula-based framework for detection of people. (Jin, Gupta, Ray & Damarla 2011) and (Jin et al. 2012) presented a feature-level fusion method based on a hidden Markov model (HMM) for personnel detection by using the seismic and PIR sensors. (Huang et al. 2011) developed a feature fusion system based on GMM by using the acoustic, seismic and ultrasound sensors to discriminate between humans and four-legged animals. Although these approaches can reduce the false alarms to some extent, the computation cost also rapidly increases. In addition, the sensitivity of these sensors is severely affected by environmental factors, such as temperature change, extreme air turbulence and adverse weather conditions.

In summary, the classification accuracy of the WSN-based target detection approach needs to be further improved. On the one hand, complicated environments with the presence of animals can cause false alarms to discriminate different types of targets. On the other hand, adverse environmental conditions may have significant effects on the sensitivity of the sensors. Although it is possible to improve the detection rate by deploying hybrid sensors within the scope of monitoring, existing research indicates that the performance is still modest. In addition, the classification algorithm for data fusion

will intensively increase the computational complexity and energy consumption, which makes them unfeasible for large-scale deployment in practice.

2.1.2 Radar-based Target Detection Approach

Radar is an object-detection system that uses electromagnetic waves to determine the range, angle or velocity of objects by calculating various parameters of the attenuation and scattering in the radar echo signal. Radar cross section (RCS) is one of the key parameters in the detection of targets which contains recognizable target characteristic such as size, shape, structure as well as the state of motion. RCS is a fictitious area that reflects the intensity of the wave back to the radar. It can be defined as follows (Balanis 1989),

$$\sigma = \lim_{R \to \infty} 4\pi R^2 \frac{|E_s|^2}{|E_t|^2} \tag{2.1}$$

where R represents the distance between the radar and the target, E_s is the scatter field intensity and E_t is the incident field intensity. Here, we assume that the target is in the condition of far-field covered by the radar. According to the above equation, RCS highly depends on several parameters, such as aspect angle, frequency, polarization and dimensions of the target. Therefore, a traditional radar system usually uses RCS to detect airborne targets such as aircraft and missiles when the environment is not so complicated (Foster 1995). However, the channel path in a foliage environment is non-line-of-sight (NLOS) and obscured by leaves and trunks. For this reason, the propagation attenuation and the multi-path effects become severe which makes some RCS statistical parameters unfeasible for target detection in a foliage environment.

To overcome this issue, there have been many efforts undertaken to investigate radar detection in foliage environments. One direction is to pursue the foliage clutter modeling and analysis in order to gain a better understanding of the clutter and improve the detection performance (Liang & Liang 2010*b*). (Sheen, Malinas, Kletzli, Lewis & Roman 1994) measured and analyzed one-way transmission properties of foliage using a bistatic and co-

herent wide-band system over the band from 300 to 1300 MHz. (Fleischman, Ayasli, Adams & Gosselin 1996) measured two-way foliage attenuation by a synthetic aperture radar (SAR) and discussed probability dependency for frequency, polarization, and depression angle. Other than SAR, in (Nashashibi, Sarabandi, Oveisgharan, Dobson, Walker & Burke 2004) and (Nashashibi & Ulaby 2005), the authors applied Millimeter-Wave (MMW) radars in measurements of foliage attenuation and ground reflectivity. These studies have shown that the foliage channel contains much spiky clutter; thus, it would be quite difficult to ensure a good accuracy for target detection in foliage environments. Although the K-distribution has been widely used for radar clutter modeling in the previous studies (Watts 1987) (Nohara & Haykin 1991), it is still inaccurate to describe the strong spatial and angular fluctuations of foliage. Based on an ultra-wideband (UWB) radar, (Kapoor, Tsihrintzis & Nandhakumar 1996) proposed an alpha-stable model and (Liang, Liang & Samn 2008) presented a log-logistic model for foliage clutter. However, the detection performance has not been further verified in these studies.

Another direction centers on the development of radar technology. Recently, advancements in foliage penetrating (FOPEN) SAR have opened new insights into the problem of detecting targets in foliage environments. FOPEN SAR operates mainly in the VHF and UHF bands to enable detection and imaging of targets concealed in foliage. Many practical FOPEN measurements have been conducted by a number of researchers in recent years. The research groups from USAFRL (Davis, Tomlinson & Maloney 1999), MIT (Fleischman et al. 1996) (Bessette, Crooks & Ayasli 1999) (Toups, Ayasli & Fleischman 1996) (Binder, Toups, Ayasli & Adams 1995), and JPL (Durden, Klein & Zebker 1991) (Durden, Klein & Zebker 1993) have reported the results of several foliage penetration experiments, using the VHF, UHF, L and S bands fully polarimetric SAR imaging over forested areas. These results have demonstrated that these lower bands have very good ability to penetrate foliage. Some advanced signal processing approaches have also been published to support better performance for target detec-

tion. (Halversen, Nanis, Owirka & Novak 1994) developed a two-pass change detection algorithm for forming several aspect-angle-diverse SAR images to enhance the target detectability. (Rau & McClellan 1998) also utilized reconstructing directional filter-banks to enhance targets. Based on the application of a set of filters, some alternative approaches have been proposed to improve the detection performance. (Allen 1996) reported a matching filtering method and (Runkle, Nguyen, McClellan & Carin 2001) employed a sequence of directional filters combined with a hidden Markov model (HMM). In addition, different pattern recognition approaches have been introduced to these studies such as Bayesian Neural Network (BNN) (MacDonald, Isenman & Roman 1997), Support Vector Machine (SVM) (Zhao & Principe 2001), Extreme learning machine (ELM) (Guo & Zhou 2018) and so on.

As shown in the above literature review, there are still practical difficulties inherent in detecting targets by utilizing radar systems. On the one hand, the fluctuations of the foliage clutter may have significant effects on the performance of identifying targets obscured in foliage. On the other hand, although FOPEN SAR provides the potential for target detection in foliage environments, most studies focus on the detection of vehicle-sized targets in the forest such as trucks and tanks; thus, a few attempts have been made to use this technology for small-sized targets detection such as humans and animals. In addition, these radar systems are not suitable for the covert operations due to the large size of the antennas. Compared to the WSN-based approach with inexpensive sensors, the radar-based one requires high power and high cost.

Although significant progress has been made for target detection in foliage environments by utilizing the WSN-based and Radar-based approaches, there are still some fundamental issues to be tackled such as installation and maintenance costs of systems, adverse effects of the environmental conditions and false alarms caused by the presence of animals. In order to solve this problem, in this thesis, we present a cost-effective monitoring approach based on DFS technology for target detection in foliage environment. The research

of DFS technology and its applications will be introduced in the next section.

2.2 Device-Free Sensing

With the rapid advancements in the Internet of Things (IoT) and the widespread use of wireless networks, virtually all entities in our environment will be enhanced by sensing. It is possible to capture the environmental changes as long as wireless networks have been deployed over a large area with guaranteed coverage. Since each transceiver within a wireless network must have a capability to generate and transmit RF signals, it would be a natural choice to fully utilize this capability for not only data communication but also for sensing. DFS is an emerging class of sensing technology which has been proposed as a way of detecting and tracking targets which only uses RF signals, such as Bluetooth, UWB, ZigBee and Wi-Fi, without the need to equip any devices or extra hardware support. In the past several years, there have been many efforts undertaken to investigate DFS technology. They can be categorized into three groups: device-free localization, device-free intrusion detection and device-free activity recognition.

2.2.1 Device-free localization

Device-free localization is a passive localization technique relying on the sensing capability of the RF signals. Since the tracked entity is neither required to carry devices nor participate actively in the localization process, device-free localization has attracted increased attention from scholars and practitioners. In order to perform localization, there are several approaches that have been proposed in the literature which can be broadly categorized into two groups: (1) location-based approach and (2) link-based approach.

- **Location-based approach**

The location-based approach is also known as fingerprinting which formulates the device-free localization as a fingerprint-matching problem. The idea of the approach was first proposed in (Youssef, Mah & Agrawala 2007) in the context of passive localization. With the object placed at various predetermined locations in the deployment area, the authors built an offline radio map by collecting all the corresponding wireless link measurements. The objects location was estimated by mapping the test location to one of these trained locations based on the trained offline radio map. This work was extended to a much larger deployment in *Nuzzer*, which is a large-scale localization system for real environments with rich multipath (Seifeldin, Saeed, Kosba, El-Keyi & Youssef 2013). The results of this study have shown that *Nuzzer* gives location estimates with less than 2-meters median distance error. In order to further mitigate the error caused by the multi-path effect in cluttered indoor environments, the probabilistic techniques have been adopted to improve the localization accuracy. The idea of this method is to formulate this localization problem into a probabilistic classification problem. It estimates received signal strength (RSS) distributions at each location according to the training information and utilizes probabilistic methods to find the match with the maximum likelihood. For example, (Savazzi, Nicoli, Carminati & Riva 2014) proposed a framework of Bayesian estimation approach to reach the localization accuracy to 1-meters and (Xiao, Wu, Yi, Wang & Ni 2013) used the maximum a posteriori probability (MAP) algorithm to achieve the localization accuracy to 0.9-meters.

In general, the location-based approach has two advantages: (1) It does not require a dense nodes deployment because there is no intersection with any radio Line-of-Sight (LOS) links with the presence of an object; (2) It can avoid modeling errors by explicit measurements of the multipath effects on RSS in each different location. However, it is also apparent that the calibration procedure of fingerprinting is relatively tedious.

- **Link-based approach**

The concept of the link-based approach is to form a consistent link-based model to relate the object's location relative to the radio link locations based on the RSS dynamics in the network. This approach analyzes the statistical relationship between an object's position and the resulting RSS of any radio links in the environment and consequently deduces the location information using geometric methods. (Zhang, Ma, Chen & Ni 2007) presented an algorithm which directly estimates track of a single object from link measurements. For each link whose RSS variation exceeds an empirical threshold, the object is likely to be located in an area which is approximated as a rectangle, centered at the midpoint of the line between the transmitter and receiver. Then the authors adopted the best-cover algorithm to estimate the objects position based on the experiments with a 44 RF-based grid array covering 36 square meters. This work was extended in (Zhang & Ni 2009) to use a probabilistic cover algorithm based on distributed dynamic clustering to improve the localization accuracy. In order to realize a real-time accurate and scalable system for device-free localization, they divided the monitored area into different triangular sections and used the support vector regression model to locate the object in each area (Zhang, Liu, Guo & Ni 2013). This series of work has performed valuable exploration and verified the feasibility of utilizing radio link information for localization.

Inspired by the computed tomography method that is widely adopted in medical and geophysical systems, another set of work following the above studies modeled the device-free localization as a radio tomographic imaging (RTI) problem (Wilson & Patwari 2010) (Wilson & Patwari 2012). When an object moves into the area of a wireless network, links which pass through that object will experience shadowing losses. This work carried out in-depth research on the use of shadowing losses on links between many pairs of nodes in a wireless network to image the attenuation of objects within the network area. Based on this work, there has been a great deal of research on RTI to realize high-performance of device-free localization. (Kaltiokallio, Bocca

& Patwari 2012) exploited channel diversities based on channel packet reception rates and fade levels to restrain the frequency domain interference. (Wang, Gao, Yu, Cheng, Wu & Wang 2013) proposed a differential scheme to process RSS measurements to improve the localization accuracy and system robustness. (Nannuru, Li, Zeng, Coates & Yang 2013) presented measurement models and particle-based algorithms for RF-tomographic approaches to track multi-targets in indoor environments.

In general, the link-based approach has two advantages: (1) it is robust to the environmental variations because the objects position is directly estimated based on its relative distance to each radio LOS link ; (2) it needs less calibration effort which means that only node positions and ambient RSS for each link is required. However, it depends on a dense nodes deployment to guarantee enough radio LOS links to cover all the tracking area.

2.2.2 Device-free Intrusion Detection

The concept of device-free intrusion detection is to record and analyze the RSS dynamics obtained from the existing wireless infrastructures for performing intrusion detection. Different from the traditional intrusion detection system that either requires special hardware support or communication devices attached to objects, this passive intrusion detection has shown the feasibility to detect intruders without any physical devices equipped with them. With wireless infrastructures becoming more and more pervasive in our daily lives, device-free intrusion detection can provide a broad range of application such as intrusion detection in industrial facilities, surveillance of the home security and search-and-rescue operations.

The device-free intrusion detection depends on the fact that RF signals that travel through in the ranges of the wireless networks are affected by absorption, reflection, refraction, and scattering. Therefore, the presence of intrusions within the wireless network will result in significant RSS variations at wireless devices which makes it possible to detect intrusion in wireless environments. In recent years, there have been many efforts undertaken to

investigate device-free intrusion detection. (Youssef et al. 2007) first demonstrated the feasibility of device-free localization in a controlled environment using the moving average and moving variance of RSS to detect intrusions. This work was extended to a real environment in (Moussa & Youssef 2009). Although the performance of algorithms developed in previous work severely degraded in this scenario, the authors presented an alternative algorithm, based on the maximum likelihood estimator (MLE) that has a significant performance increase without affecting the systems precision. However, these studies are limited as only a single intrusion indicator can be exploited. In order to improve the detection capability to identify different intrusion patterns in real world (e.g. an intruder is standing and hiding or a person is trapped in a fire building), (Yang, Ge, Xiong, Chen & Liu 2010) proposed a joint learning approach which utilized grid-based clustering over K-neighborhood to effectively diagnose the presence of intrusions in Zigbee networks.

Other than these studies, the RTI technique has been investigated to further improve detection accuracy. (Wilson & Patwari 2011) first applied an inverse imaging algorithm to obtain an attenuation map and then made improvement by leveraging motion-induced variance of RSS measurements. (Li, Chen, Coates & Yang 2011) presented a sequential Monte Carlo (SMC) method incorporated with on-line expectation maximization (EM) to estimate model parameters. However, the majority of these studies for RF tomographic intrusion detection have focused on a single target in a wireless network. In order to realize detecting multiple targets, the authors in (Thouin, Nannuru & Coates 2011) considered the attenuation effect is the sum of attenuations caused by all targets and developed a multi-target tracking algorithm based on a particle approximation of a moment-based filter. The approach was extended to provide some experimental verification for up to four targets (Nannuru, Li, Coates, Yang et al. 2011).

In general, device-free intrusion detection brings several advantages over other traditional technologies owing to the following facts: (1) It can perform based on RSS measurements from low-cost commercial wireless devices,

which are relatively inexpensive and can be deployed quickly; (2) It is able to work in darkness, smoke and to see through walls; (3) It does not raise high privacy concerns as do video cameras. However, device-free intrusion detection still remains a challenging issue due to the presence of large amounts of multi-path clutters in real environments.

2.2.3 Device-free Activity Recognition

Activity recognition has become increasingly important and has the potential to support a broad spectrum of promising applications such as smart surveillance, elder care, virtual reality, advanced user interface, etc. Traditional approaches involve wearable sensors and specialized hardware installations. Device-free activity recognition has been proposed as a way of identifying human activities through the use of existing wireless networks while eliminating the need for a human to carry any device. The concept of device-free activity recognition is to utilize the variations in the transmission channel to recognize human activities in a given environment. Existing solutions for device-free activity recognition can be grouped into two categories: (1) RSS-based approach and (2) channel state information (CSI)-based approach.

- **RSS-based approach**

The RSS-based approach is based on the fact that the existence of an entity in wireless environments affects the RF signals, especially when humans are performing different activities. The RSS at transceivers should be relatively stable if there is no movement or changes in wireless environments. However, the presence of a human will results in changes in RSS values, whereas the degree of the RSS variation is correlated with the level of human motion. Therefore, different human activities will generate correlated characteristic patterns in the received superimposed RF signals. By identifying and interpreting these patterns, it is possible to recognize activities or gestures performed by device-free entities in the RF channel.

There have been extensive studies on the RSS-based approach for device-free activity recognition. (Sigg, Scholz, Shi, Ji & Beigl 2014) first investigated the feasibility of recognizing activities based on RSS fluctuations. The authors developed a DFAR system for device-free activity recognition which achieved recognition rates of over 80% for four activities including crawling, lying down, standing up and walking. However, this system relies on sophisticated Software Defined Radio (SDR) devices from which one continually transmits a signal that is read and analyzed by other nodes. In order to directly use RSS in simple transceiver hardware, this work was extended to utilize Wi-Fi RSS fluctuations on an off-the-shelf mobile phone for the recognition of activities and gestures. The results demonstrated the feasibility of distinguishing simple activities and to some extent also gestures based on RSS fluctuations. However, the accuracies stayed below what would be possible with standard sensors such as accelerometers. In order to improve the performance, (Abdelnasser, Youssef & Harras 2015) presented a WiGest system by leveraging changes in Wi-Fi RSS to sense in-air hand gestures around the users mobile device which achieved overall gesture detection accuracy of 89%.

In general, the RSS-based approach can be widely available in commercial off-the-shelf Wi-Fi devices. However, the performance of device-free activity recognition based on RSS is limited by the disadvantage of RSS itself. RSS is inherently a coarse measurement which only provides coarse-grained information about the channel variations and does not contain fine-grained information about small-scale fading and multipath effects caused by the micro-movements. In addition, strong multipaths make RSS suffer unpredictable fluctuations in dense multipath propagation. Therefore, RSS-based techniques have difficulties providing high recognition accuracy in most environments.

- **CSI-based approach**

The idea of the CSI-based approach for device-free activity recognition is to explore the change rules of CSI when the wireless environment is affected

by human activities. CSI represents the channel properties of a communication link which describe how a signal propagates in the channel combining the effect of time delay, amplitude attenuation and phase shift. Compared with RSS, CSI measurements provide more fine-grained information on each subcarrier with both amplitude and phase information for device-free activity recognition.

As CSI is an upgrade for RSS, it is a natural choice to adopt CSI to boost the recognition performance. (Wang, Wu & Ni 2017) presented a WiFall system that employs the time variability and special diversity of CSI for fall detection in an indoor environment. (Wang, Liu, Chen, Gruteser, Yang & Liu 2014) developed an E-eyes system that utilizes CSI signal measurements to identify household activities at home such as sleeping on the bed, sitting on the bed, watching TV on a sofa, taking a shower and washing dishes. (Nandakumar, Kellogg & Gollakota 2014) employed off-the-shelf Wi-Fi devices that leverage the CSI information to classify four arm gestures such as push, pull, lever, and punch. However, all of these studies have focused on the recognition for macro-movements. As CSI takes the advantage of multipath effects and captures the detailed changes on different subcarriers, it is suitable to recognize micro-movements. (Wang, Zou, Zhou, Wu & Ni 2016) proposed a WiHear system that uses CSI values to identify mouth movements while talking for achieving lip reading. This work introduced Mouth Motion Profile that leverages partial multipath effects and wavelet packet transformation to solve this micro-movement detection. (Ali, Liu, Wang & Shahzad 2015) presented a WiKey system that exploits the variations in CSI values to recognize keystrokes. In order to identify the micro-movements of hands and fingers in typing, WiKey adopted an extraction algorithm that automatically detects and segments the recorded CSI time series to extract the waveforms for individual keystrokes.

In general, as CSI is a finer measurement of the wireless propagation channel, the CSI-based approach can provide high performance for device-free activity recognition. However, the CSI-based approach is only accessible

on specific platforms because the resolution of CSI is limited by the operating bandwidth of Wi-Fi (IEEE 802.11n/ac channel). Therefore, the majority of current CSI-based studies rely on COTS Wi-FI network interface cards (NICs) (such as Intel 5300 and Atheros 9390) to obtain CSI values.

As shown in the above literature review, device-free sensing-based techniques have the advantages of long-range, low-cost and the ability to work in darkness and NLOS scenarios while offering good privacy protection. However, all of these applications are based on situations where performance validation is conducted in indoor environments or open-field outdoor environments. Performance of DFS-based technologies in a cluttered outdoor environment has not yet been fully explored. Therefore, in this thesis, the possibility of using DFS technology for target detection and classification in a foliage environment is investigated. Some more related works are referred to in the following chapters.

Chapter 3

A Device-Free Sensing Approach for Human and Animal Classification

The well-known IoT is recently being considered for critical missions such as search and rescue, surveillance and border patrol. One of the most critical issues that these applications are currently facing is how to correctly distinguish between human and animal targets in a cost-effective way. In this chapter, we first present a relatively low-cost but robust approach that uses a combination of device-free sensing and machine-learning technologies to tackle this issue. In order to validate the feasibility of the presented approach, a variety of data is collected in a cornfield using impulse-radio ultra-wideband (IR-UWB) transceivers. These data are then used to investigate the influence of different statistical properties of the RF signal on the accuracy of human and animal target classification. Based on the probability density function (PDF) of different statistical properties, two distinguishing features for target classification are found, namely standard deviation and root mean square delay spread. Using them, the impact on the classification accuracy due to different classifiers, number of training samples and different values of SNR are extensively verified which indicates that the pre-

sented approach has a great potential to be deployed in an outdoor cluttered environment.

3.1 Introduction

Personnel detection in terms of human and small animal targets classification has been found very useful for many applications, ranging from military to surveillance (Chan, Kuga & Ishimaru 1999) (Frolind, Gustavsson, Lundberg & Ulander 2012) (Jin et al. 2012) (Guan, Yin, Guo & Wang 2016) (Damarla, Bradley, Mehmood & Sabatier 2013). The traditional approaches have been revealed to be deficient due to ever-increasing requests for safety, security and environment protection at local and national level. Previously, the most performed studies are focused on using either SAR or hybrid-sensor systems for personnel detection. Although these approaches can effectively differentiate targets with very low false alarm probability, their costs of implementation need to be dramatically reduced; otherwise, they are not going to be feasible for target detection with the presence of animals that are similar to human in terms of the physical size. As far as cost reduction is concerned, several novel detection approaches based on micro-Doppler signatures have been recently presented in the literature. Using these approaches, either a human doing different activities (Wang, Liu & Fathy 2013) (Ding & Tang 2014) (Du, Ma, Wang & Liu 2014) or different humans doing the same activity (Javier & Kim 2014) (Kim & Moon 2016) (Fioranelli, Ritchie & Griffiths 2016) can be accurately classified. Moreover, humans and dogs can be distinguished by using stride information from the targets, as demonstrated in (Kim, Ha & Kwon 2015). However, the performance of these approaches has only been verified in the open-field environment. Their classification accuracy may be severely deteriorated, if clutters are introduced in the surrounding area. In order to dramatically reduce system cost without compromising performance, a cost-effective monitoring system with a high reliability is urgently required for personnel detection.

There is an emerging class of sensing technology, known as DFS, which only uses RF signals as sensing devices to detect some environmental variations. Thus, it requires no additional hardware but an RF transceiver which shows a potential to dramatically reduce the overall cost. Although this technology has been used to successfully demonstrate human target detection either at an indoor environment or in an open field, no attempt has been made to transfer the technology to applications that are operated at outdoor with changing atmosphere and ground conditions. Thus, there are still several challenges for us to overcome. Since the outdoor clutter may be time-varying, they could significantly affect propagation of an RF signal in a non-predictable way. As DFS-based approach uses RF signals as sensing devices, the selection of the most appropriate RF signals plays a critical role. According to theory, the impulse-shaped signal with extremely short duration pulses is immune or invulnerable from sensitivity or multi-path effects or fading problems which is a better option than the continuous-wave (CW) signal (Wang & Fathy 2012) (Kumar, Li, Liang, Zhang & Wu 2014). Thus, an IR-UWB signal is selected in this work. In addition, animals such as goats and dogs, may have similar dielectric properties as human beings that could also adversely affect the detection accuracy of human targets. To ensure that the types of the detected target can be correctly classified, there is no doubt that the selection of distinct features is a critical task. Until now, very few papers discuss this issue in the literature. It is still unknown how to distinguish humans and animals in an effective way.

In this chapter, we present an effective and robust solution to tackle this issue. This solution is based on a combination of IR-UWB and machine-learning technologies. Although continuous improvement of sensing technology naturally pushes the state of the art to either lower cost or higher performance, the innovations developed in this work will radically disrupt this progression and create a whole new standard for cost versus performance that will enable the development of applications which were previously unattainable. Several typical statistical properties (SP) of the received RF signals

are investigated by means of a probability density function (PDF) so that the computational cost can be minimized without compromising detection accuracy. Based on our experimental results, two distinguishing features are found to be particularly suitable for human and animal target classification in a cornfield. Using these two features only, the impact on the classification accuracy due to different classifiers, the number of training samples and variations of SNR is extensively investigated. Simulation results demonstrate the feasibility of the presented cost-effective sensing approach for human and animal target classification in outdoor environments with the existence of clutters.

The rest of this chapter is organized as follows. Section 3.2 briefly introduces the data measurement and collection in real scenarios. In Section 3.3, we present the details of our proposed feature extraction and selection method. We provide the experimental results and analysis in Section 3.4, and finally summarize this chapter in Section 3.5.

3.2 Experiment Setup and Data Acquisition

To verify the performance of the developed system, in particular the accuracy of distinguishing between human and animal targets in an outdoor environment with the existence of clutters, a variety of data have been taken in a cornfield. The experimental setup is shown in Figure 3.1. The transceivers are placed at fixed locations with a constant height, 0.5 m above the ground. Four scenarios are used for data collection purposes. In scenario 1, a penetration measurement was taken without any target placed between a transmitter and a receiver. In scenarios 2-4, three different targets are used, including (1) human (a crouched man with 65 kg weight and 80 cm height), (2) dog (approximately 70 cm length and 40 cm height), and (3) goat (approximately 60 cm height). Since the detection and classification accuracies may be adversely affected by the selected locations where the target is placed, eleven different locations (A, B, C, D, E, F, G, H, I, J and K) within a region

between the transceivers are used to ensure that the system can effectively detect and classify the concealed target in the entire monitoring area. The detailed selection of locations is given in Figure 3.2. On the other hand, it is also worthwhile to mention that the resolution of the scanned (captured) waveform is 61 picoseconds. Since there are 350 sampling points (limited by the used system) as shown in Figure 3.3 (a), the overall duration of each captured waveform is 61 ps $\times$ 350 = 21.35 ns.

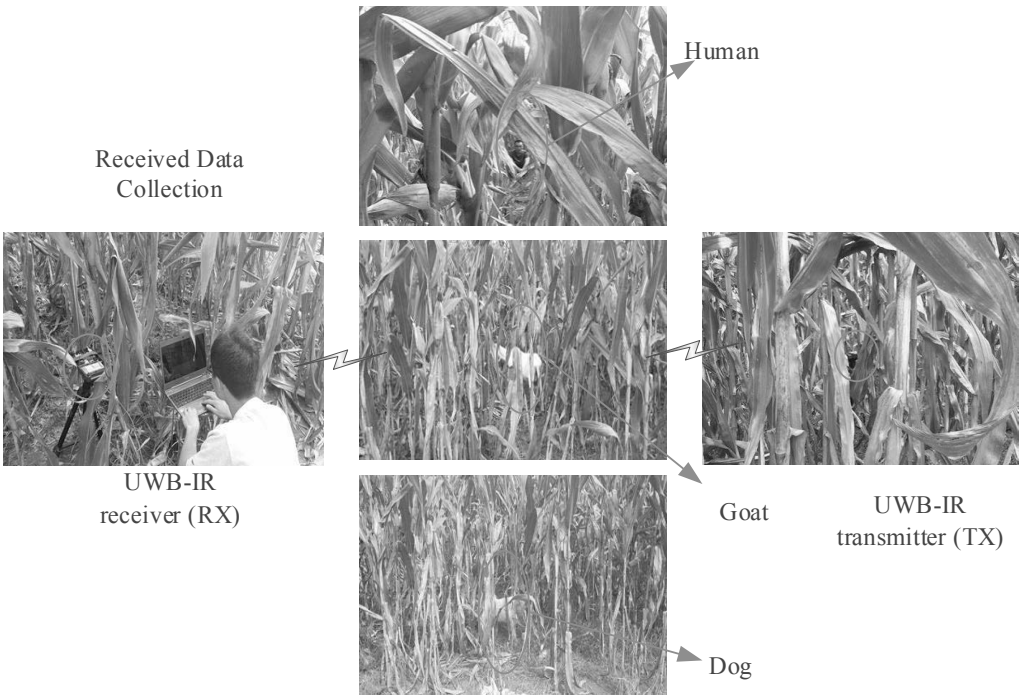

Figure 3.1: Measurement setup

Note that the corn plants are separated by approximately 0.3 m, and the heights are up to approximately 1.7 m. To ensure the reliability of the system, many samples are collected: in each scenario, 500 samples are taken at every location. As there are 11 different locations, an overall 5,500 samples for each scenario are collected to form a database. These collected data are used for the purpose of machine learning and will be explained in detail in the following sections.

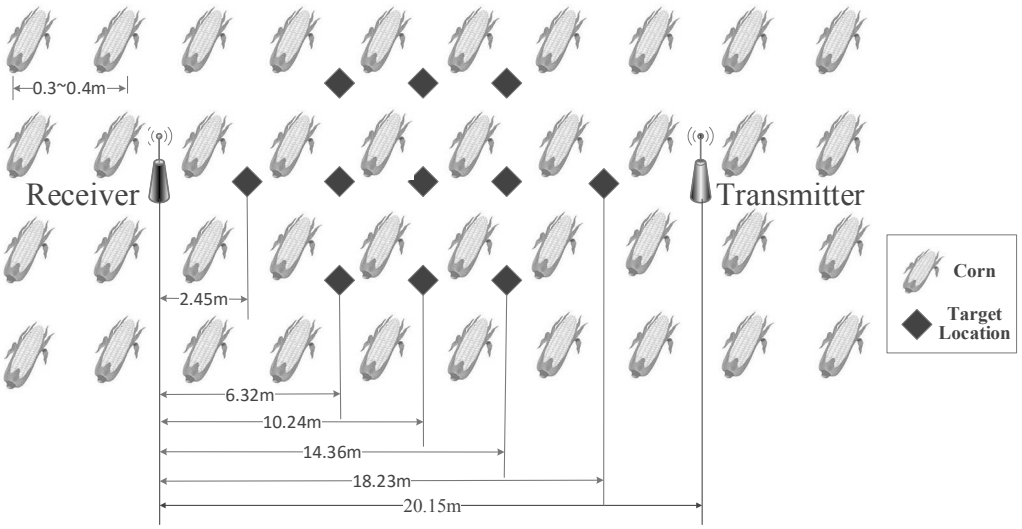

Figure 3.2: The selected locations for data collection in a cornfield

3.3 Proposed Method for Feature Extraction and Selection

This section is organized as follows. Section 3.3.1 briefly introduces the data preprocessing of the received RF signals collected in Section 3.2 and Section 3.3.2 presents the feature extraction and selection approach.

3.3.1 Data Preprocessing

IR-UWB technology is selected in the present approach because, not only is it robust against noise but also is more energy efficient than the conventional CW-based technology. The measurements were taken using PulsON 400 (P400) by the Time Domain Co., Ltd. The operation frequency of the transceiver is from 3.1 to 5.3 GHz with the center frequency at 4.2 GHz. Planar elliptical dipole antennas with a gain of 3 dBi are used for transceivers. In addition, the receiver is connected to a PC so that the collected data can be directly acquired and recorded digitally. More details of the P400 specifications and key performance parameters can be found in Table 3.1. As

Table 3.1: P400 Specifications and Key Performance Parameters

Physical Parameters	
Dimensions	4”× 3”× 0.85” = 10.2 inˆ3
Temperature	Operating: -10°C to 65°C Storage: -40°C to 85°C
Power Requirements	5.75V to 30V DC
Power Consumption	5 Watts
RF Characteristics	
Operating Band	3.1GHz to 5.3 GHz
Center Frequency	4.3 GHz
Transmit power	Mode 1: -14.5 dBm Mode 2: +2.3 dBm
Antenna Ports A&B	Standard 50 Ohm SMA coaxial connector
Noise Figure	4.8 dB
Transmit Pulse Repetition Rate	10.1MHz (default - others available)
RF Communications	
Channelization	7 user selectable pseudo-random pulse interval channels
Raw (Symbol) rates:	158k, 79k, 39.5k, 19.7k, 9.86kbps
Max Distance (FCC Part 15 0dB Antennas, Freespace)	88m, 125m, 177m, 250m, 354m
Communications type	Packet transmission
Max user bytes/packet	1024

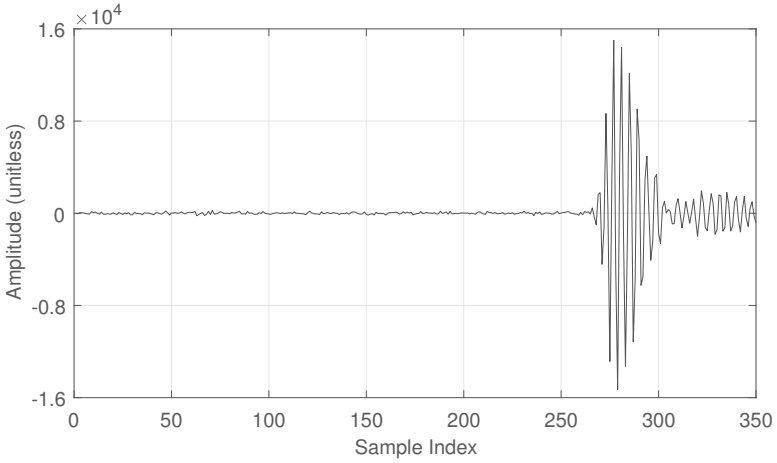

(a)

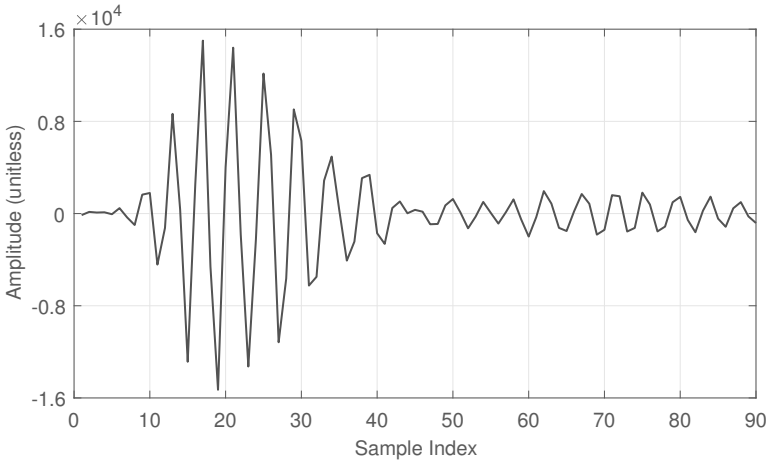

(b)

Figure 3.3: Waveforms of the raw RF signals at the receiver without any target placed in the surrounding region: (a) without preprocessing, (b) with preprocessing

mentioned, an RF signal can be partially blocked and reflected which results in different scattering paths. This phenomenon can be represented as:

$$r(t) = \sum_{k=1}^{N} A_k p(t - t_k) \tag{3.1}$$

where $r(t)$ is the received signal, A_k is the amplitude of the kth multipath, $p(t)$ is the envelope of the template signal, $t_k$is the time delay of the kth path and N is the number of scattering paths. As shown in Equation (3.1), this model includes all multipath reflections. Since the envelope of the received waveform can be significantly affected by the type of the detected target, any changes in the targets, including the physical size and material, could be very well reflected by the received waveform. It is noted that to improve classification accuracy, only the part that contains the strong impulse is selected for feature extraction and signal preprocessing is required to remove unwanted noise. As illustrated in Figure 3.3, two measured waveforms, namely with and without signal preprocessing, are compared.

To show the challenge of human and animal target classification, the waveforms of the received raw RF signals with different targets, including human, dog and goat, are plotted in Figure 3.4 (a), (b) and (c), respectively. Although distinct differences can be found for the scenario, where no target is placed, the differences between human and animal targets are not obvious at all. Thus, using the conventional approach that only uses the strength of RF signals is no longer appropriate.

3.3.2 Feature Extraction and Selection

As previously demonstrated, once a target is placed between a transmitter and a receiver, the channel condition varies, which influences the received RF signals. Since an impulse-like RF signal has rich multipath features, some insight regarding target classification may be provided by investigating the characteristics of these signals. To capture the salient differences of the received RF signals as different targets are placed, a number of features can be extracted from the waveform of every received RF signal *r(t)*. The statistical properties of IR-UWB signals that are commonly used for identification of NLOS and LOS are used for features extraction in this work. Eight classical statistics are selected because they have been successfully applied for indoor target localization. However, the feasibility of using them for human and

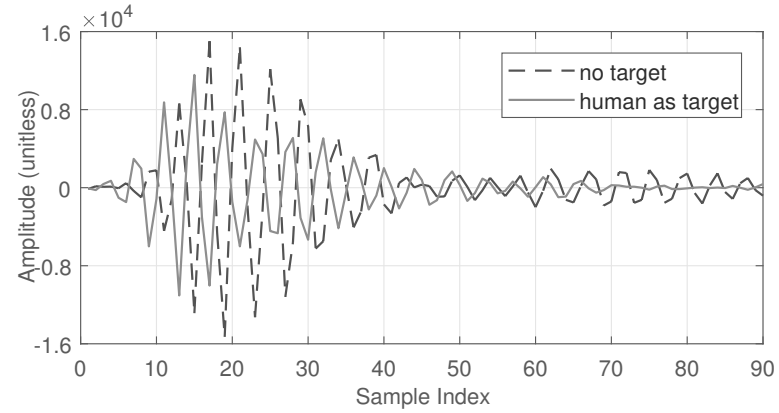

(a)

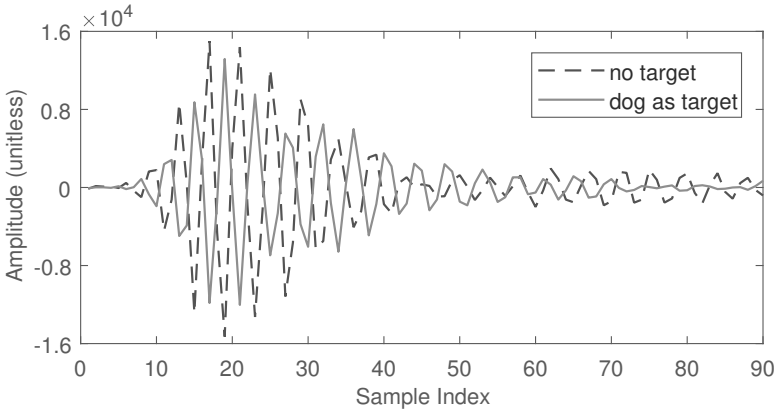

(b)

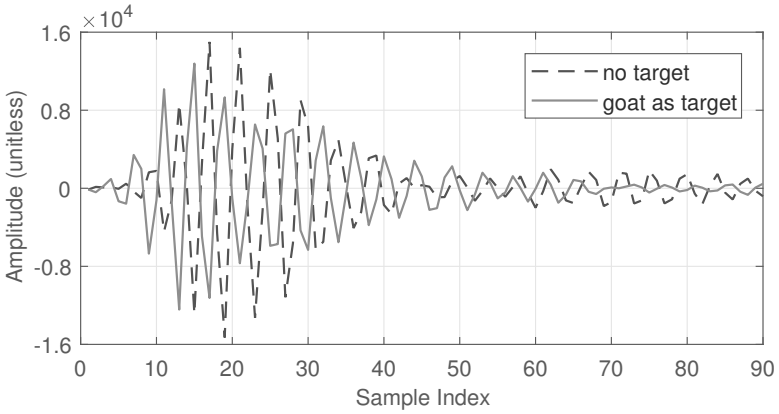

(c)

Figure 3.4: Measured waveforms at the receiver with three different targets, (a) human, (b) dog and (c) goat

animal classification in outdoor environment has not been attempted.

The PDFs of the statistics of multipath components (MPCs) can be obtained using the previously collected data. Although multiple features can be used for target classification, it is desirable to minimize the dimension of the selected features. Consequently, not only the average classification accuracy but also the computational efficiency would be significantly enhanced which is essential for autonomous sensing. For this reason, the characteristics of different features are analyzed in terms of PDF so that the most distinguishing features can be selected. It is noted that all the extracted features in this chapter are normalized between 0 and 1 for simplicity. If a collection of extracted feature values is given as $x = (x_1, x_2, \ldots, x_k)$, their corresponding normalized data $z = (z_1, z_2, \ldots, z_k)$ can be expressed as:

$$z_k = \frac{x_k - \min(x)}{\max(x) - \min(x)} \tag{3.2}$$

Due to the fact that for personnel detection, it is not necessary to distinguish between goat and dog targets, the previously defined scenarios are merged into three cases. The targets are defined as no target, human and animal. Note that the case of animal is formed by a combination of goat and dog with a ratio of 1:1. The statistics of MPCs can be categorized into either amplitude-based parameters (in the time domain) or delay-based parameters (in the frequency domain). For the amplitude-based parameters, they can be divided into two types of parameters, namely absolute parameter and relative parameter. The type of absolute parameter consists of the maximum amplitude of the received signal, the number of the MPCs within 10 dB of the strongest path for each received signal and the number of MPCs that contain 90%of the received energy. These parameters can be expressed using the following equations.

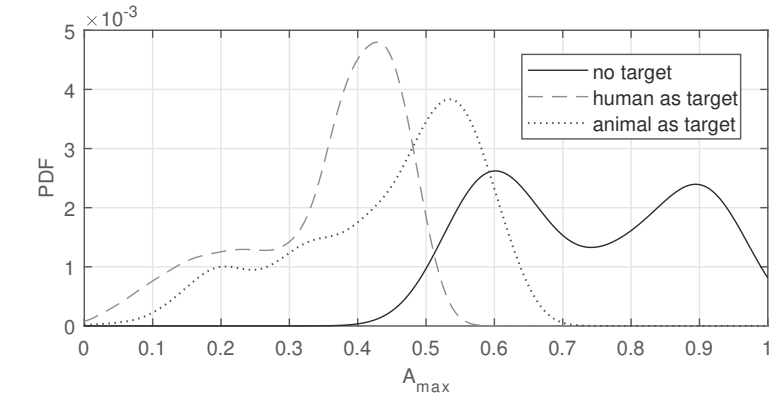

(a)

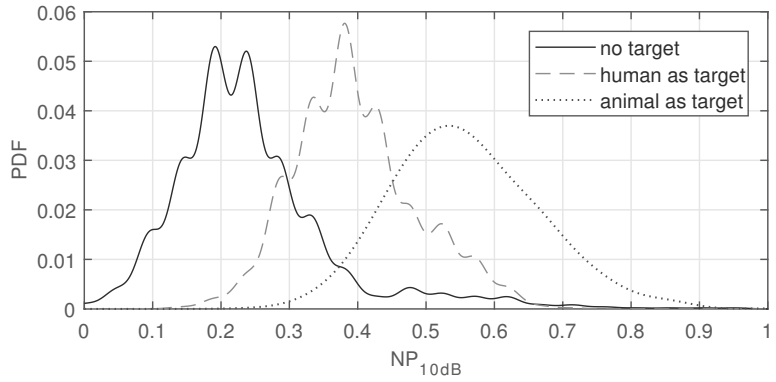

(b)

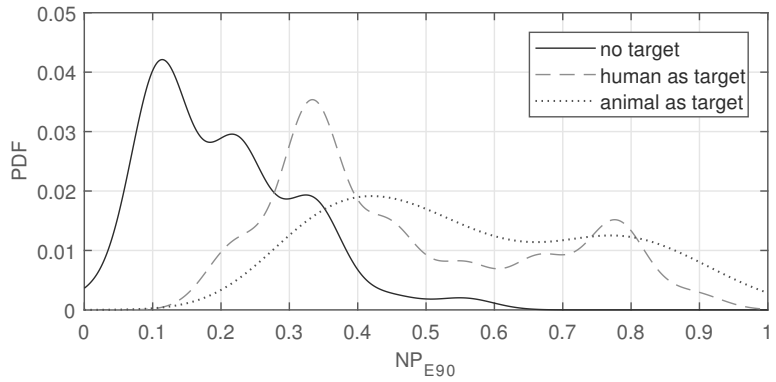

(c)

Figure 3.5: Calculated PDF as a function of selected statistical feature: (a) maximum amplitude, (b) number of MPCs within 10 dB of the strongest path, (c) number of MPCs that contain 90% of the received energy

The maximum amplitude of the received signal:

$$A_{\max} = \max_{t} |r(t)| \tag{3.3}$$

The number of the MPCs within 10 dB of the strongest path for each received signal:

$$NP_{10dB} = \sum_{r(t)} (|r(t)| > -A_{\max}/10) \tag{3.4}$$

The number of MPCs that contain 90% of the received energy:

$$NP_{E90} = \min_{n} \left(\sum_{t=1}^{n} |r(t)|^2 > 0.9E_r \right) \tag{3.5}$$

Using the previously obtained measurement samples, the calculated PDFs of these three features for all cases are depicted in Figure 3.5 (a), (b) and (c), respectively. As illustrated in Figure 3.5 (a), there is a relatively large overlap between animal and human cases while there is another overlap between animal and no target. Very similar results can also be observed from Figure 3.5 (b) and (c). This indicates that none of these three statistical properties can be used to effectively distinguish not only human and animal targets but also correctly detect the existence of a target. This is mainly due to the fact that outdoor environments are highly dispersive which could severely affect the type of absolute parameters. Moreover, the results also indicate a similarity between human and animal targets. On the other hand, the type of a relative parameter consists of mean, standard deviation and Kurtosis. These parameters can be expressed using the following equations.

The mean of the absolute value of *r(t)*:

$$\mu_{|r|} = \frac{1}{T} \int_{T} |r(t)| \, dt \tag{3.6}$$

The standard deviation of the absolute value of *r(t)*:

$$\sigma^2_{|r|} = \frac{1}{T} \int_{T} \left[|r(t)| - \mu_{|r|} \right]^2 dt \tag{3.7}$$

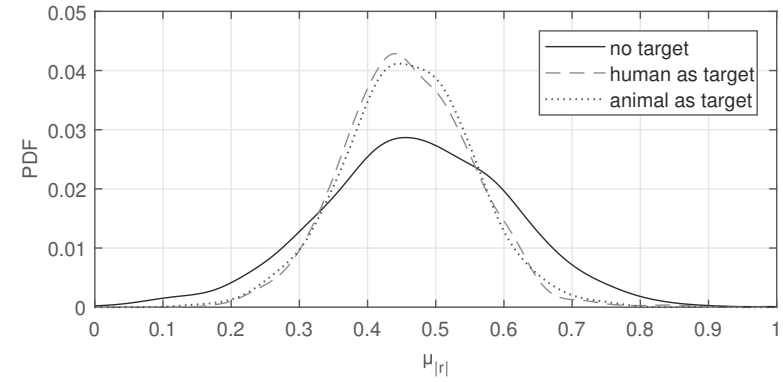

(a)

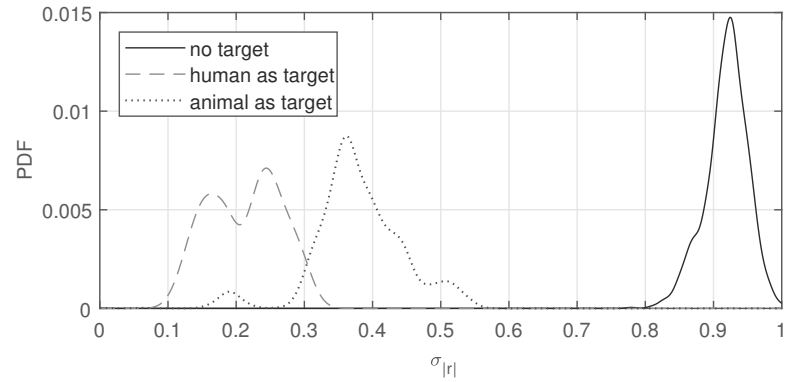

(b)

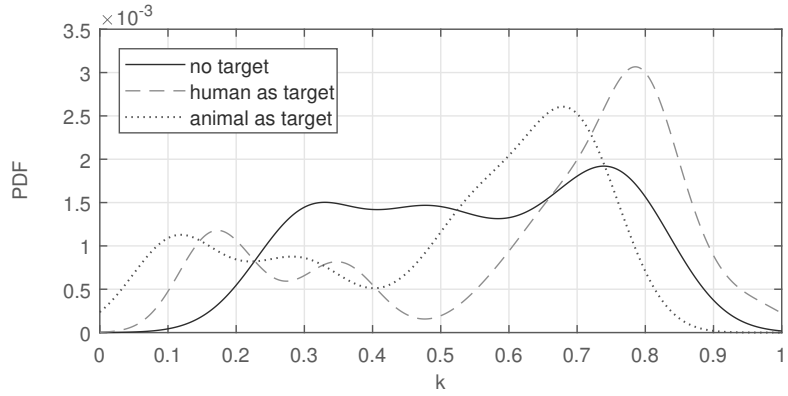

(c)

Figure 3.6: Calculated PDF as a function of selected statistical feature: (a) mean, (b) standard deviation, (c) Kurtosis.

Kurtosis:

$$k=\frac{1}{\sigma_{|r|}^4 T}\int_T \left[|r\left(t\right)|-\mu_{|r|}\right]^4 dt \tag{3.8}$$

The calculated PDFs as functions of these three features are plotted in Figure 3.6 (a), (b) and (c), respectively. It is evident that the PDF of the standard deviation (as shown in Figure 3.6 (b)) is more distinctive than the other two cases which means that this feature is very well suited for target classification. The PDFs of both mean and Kurtosis have relatively similar characteristics. Thus, neither of them can be effectively used for target classification. In particular, the PDFs of the mean are almost identical for human and animal targets which once again indicates that human and animal targets have a strong similarity. Moreover, Kurtosis is a measure of whether the data are peaked or flat relative to a normal distribution. As previously illustrated in Figure 3.4, the received RF signals for different cases seem to have similar waveforms which explains why it is difficult to use Kurtosis as a feature in the presented system.

In order to ensure the accuracy of the presented approach, the delay-based statistics of MPCs have also been taken into consideration. Two important statistics that characterize the delay information of the MPCs are the mean excess delay and the root mean square (RMS) delay spread which are given below.

The mean excess delay:

$$\tau_m = \frac{\int_{-\infty}^{+\infty} t|r\left(t\right)|^2 dt}{\int_{-\infty}^{+\infty} |r\left(t\right)|^2 dt} \tag{3.9}$$

The RMS delay spread:

$$\tau_{RMS} = \sqrt{\frac{\int_{-\infty}^{+\infty} \left(t-\tau_m\right)^2 |r\left(t\right)|^2 dt}{\int_{-\infty}^{+\infty} |r\left(t\right)|^2 dt}} \tag{3.10}$$

The calculated PDFs of these two features are given in Figure 3.7. As can be seen in Figure 3.7 (a), using the PDF of the mean excess delay is insuffi-

cient for target classification. It is interesting to see that the characteristic of this PDF is similar to the ones obtained from Kurtosis and NP_{E90}. This phenomenon once again indicates that a time-varying channel due to clutter would severely affect the accuracy of classification. As illustrated in Figure 3.7 (b), τ_{RMS} can also provide a good indication among three different types of target. Although using a single feature, either Figure 3.6 (b) or Figure 3.7 (b), could potentially differentiate between different targets, using two features would surely enhance the reliability of the presented approach. Based on the above discussion, the standard deviation and RMS delay spread are selected as input parameters for target classification in this work.

3.4 Target Classification and Results Discussion

In order to verify the performance of the presented approach for target classification, three classical classifiers are selected, including the support vector machine (SVM), the k-nearest neighbor (KNN) classifier and back-propagation neural network (BPNN). The radial basis function (RBF) kernel function is accepted for constructing the SVM. The penalization parameter of the SVM and the RBF kernel function width is searched by a grid-search-parameter optimization approach to minimize the average classification error for each SVM. For the KNN classifier, the Euclidean distance is used as a similarity measure in the experiment for KNN and the number of neighbors that is selected to be 10. Moreover, three-layer BPNN is applied to the target classification. The number of input nodes is determined according to the feature dimensions and the output layer contains 3 nodes which is the number of target types in this work. The optimal parameters of the nodes for the hidden layer, the target error, the training rate and the momentum were determined to be 25, 0.005, 0.1 and 0.01, respectively.

The previously obtained data are divided into two types: training and testing, in which the training samples are used to calculate the fitness func-

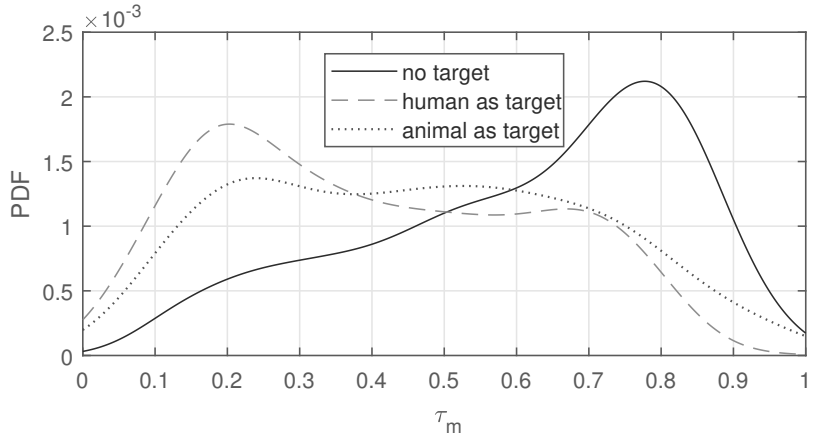

(a)

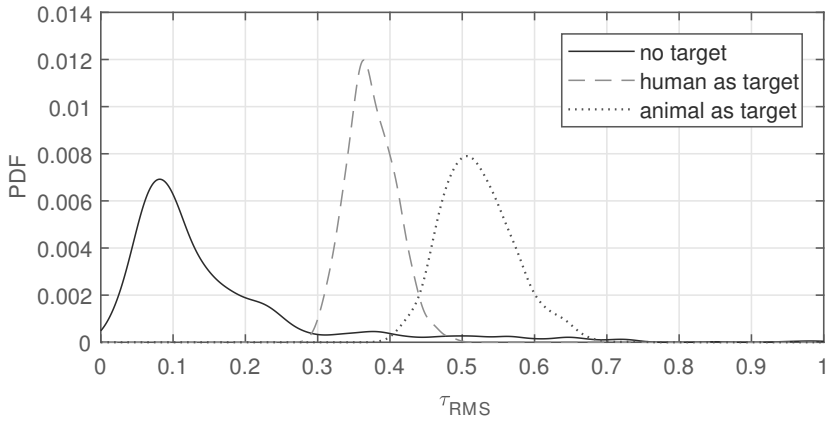

(b)

Figure 3.7: Calculated PDF as a function of selected statistical feature: (a) mean excess delay, (b) RMS delay spread

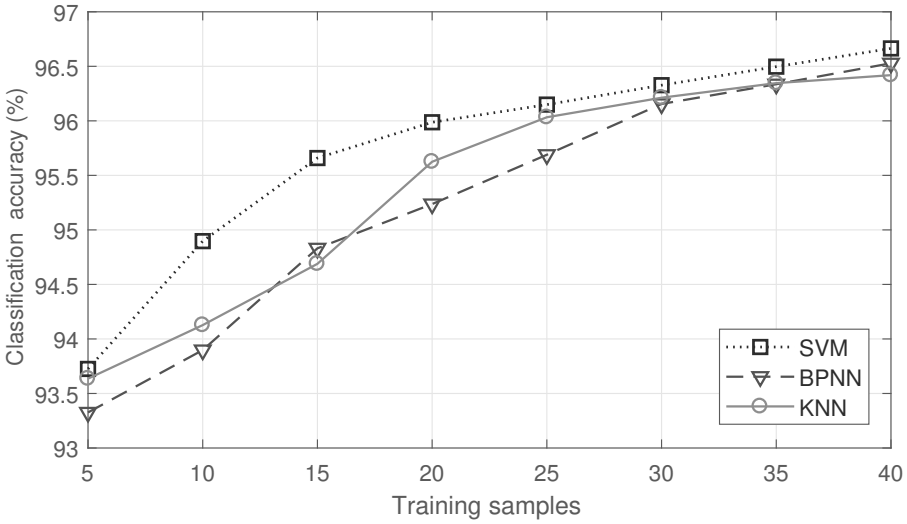
Classification accuracy (%)
Training samples
SVM
BPNN
KNN

(a)

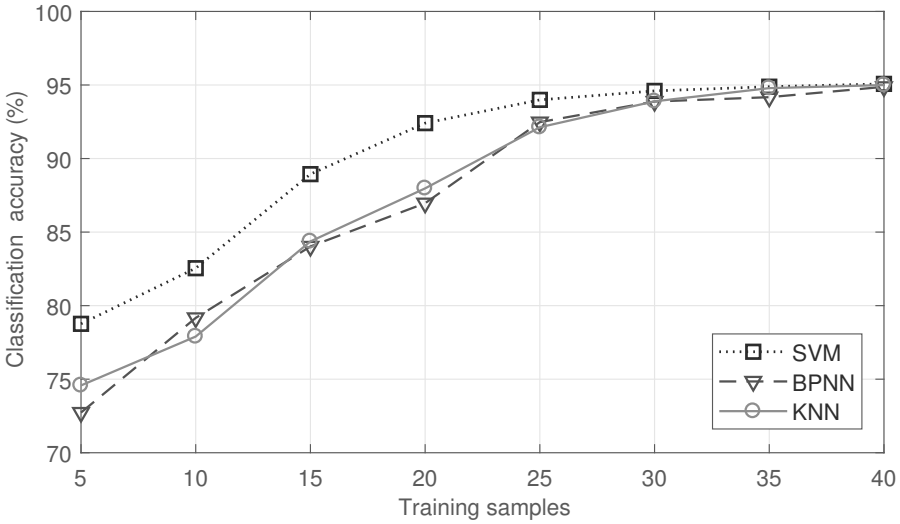
Classification accuracy (%)
Training samples
SVM
BPNN
KNN

(b)

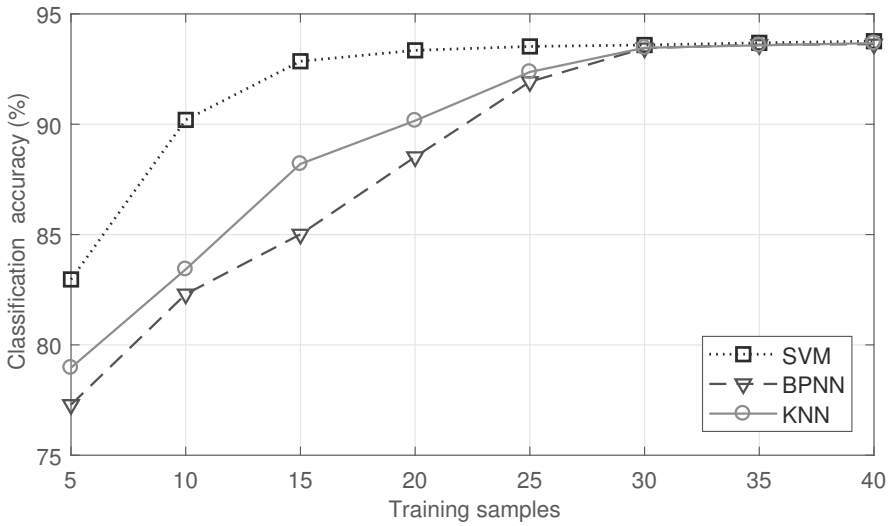

(c)

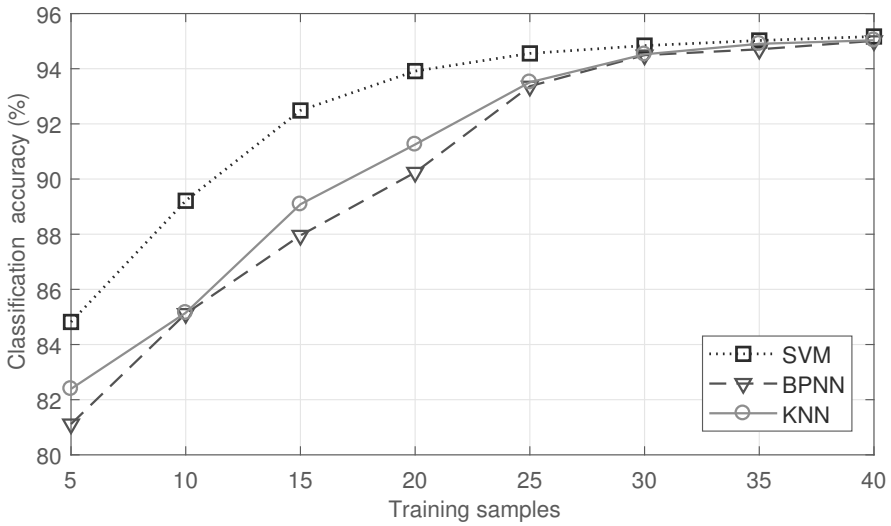

(d)

Figure 3.8: Measured classification accuracy as a function of training samples: (a) no target, (b) human as target, (c) animal as target, (d) average of three targets

tion so that the classifier can be effectively trained, while the testing samples are used to verify the performance of the sensing system. In addition, all data are randomly selected for training and testing. Once the data have been used for training, they will not be used again for testing. As the presented approach is targeted for autonomous sensing, it is essential to investigate the impact on classification accuracy of the selected number of training samples. As a rule of thumb, the more training samples are used, the higher the accuracy can be achieved but with an increased computational cost. For autonomous sensing, as the computational capability of the system is constrained by the limited battery capacity, special attention needs to be paid to the trade-off between accuracy and complexity. For every target at each location, 55 testing samples are used while the number of samples used for training is varied for evaluation purposes. Thus, there are overall $11 \times N$ training samples and 550 testing samples are used to fully investigate the trade-off between computational efficiency and classification accuracy where N ranges from 5 to 40 with a step of 5. By using RMS delay spread and standard deviation as extracted features and applying 275 training samples for each target type, the classification accuracy of the presented approach is shown in Figure 3.8. As illustrated, although the same accuracy can be achieved using the different classifier, using the SVM classifier does show a distinct advantage over using the other classifiers. This is particularly true if the number of training samples is constrained.

Besides minimizing the number of samples used for training, another serious concern is the reliability of the system. As RF signals can be easily attenuated due to environmental variations, evaluating the impact of the SNR on the classification accuracy can be used to verify the reliability of the designed system. Therefore, additional white noise is added to the original collected data so that the SNR can be effectively varied. To evaluate the robustness of the system, the noise level is changed from 0 dB to 30 dB with a step of 5 dB. During the calculation, there are 275 training samples and 550 testing samples used for each target. The corresponding results are shown in

Figure 3.9. As illustrated, both KNN and SVM classifiers have demonstrated very good immunity against noise.

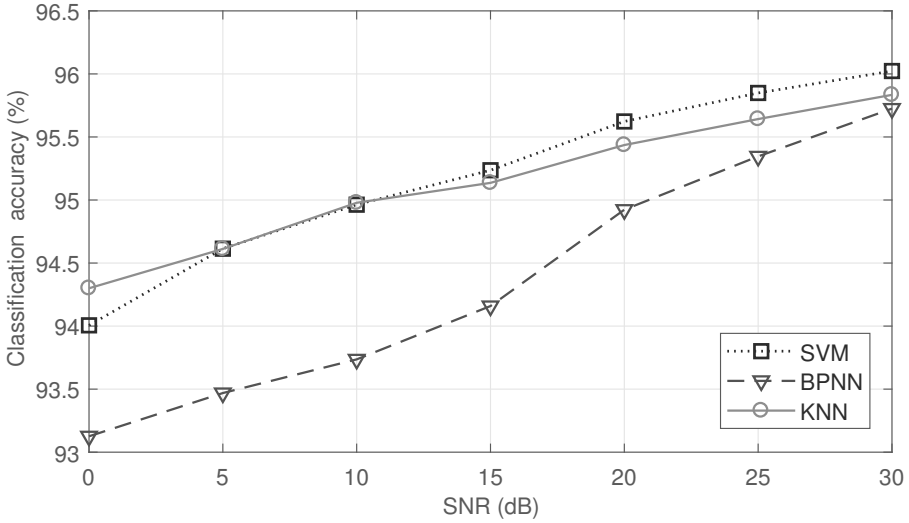

(a)

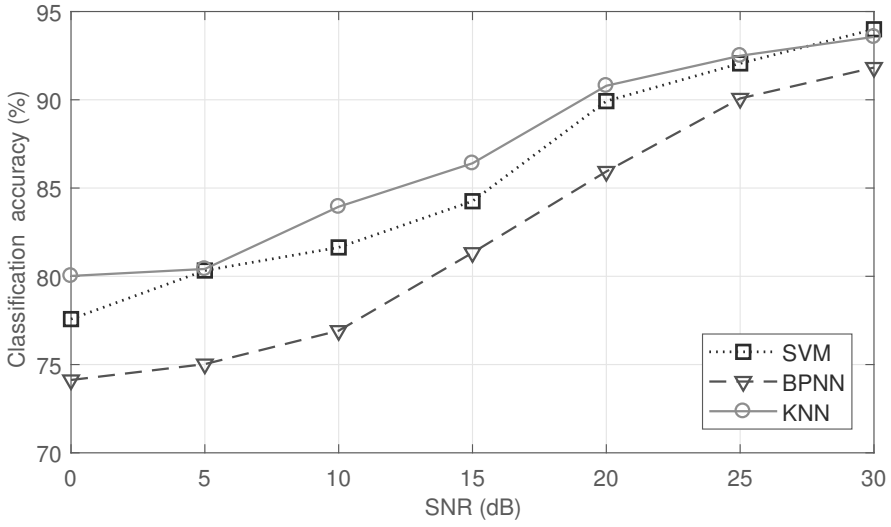

(b)

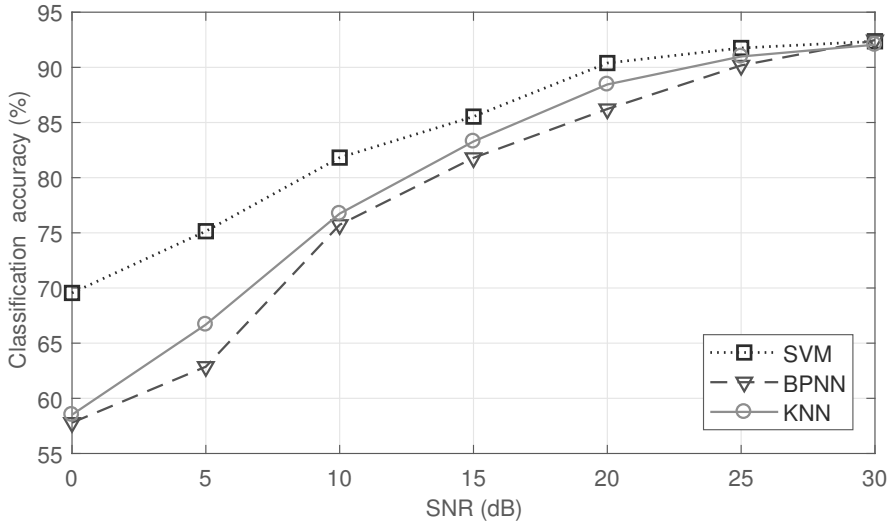

(c)

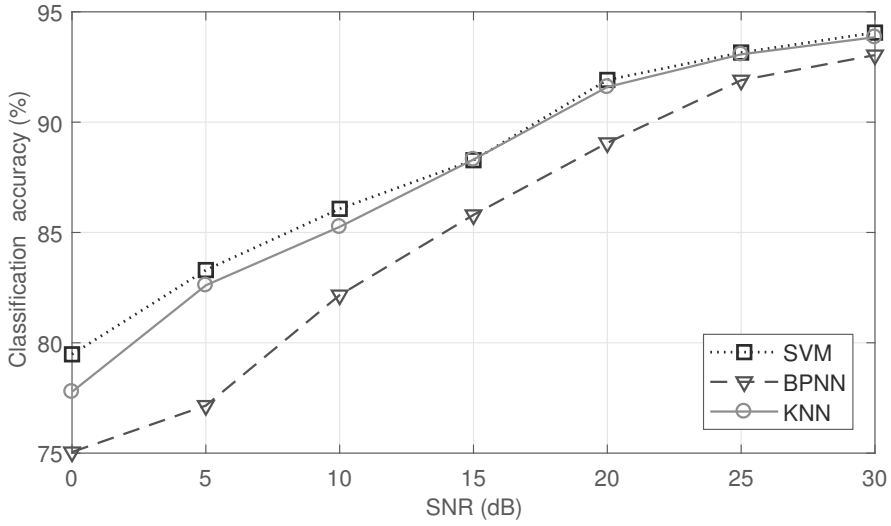

(d)

Figure 3.9: Measured classification accuracy as a function of SNR: (a) no target, (b) human as target, (c) animal as target, (d) average of three targets

The measured classification accuracy using different classifiers is given in Table 3.2, Table 3.3, and Table 3.4, respectively. In Table 3.5, the accuracy of using different classifiers is summarized. Note that, to verify the accuracy of the system in a fairly reasonable way, each experiment is carried out 30 times. The mean and standard deviation for the overall measurements are calculated and summarized in Table 3.5. The Average row shows the average accuracy rate for all the target types.

Table 3.2: The Measured Classification Results Using SVM Classifier

Target type of samples	Test results		
	No target	Human	Animal
No target	531	10	9
Human	7	516	27
Animal	9	33	508

Table 3.3: The Measured Classification Results Using BPNN Classifier

Target type of samples	Test results		
	No target	Human	Animal
No target	526	11	13
Human	9	507	34
Animal	12	33	505

Table 3.4: The Measured Classification Results Using KNN Classifier

Target type of samples	Test results		
	SVM	BPNN	KNN
No target	527	10	13
Human	9	509	32
Animal	10	32	508

Table 3.5: Summary of Classification Accuracy Using Different Classifier

Target type	Classification rate (%)		
	SVM	BPNN	KNN
No target	96.64 ± 0.72	95.73 ± 0.82	95.86 ± 0.79
Human	93.72 ± 0.97	92.14 ± 1.16	92.51 ± 1.18
Animal	92.26 ± 1.13	91.79 ± 1.23	92.38 ± 1.17
Average	94.21 ± 0.89	93.22 ± 1.08	93.58 ± 0.98

3.5 Summary

In this chapter, the possibility of using a cost-effective approach for human and animal target classification in an outdoor environment with the existence of clutters has been extensively explored. The conceptual framework of this approach is based on a combination of DFS and machine-learning technologies. To extensively verify the performance of the presented approach, a variety of samples have been measured under three different scenarios, including no target, human and animal targets. The influence of using different SP of the received RF signals for target classification is analyzed and compared using PDFs, so that the computational cost can be minimized without compromising the accuracy. It has been found that using two statistical properties, namely standard deviation and RMS delay spread, appears to be sufficient for our application. In addition, the impact of using different types of classifiers, variation of SNR as well as the number of training samples on classification accuracy is also investigated. Among different classifiers, namely BPNN, KNN and SVM, it has demonstrated that the SVM classifier is very robust against noise while maintaining good accuracy with the least number of training samples. The average classification accuracy is greater than 91% in terms of distinguishing between human and animal targets which is similar to other state-of-the-art systems that use physical sensors but with a great potential to dramatically reduce hardware and com-

putational cost. Therefore, we could firmly conclude that it is possible to use the presented approach to form a cost-effective sensing solution for human and animal target classification in cluttered outdoor environments.

Chapter 4

HOC-based Feature Extraction Approach for Target Detection in High-Clutter Environment

In this chapter, the possibility of using DFS technology for target detection in a high-clutter environment is investigated. Although in the previous chapter we used the algorithm that is based on statistical properties of the received-signal for target detection in a cornfield with the existence of low clutters, it is still questionable if this RSS-based algorithm is fully functional for detection of a target that is embedded in strong clutters such as a foliage environment. To answer this question, a variety of the measured data have been taken using different targets in a foliage environment. Applying these data along with SVM, the impact on detection accuracy due to different classification algorithms is studied. An algorithm that is based on the extraction of the high-order cumulant (HOC) of the signals is presented while the RSS-based one is used as a benchmark. The measurement results show that the classification accuracy of the HOC-based algorithm is better than the RSS-based one by at least 17%. Moreover, to ensure the reliability of the HOC-based approach, the impact on classification accuracy due to different numbers of training samples and different values of SNR are extensively verified using

experimentally recorded samples.

4.1 Introduction

DFS is an emerging technology that uses RF signals as sensing medium to detect some environmental variations. To accelerate the pace of deploying this technology for applications that need to be operated in high-clutter environments, such as target detection in a foliage environment, good detection accuracy must be ensured. In theory, a transmitted signal consists of several components, and they travel with different paths to arrive at the receiver. RF signals can be easily blocked, reflected or scattered by different targets and therefore each target would result in signals to have different patterns. By identifying and interpreting these patterns, it is possible to detect and even classify the types of targets. Based on this principle, it has been successfully demonstrated that this technology is useful for many applications that operated at indoor environments. In (Patwari & Wilson 2010) (Chen, Edelstein, Li, Coates, Rabbat & Men 2011) (Wei, Hu, Yang & Chou 2015), by detecting the RSS, some simple but very useful tasks can be accomplished using the CW signals, including localization, activity recognition and motion tracking. To further investigate the possibility of using this technology in an outdoor environment, in Chapter 3 we extract statistical parameters from IR-UWB signals to distinguish between human and animal targets in a cornfield with the existence of low clutters.

Although significant progress has been made for using DFS technology as summarized above, deploying this technology in foliage or any other environment that has strong clutters is yet been fully explored. There are still some fundamental issues that need to be tacked (Liang 2011) (Li, Zhao, Zhang, Sun & Zhou 2013). In a foliage environment, not only strength of the RF signal tends to be rapidly attenuated which could overwhelm the weak signals that may contain important features of targets but also the clutters can generate additional noise that would adversely affect SNR of the RF signal.

Note that comparing to target detection, the situation would be even more complicated to target classification. In practice, due to multipath propagation of RF signals, the RSS is spread and reduced in intensity, if there is any target placed between the transmitter and the receiver. Thus, it is relatively straightforward to detect the existence of a target. As long as the RSS is attenuated more than a certain level, the correct decision can be made. However, this is not the case for target classification. In order to correctly classify different targets, the key features of the targets must be extensively analyzed. Due to the nature of DFS technology, these features may be very similar and can be adversely affected by time-varying noise and clutters. If the RSS is relatively weak and the energy of the signals is widely spread, the RSS-based features may not be sufficient to distinguish similar targets, such as human and animal. Therefore, as noise immunity of RSS-based features is limited, a more sophisticated feature extraction method needs to be adopted.

To find an appropriate solution for target detection in a high-clutter environment, unlike conventional DFS-based systems using RSS-based classification algorithms at indoor or in open-field outdoor environments, in this chapter, an IR-UWB signal is utilized for sensing and its high-order cumulant is extracted as a key feature to improve the immunity of the system against the noise generated by clutters (trees and their branches). Using this system, a variety of the samples are taken in a foliage environment. These samples are then extensively used to verify the performance as well as the robustness of the system. In particular, the measurement results show that the classification accuracy of the HOC-based algorithm is better than the RSS-based one by at least 17%. Moreover, the impact on classification accuracy due to the different number of training samples and different values of SNR is extensively verified.

The rest of this chapter is organized as follows. Section 4.2 briefly introduces the data measurement and collection taken in a foliage environment. In Section 4.3, we present the details of our proposed feature extraction method based on HOC. We provide the experimental results and analysis in Section

4.4, and finally summarize this chapter in Section 4.5.

4.2 Experimental Setup and Data Collection

To verify the performance of the presented approach, in particular the accuracy of distinguishing between human and small-animal targets in a high-clutter environment, a variety of data have been taken in a foliage environment. The foliage environment applied in this work is dominated by a mixture of small- and medium-sized trees with different amounts of brush and shrubs. The diameter of the trunk is varied in the range of 2 to 20 cm and is up to approximately 10 m tall. The trees are spaced varying from 0.5 to 2 m and a small amount of underbrush was scattered throughout the area in the space. The operating frequency of the IR-UWB transceiver is from 3.1 to 5.3 GHz with the center frequency at 4.2 GHz. Planar elliptical dipole antennas with a gain of 3 dBi are used for transceivers. In addition, the receiver is connected to a PC so that the collected data can be directly acquired and recorded.

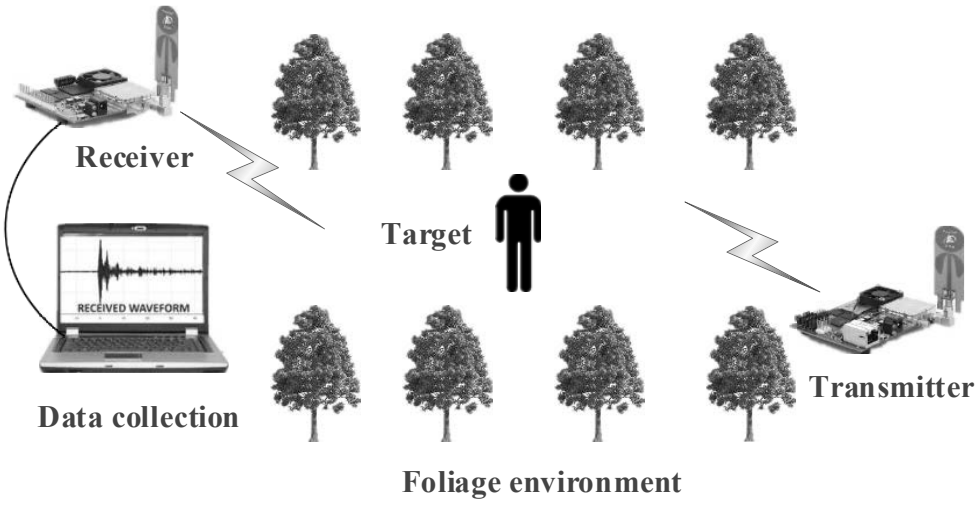

Figure 4.1: Measurement setup

The experimental setup is shown in Figure 4.1. The transceivers are placed at fixed locations at a constant height, 0.5 m above the ground. Three

scenarios are used for data collection. A penetration measurement was taken without any target placed between a transmitter and a receiver, in scenario 1. In scenarios 2 and 3, two different targets are used, including (1) a human (a crouched man with 65 kg weight and 80 cm height) and (2) a dog (approximately 70 cm length and 40 cm height). Since the detection and classification accuracies may be adversely affected by the selected locations where the target is placed, five different locations (A, B, C, D and E) within a region between the transceivers are used to ensure that the system can effectively detect and classify the concealed target in the entire monitoring area. These locations are illustrated in Figure 4.2.

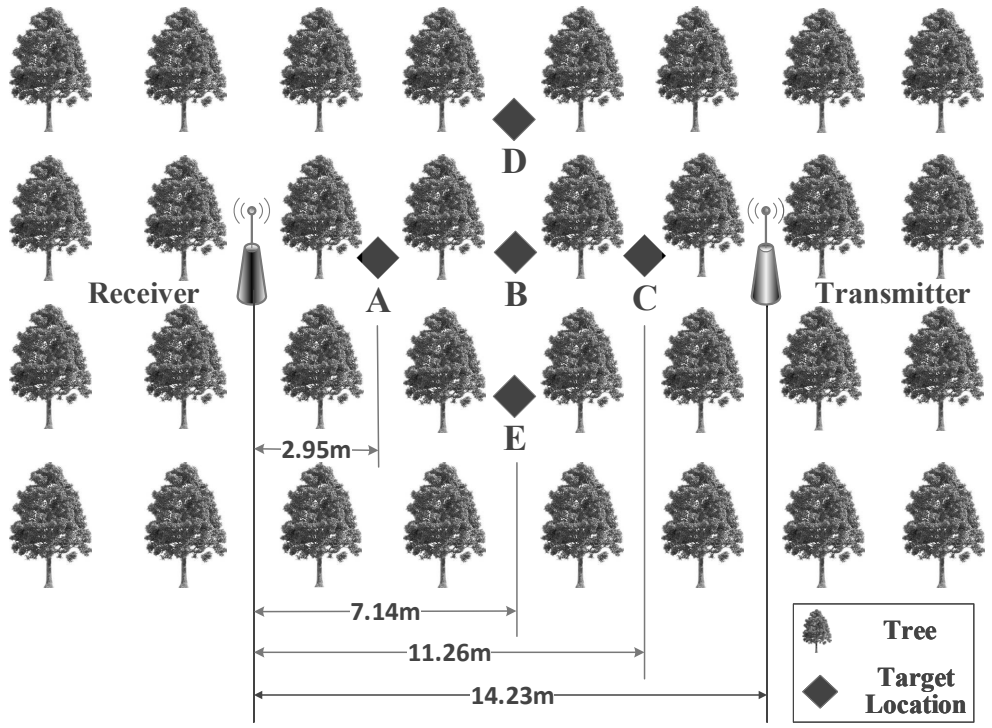

Figure 4.2: The selected locations for data collection in a foliage environment.

To ensure the reliability of the approach, 480 samples are taken at every location for each scenario. As there are 5 different locations, an overall 2,400 samples for each scenario are collected to form a database. These collected data are used for the purpose of machine learning and will be explained

in detail in the next Section. To show the challenge of human/dog target classification, the waveforms of the received raw RF signals with different scenarios are plotted in Figure 4.3. Although distinct differences can be seen for the scenarios with and without any target, the differences between humans and dogs are difficult to distinguish. The features from different scenarios must be extracted in an effective way, otherwise it is impossible to correctly classify the different targets. For this reason, a feature extraction method based on a high-order cumulant is selected in this work.

4.3 HOC-based Feature Extraction

This section is organized as follows. Section 4.3.1 briefly introduces the the basics theory of HOC and Section 4.3.2 presents the feature extraction method based on HOC.

4.3.1 Brief Introduction to HOC

The HOC-based method for signal processing has lately regained the spotlight owing to the achievement of excellent empirical performance in several different domains of application such as pattern recognition (Chandran & Elgar 1991) (Chandran, Carswell, Boashash & Elgar 1997) (Orlic & Dukic 2009) (Mustapha & Dimitrakopoulos 2010), study of machine faults (Benbouzid 2000) (Chow & Tan 2000) (Liang, Iwnicki & Zhao 2013), analysis of electrocardiogram (ECG) (Khadra, Al-Fahoum & Binajjaj 2005) (Martis, Acharya, Lim, Mandana, Ray & Chakraborty 2013) and electroencephalogram (EEG) signals (Muthuswamy, Sherman & Thakor 1999) (Acharya, Sree & Suri 2011), although the main concept has been around for some decades. The basic principle of HOC is briefly introduced here (Mendel 1991).

If a collection of random variables is given as $\{x_1, x_2, \ldots, x_k\}$, their corresponding *kth*-order cumulant can be defined as the coefficient of $\{v_1, v_2, \ldots, v_k\}$

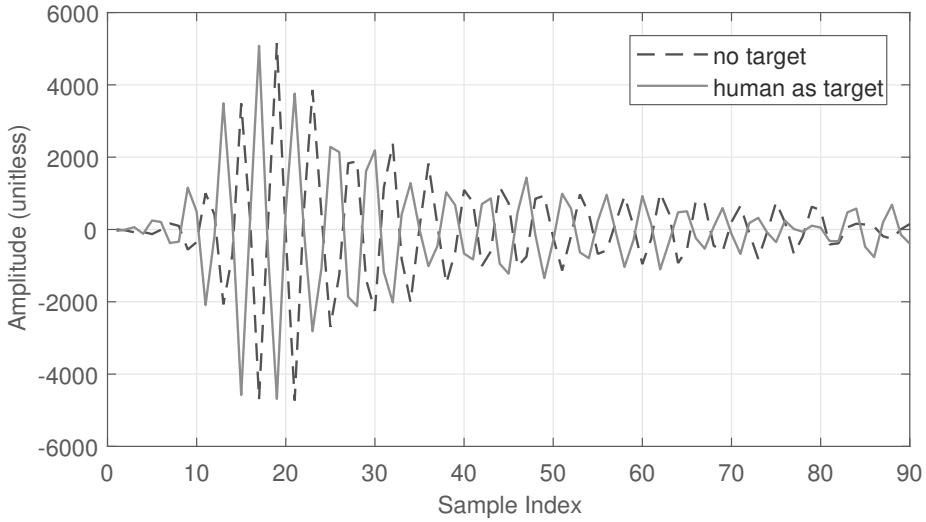
no target
human as target
Amplitude (unitless)
Sample Index
6000
4000
2000
0
-2000
-4000
-6000
0
10
20
30
40
50
60
70
80
90

(a)

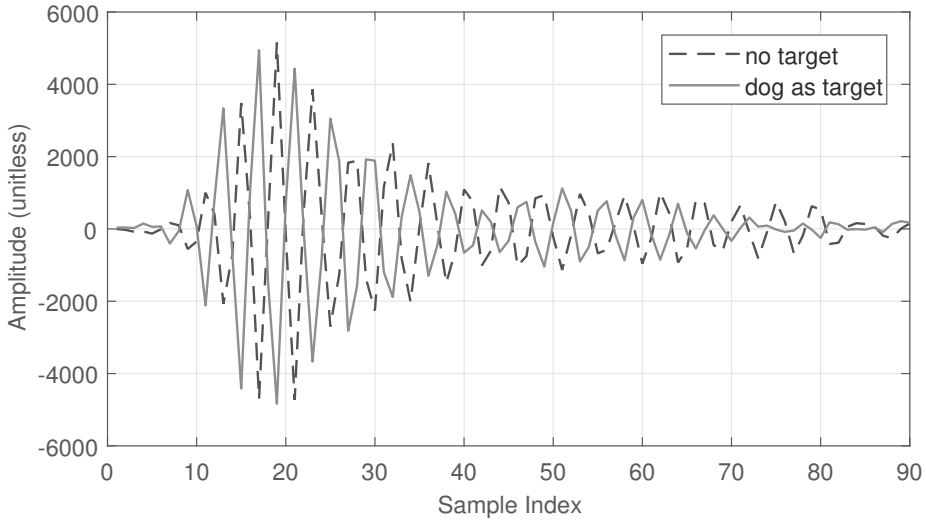
no target
dog as target
Amplitude (unitless)
Sample Index
6000
4000
2000
0
-2000
-4000
-6000
0
10
20
30
40
50
60
70
80
90

(b)

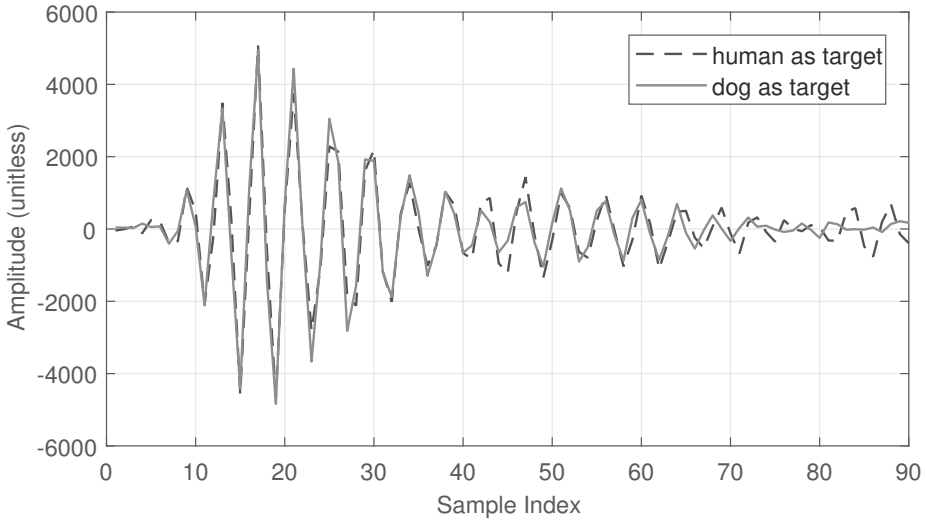

(c)

Figure 4.3: Measured waveform at the receiver under different senarios: (a) no target vs human target, (b) no target vs dog target, (d) human vs dog targets

in the Taylor series expansion of the cumulant-generating function,

$$\psi(v) = \ln E\{exp(jv'x)\} \tag{4.1}$$

where $E[\cdot]$ is the expectation operator, representing the statistics average. The *kth*-order cumulant of x is defined as,

$$cum(x_1, x_2, \ldots, x_k) = (-j)^k [\partial/\partial v_1 \partial v_2 \ldots \partial v_k] \psi(v)\Big|_{v=0} \tag{4.2}$$

When the average of the random variables is non-zero, the expression of the third-order and above are very complicated. Thus, in practice, the zero-mean processing is adopted to the raw signal so that the higher-order cumulant can be simplified. Let $\{x(t)\}$ be a zero-mean of *kth*-order stationary random process. The *kth*-order cumulant of this process is denoted as $C_{kx}(\tau_1, \tau_2, \ldots, \tau_{k-1})$, which is defined for the joint *kth*-order cumulant of the

random variable $x(t)$, $x(t+\tau_1)$, ..., $x(t+\tau_{k-1})$, i.e.,

$$C_{kx}(\tau_1, \tau_2, \ldots, \tau_{k-1}) = cum(x(t), x(t+\tau_1), \ldots, x(t+\tau_{k-1})) \tag{4.3}$$

where τ_1, τ_2, ..., τ_{k-1} are time delays. Following from Equation (4.4) to Equation (4.6), the corresponding second-, third- and fourth-order cumulants of zero-mean $x(t)$ can be expressed as,

$$C_{2x}(\tau) = E\{x(t)x(t+\tau)\} \tag{4.4}$$

$$C_{3x}(\tau) = E\{x(t)x(t+\tau_1)x(t+\tau_2)\} \tag{4.5}$$

$$\begin{aligned} C_{4x}(\tau) = E\{x(t)x(t+\tau_1)x(t+\tau_2)x(t+\tau_3)\} - C_{2x}(\tau_1)C_{2x}(\tau_2-\tau_3) \\ -C_{2x}(\tau_2)C_{2x}(\tau_3-\tau_1) \ - C_{2x}(\tau_3)C_{2x}(\tau_1-\tau_2) \end{aligned} \tag{4.6}$$

For a zero-mean Gaussian random process, the cumulants have the following conclusions,

$$C_{1x} = 0, \ C_{2x} = \sigma^2, \ C_{kx} = 0 \ \ (k \geq 3) \tag{4.7}$$

As indicated in Equation (4.7), if a signal contains additive Gaussian noise, including colored or white noise, the influence of noise can be minimized by using higher-order cumulants which proves the fact that the HOC-based approach is inherently suitable for this case. However, this requires excessive number crunching. In order to extract useful information from higher-order cumulants of non-Gaussian stationary processes, one-dimensional (1-D) slices of multi-dimensional cumulants are often used. This is mainly due to the fact that a 1-D slice of a higher-order cumulant retains all the useful characteristics of the signal. Therefore, computational efficiency can be significantly improved by using 1-D slices. The 1-D slice of a third-order cumulant $C_{3x}(\tau_1, \tau_2)$ can be defined as,

$$C_{3x}(0, \tau) = cum(x(t)\, x(t)\, x(t+\tau)) \tag{4.8}$$

and

$$C_{3x}(\tau,\tau)=cum\left(x\left(t\right)x\left(t+\tau\right)x\left(t+\tau\right)\right) \tag{4.9}$$

If a random process is symmetrically distributed, then its third-order cumulant equals zero whereas some non-symmetrical process has an extremely small third-order cumulant and much larger fourth-order cumulant. The one-dimensional slices of fourth-order cumulant $C_{4x}\left(\tau_1,\tau_2,\tau_3\right)$ is defined as following,

$$C_{4x}(0,0,\tau)=cum\left(x\left(t\right)x\left(t\right)x\left(t\right)x\left(t+\tau\right)\right) \tag{4.10}$$

$$C_{4x}(0,\tau,\tau)=cum\left(x\left(t\right)x\left(t\right)x\left(t+\tau\right)x\left(t+\tau\right)\right) \tag{4.11}$$

$$C_{4x}(\tau,\tau,\tau)=cum\left(x\left(t\right)x\left(t+\tau\right)x\left(t+\tau\right)x\left(t+\tau\right)\right) \tag{4.12}$$

4.3.2 Proposed HOC-based Feature Extraction

Since the HOC of Gaussian signals is statistically zero, HOC-based methods can be used to separate additive mixtures of independent non-Gaussian signals and Gaussian noise (Nikias & Mendel 1993). This feature can be exploited to detect and classify non-Gaussian signals and provide high noise immunity in applications where the signal source is corrupted with Gaussian noise. As previously mentioned, one of the critical hurdles to enable DFS for target recognition in a foliage environment is to enhance the immunity of the system against the noise generated by clutters (trees and their branches). In addition, HOC contains both amplitude and phase information of a signal which is very useful for target classification because distinct features can be extracted from a higher-order domain. Therefore, a HOC-based method is selected in this work due to the fact that it may have a promising potential to reduce false alarm triggering.

In this chapter, the following procedures are used for feature extraction from the received RF signals. Firstly, zero-mean processing needs to be applied for the raw RF signals. In the experiment, using the platform presented in Figure 4.2, only the signals that have been sampled can be extracted at the output and it is impossible to obtain the true values of the HOC. Thus, the zero-mean processing is required to simplify the HOC. This is particularly true for this case, as by no means the average of the received RF signal is zero. Secondly, the fourth-order cumulant is selected because the third-order cumulant of the received RF signal is much smaller than its fourth-order ones. Finally, 1-D slices of fourth-order cumulants are used to extract useful information from the HOC of non-Gaussian stationary processes. It is noted that although different types of 1-D slices of fourth-order cumulants are possible, as shown in Equation (4.10)-Equation (4.12), including radial, vertical, horizontal, diagonal and offset-diagonal. The vertical slice is selected in this work mainly because it can provide a simple but effective way to extract important information from the received signals which improves the accuracy of target classification without a significantly increased computational cost. Consequently, the estimated values of the fourth-order cumulants using 1-D

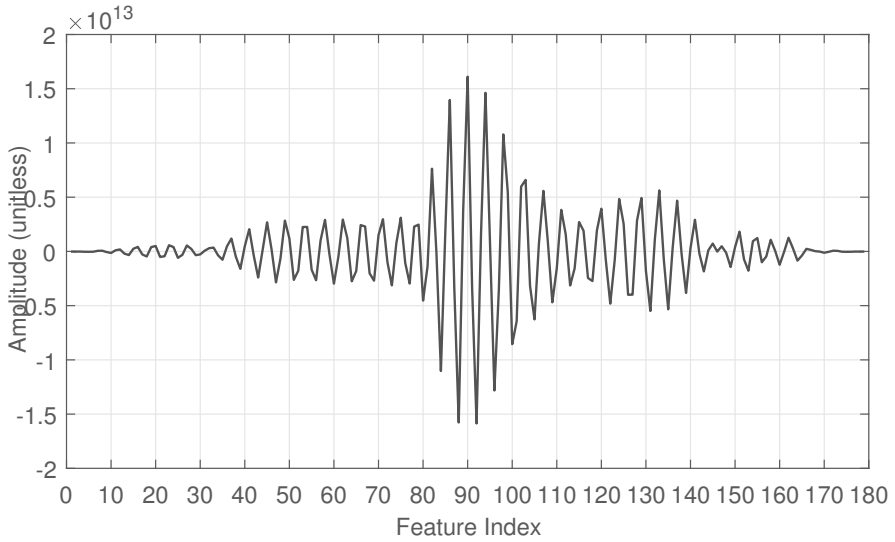

(a)

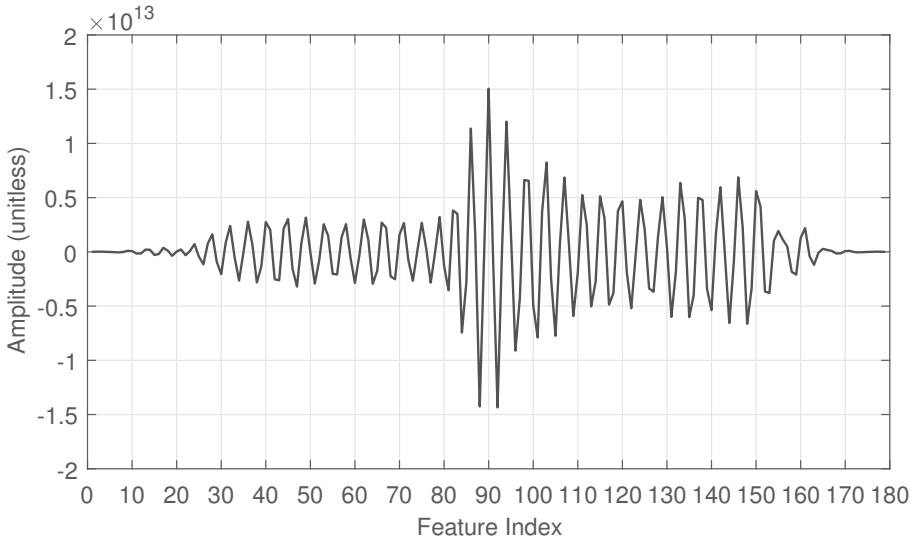

(b)

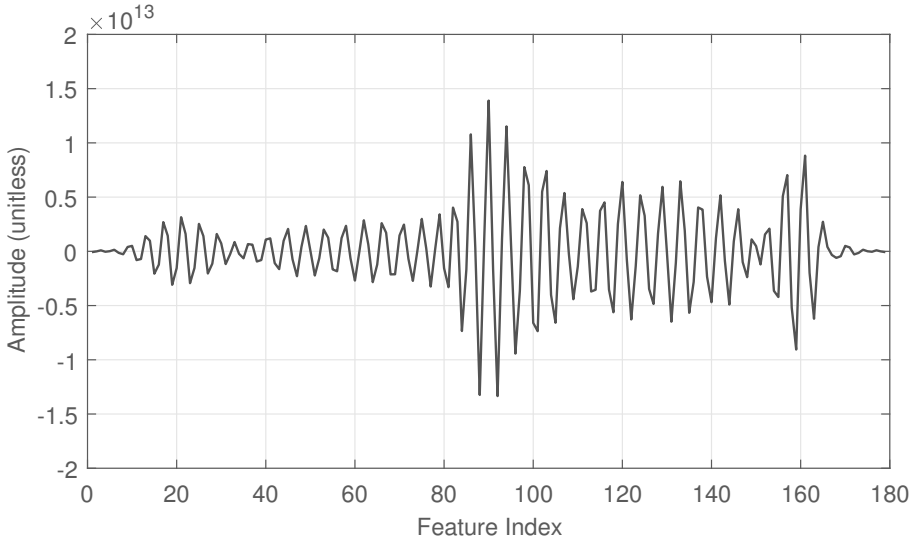

(c)

Figure 4.4: Extracted features using the presented appraoch: (a) no target, (b) human as target, (c) dog as target

vertical slices $\hat{c}_{4x}(0,0,\tau)$ from a finite set of measured data samples $x(1)$, $x(2)$, ..., $x(n)$, can be expressed as,

$$\begin{aligned}\hat{c}_{4x}(0,0,\tau) = \tfrac{1}{N}\sum_{n=1}^{N}\left[x(n)-\hat{m}_{1x}\right]^3\left[x(n+\tau)-\hat{m}_{1x}\right] \\ -\tfrac{3}{N^2}\sum_{n=1}^{N}\left[x(n)-\hat{m}_{1x}\right]\left[x(n+\tau)-\hat{m}_{1x}\right]\sum_{n=1}^{N}\left[x(n)-\hat{m}_{1x}\right]^2\end{aligned} \tag{4.13}$$

where $\hat{m}_{1x}=\frac{1}{N}\sum_{n=1}^{N}x(n)$.

To demonstrate the effectiveness of using the presented HOC-based method, the features of different targets are extracted and plotted in 4.4. Unlike the results in Figure 4.3, the distinct features are shown for the different cases, not only with and without a target but also with human or dog targets.

4.4 Target Classification and Results Discussion

In order to verify the performance of the presented approach for target classification, an SVM classifier is used. The previously obtained data are divided into two types: training and testing, in which the training samples are used to calculate a fitness function so that the classifier can be effectively trained, while the testing samples are used to verify the performance of the sensing system. As a rule of thumb, the more training samples are used, the higher accuracy can be achieved but with an increased computational cost. It is therefore essential to investigate the impact on classification accuracy of different numbers of training samples so that the trade-off between accuracy and complexity can be effectively optimized.

For every target at each location, 110 testing samples are used while the number of samples used for training is varied for evaluation purposes. Thus, there are overall 5 × N training samples, and 550 testing samples are used to fully investigate the trade-off between computational efficiency and

classification accuracy, where N ranges from 10 to 110 with a step of 10. In order to verify the superiority of the HOC-based features, RSS-based ones are also used for comparison. The seven RSS-based features are listed in Table 4.1. The corresponding results in terms of average classification accuracy for all target types are shown in Figure 4.5. As illustrated, using the HOC-based approach does show a distinct advantage over using the RSS-based one. In all cases, the accuracy still can be improved by more than 10%. This is particularly true if a higher number of training samples is used.

Table 4.1: Seven Typical RSS-based Parameters

Energy of *r(t)*	$E_r = \int_{-\infty}^{+\infty} \lvert r(t)\rvert^2 dt$
Maximum amplitude of *r(t)*	$A_{\max} = \max_t \lvert r(t)\rvert$
Mean excess delay	$\tau_m = \int_{-\infty}^{+\infty} t\,\lvert r(t)\rvert^2 dt \Big/ \int_{-\infty}^{+\infty} \lvert r(t)\rvert^2 dt$
RMS delay spread	$\tau_{RMS} = \sqrt{\int_{-\infty}^{+\infty} (t-\tau_m)^2 \lvert r(t)\rvert^2 dt \Big/ \int_{-\infty}^{+\infty} \lvert r(t)\rvert^2 dt}$
Mean of $\lvert r(t)\rvert$	$\mu_{\lvert r\rvert} = \frac{1}{T}\int_T \lvert r(t)\rvert dt$
Standard deviation of $\lvert r(t)\rvert$	$\sigma^2_{\lvert r\rvert} = \frac{1}{T}\int_T \left[\left\lvert r(t) - \mu_{\lvert r\rvert}\right\rvert^2\right] dt$
Kurtosis of $\lvert r(t)\rvert$	$k = \frac{1}{\sigma^4_{\lvert r\rvert} T}\int_T \left[\lvert r(t)\rvert - \mu_{\lvert r\rvert}\right]^4 dt$

Note: *r(t)* is the target waveform and the resolution of the scan waveform is 61 *ps*.

Besides minimizing the number of samples used for training, another serious concern is the reliability of the system. As RF signals can be easily attenuated due to environmental variations, evaluating the impact of the SNR on the classification accuracy would verify the reliability of the designed system. Therefore, additional white noise is added to the original collected data so that the SNR can be effectively varied. To evaluate the robustness of the system, the noise level is changed from 0 dB to 30 dB with a step of 5 dB. During the calculation, there are 350 training samples and 550 testing samples used for each target. The corresponding results are given in Figure 4.6. As illustrated, the HOC-based approach is always better than

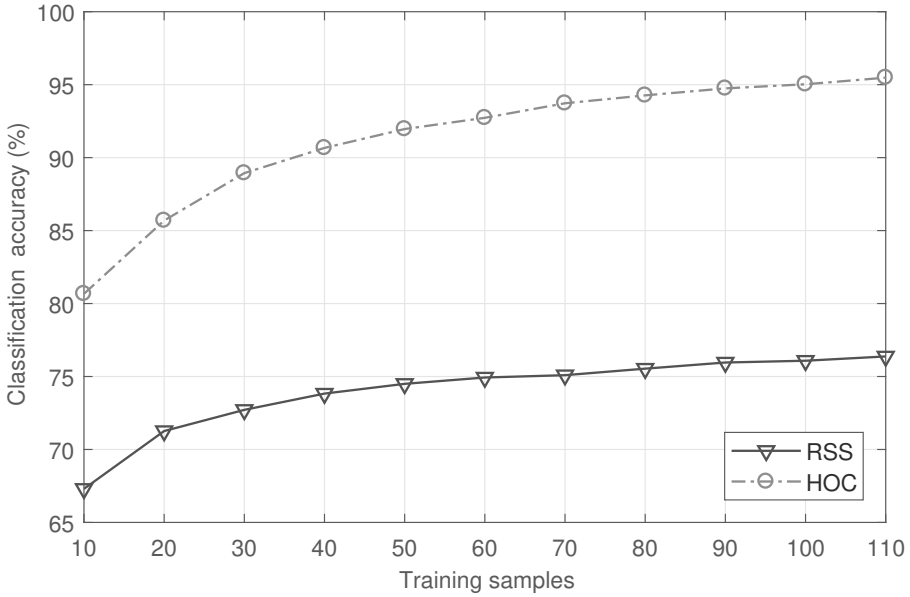

Figure 4.5: Classification accuracy as a function of number of training samples

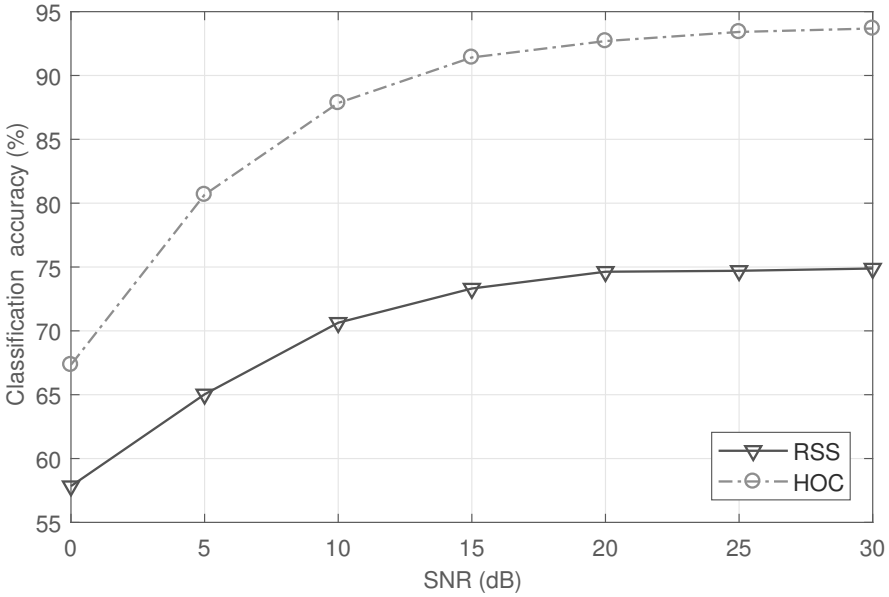

Figure 4.6: Classification accuracy as a function of SNR

the RSS-based one. To demonstrate the improvement of using the presented approach for target detection, the measured classification accuracy using two different methods for feature extractions, namely RSS and HOC, are compared in Table 4.2. Note that, to verify the accuracy of the system in a fairly reasonable way, each experiment is carried out 50 times. The Average row shows the average accuracy rate for all target types.

Table 4.2: Summary of Classification Accuracy using Different Feature Extractions

Target type	Classification rate (%)	
	HOC-based	RSS-based
No target	94.27 ± 0.85	81.56 ± 1.72
Human	90.16 ± 1.12	69.69 ± 1.97
Animal	96.70 ± 1.07	74.17 ± 1.43
Average)	93.71 ± 0.77	75.14 ± 0.93

4.5 Summary

The performance analysis of using DFS technology for target detection in a foliage environment has been investigated in this chapter. To ensure the good classification accuracy, a HOC-based feature extraction algorithm is presented. The performance improvement of using the HOC-based algorithm over the RSS-based one has been observed from the illustrative example. Without using any sensing devices but RF transceivers, a variety of samples have been measured under three different scenarios in a foliage environment, namely no target and with the targets of human and dog, respectively. Using these measured samples along with SVM classifier for target classification, the average accuracy of the HOC-based algorithm is greater than 93.71% while the RSS-based one can only achieve an accuracy of 75.14% under the same scenarios. Furthermore, the impact on classification accuracy due to

the number of training samples and SNR variations are investigated. Based on the results obtained from the illustrative example, we could conclude that the HOC-based algorithm has improved the robustness and is more accurate than the RSS-based one. Therefore, it is likely to be a useful approach for target detection and classification in a high-clutter foliage environment.

Chapter 5

Foliage Penetrating Target Classification with Seasonal Variation based on DEFPA-SVM

Foliage penetrating (FOPEN) has been found to be a critical mission for a variety of applications, ranging from surveillance to military. In the previous chapters, an emerging technology namely DFS has been introduced to the domain of FOPEN. Although the feasibility of using this technology for target detection beneath foliage has been explored to some extent, it is questionable if the same technology can be transferred to a realistic environment. As far as FOPEN is concerned, the impact of seasonal variations on detection accuracy can be severe. To address this concern, in this chapter, an experiment is conducted in four seasons and how to ensure reasonable detection accuracy with seasonal variations is intensively investigated. To fully evaluate the potential of using the DFS for FOPEN, in this chapter we propose a new recognition method using an optimization-based support vector machine (SVM) to recognize targets obscured by foliage in different seasons. To seek the optimal parameters of SVM, a new hybrid differential evolution and flower pollina-

tion optimization algorithm (DEFPA) is developed to determine the optimal parameters for SVM with the highest accuracy and generalization ability. Consequently, the adverse effects on detection accuracy due to variations of weather conditions in four seasons can be accommodated. According to the experimental result, it is shown that the average classification accuracy of the presented approach can be improved under all seasons with ensured robustness.

5.1 Introduction

FOPEN, in particular human detection, has been a long-standing subject of intensive study (Ivashov, Razevig, Sheyko & Vasilyev 2004) (Gallagher & Narayanan 2013) (Aziz, Abdullah & Yusof 2017). In order to effectively solve this problem, a target classification approach using a DFS-based technology is proposed. Previously, the studies of Chapter 3 and Chapter 4 focused on either using the RSS-based or the HOC-based algorithm for FOPEN target classification. Although both approaches can effectively differentiate targets with a low false-alarm probability, deploying the approaches amongst foliage under different weather conditions has not yet been fully explored which makes them infeasible in practice. Therefore, to this date, the detection and recognition of foliage covered targets still has some fundamental issues to be tackled. In particular, the classification accuracy needs to be significantly improved before it can be considered a practical approach.

In an outdoor environment, the classification accuracy can be dramatically degraded by many factors. First of all, most outdoor scenarios are based on NLOS, such as FOPEN. The trunks, branches and leaves of trees can rapidly attenuate the strength of RF signals. As a result, the weak signals that may contain important features of targets are likely to be overwhelmed. Secondly, foliage is an intrinsically time-variant channel environment due to changes of atmosphere and ground conditions. Strong winds could result in moving the branches and leaves of trees and generate a large

amount of time-varying clutter and noise which is quite undesirable. As far as classification is concerned, the extracted features from received RF signals must be not only sufficiently distinctive among different types of target but also robust enough against noise. Finally, different weather conditions and seasons could also affect the performance of the presented approach due to variations of humidity and foliage density. If the classifier were only trained using the datasets obtained in a specific condition, it would be quite difficult to ensure good accuracy. To overcome this issue, it is desirable to train the classifier with more and more datasets. Ideally, all weather conditions under four seasons should be included. The classical SVM classifier has been successfully applied to target classification (Tang, Zhang, Chawla & Krasser 2009) (Muñoz-Marí, Bovolo, Gómez-Chova, Bruzzone & Camp-Valls 2010) (Bahrampour, Ray, Sarkar, Damarla & Nasrabadi 2013) (Geng, Chen, Fu, Bao & Pahlavan 2016). However, its performance is strongly dependent upon the optimized parameters of the SVM. Using an enormous amount of training datasets to obtain the best-optimized parameters for SVM could significantly increase the computational cost. Thus, how to determine the optimal parameters for a classifier in a simple but effective way also needs to be investigated in detail.

In this chapter, IR-UWB signals are utilized for sensing and their high-order cumulants (HOC) described in Section 5.3 are extracted as key features. In addition, a hybrid differential evolution and flower pollination algorithm (DEFPA) is used in conjunction with an SVM to ensure a good classification accuracy achieved in an effective way. To demonstrate the performance of the presented approach, three targets that have a similar physical size, namely a human, a wooden board and an iron cupboard, are used in a foliage environment. A variety of data samples are taken in four seasons with different weather conditions, including sunny, rainy, snowy and foggy. These data samples are then used to extensively verify the performance of the presented approach in terms of accuracy and robustness. In particular, the impact on classification accuracy due to different classifiers, numbers of training samples

and the values of SNR are carefully evaluated. According to the experimental results, an average accuracy of 94% is achieved in terms of human target classification which is similar to other SAR and hybrid-sensor systems.

The rest of this chapter is structured as follow. Section 5.2 introduces the data measurement and collection taken in a foliage environment under four different weather conditions. Section 5.3 presents the basic idea of SVM. In Section 5.4, a differential evolution algorithm, flower pollination optimization algorithm, hybrid DEFPA algorithm and the optimization procedure to the SVM are presented. The experimental results are reported in Section 5.5. Finally, the conclusion is shown in Section 5.6.

5.2 Experimental Setup and Data Collection

To verify the feasibility of the aforementioned approach, in particular, the accuracy of distinguishing between different targets in four seasons with different weather conditions, a variety of data samples have been taken in a foliage environment. The experimental setup is the same as Figure 4.1. The operating frequency of the used IR-UWB transceiver covers from 3.1 to 5.3 GHz with the center frequency at 4.2 GHz. The transceiver is combined with planar elliptical dipole antennas to form a prototype that is used for data collection. In addition, the prototype is connected to a PC so that the collected data can be directly acquired and recorded.

The measurements were performed in a park which contains a mixture of hardwood trees and low-lying undergrowth. As illustrated in Figure 5.1, measurements were performed under four typical weather conditions in different seasons, namely sunny, rainy, snowy and foggy. Consequently, four datasets are generated and used in this work. These datasets were collected in four seasons in 2016. For all measurements, the transceiver is placed at a fixed location at a constant height of 1.5 m above the ground. The distance between the transmitter and the receiver is approximately 20 m in all scenarios. Three target types, including human (target type I), iron cupboard

(target type II) and wooden board (target type III), are employed for classification. The height and weight of the human target are 175 cm and 68 kg, respectively. The dimension of the iron cupboard is 50 cm × 40cm × 140 cm (length × width × height). The size of the wooden board is 60 cm × 180 cm (width × height) and the thickness of the board is 2.5 cm.

To ensure that the experimental setup is appropriate and the prototype is fully functional, a penetration measurement was firstly taken without any placed target. Once the functionality of the prototype is confirmed, different types of target are then placed between a transmitter and a receiver for testing purposes. Since the detection, as well as classification accuracy, may be adversely affected by the selected locations where the target is placed, eight different locations (A, B, C, D, E, F, G and H) are used to ensure that the system can effectively detect and classify the placed target in the entire monitoring area. These locations are summarized in Figure 5.2. To improve the classification accuracy, only the later part with 90 sampling points that contain strong impulse is selected for feature extraction and signal pre-processing is required to remove unwanted waveform.

In order to collect enough data samples for the experiment, at every location, 500 data samples are taken for each type of target under each weather condition. As there are eight different locations, an overall 16,000 data samples of data for each type of target are collected to form a database. These collected data are used for the purpose of target classification as will be explained in detail later on. To illustrate the challenge of target classification using a DFS-based technology, two typical scenarios are used as examples and their corresponding waveforms of the received signals are given. In Figure 5.3, the waveforms measured with different targets are compared with no target under a snowy condition. As can be seen, although it is relatively easy to identify if there is any target placed between transmitter and receiver, it may not be possible to correctly classify its type unless the features from different targets can be extracted in a more distinguished way. For this reason, the higher-order cumulant (HOC) based algorithm is selected for

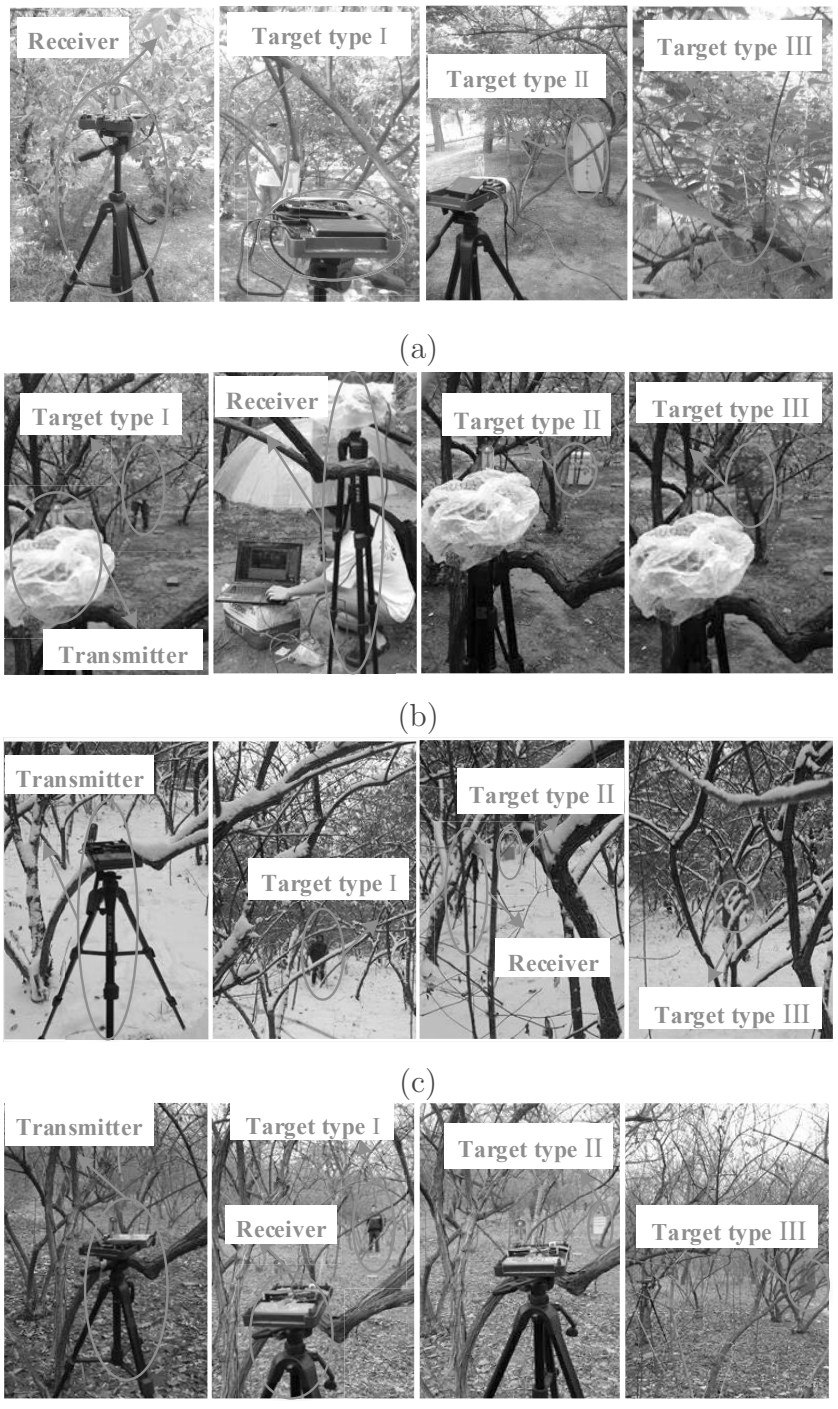

Figure 5.1: Seasonal variations: (a) sunny, (b) rainy, (c) snowy and (d) foggy

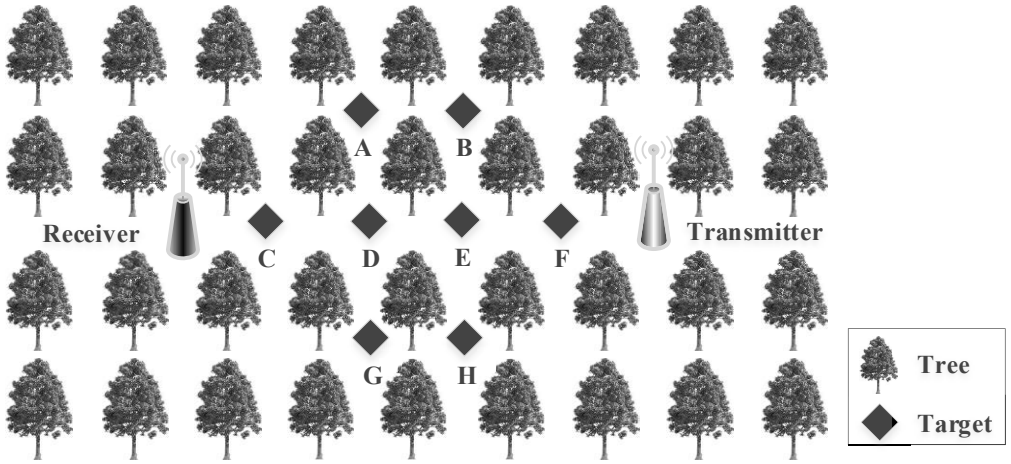

Figure 5.2: Indication of the selected location for data collection in a foliage environment

feature extraction in this work. The detail of this method has been shown in the Section 4.3.

On the other hand, the waveforms measured for the same target (human) with different weather conditions in different seasons are shown in Figure 5.4. As illustrated, the weather condition could have a significant impact on the received signals. Therefore, it indicates that multiple datasets must be created and then used for target classification; otherwise, the classification accuracy is very likely to be poor.

5.3 Support Vector Machine

This section is organized as follows. Section 5.3.1 briefly introduces the basics theory of SVM. Section 5.3.2 presents the classical optimization methods for the selection of the SVM parameters.

5.3.1 Brief Introduction to SVM

SVM has been developed by Vapnik (Vapnik 1998), which is a novel machine learning method based on statistical learning theory (Vapnik 2013). Based on

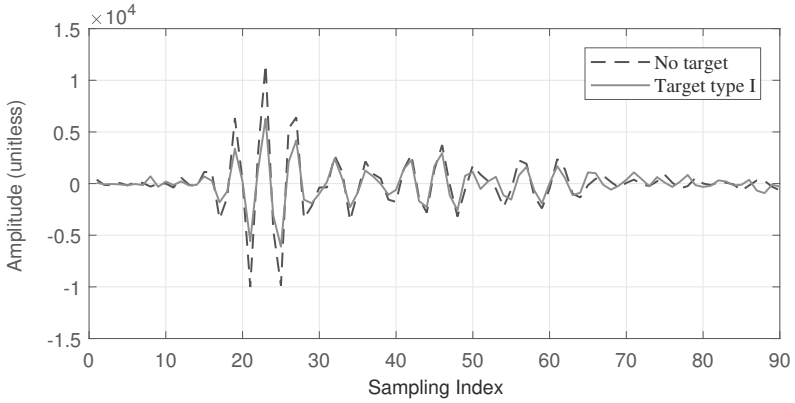

(a)

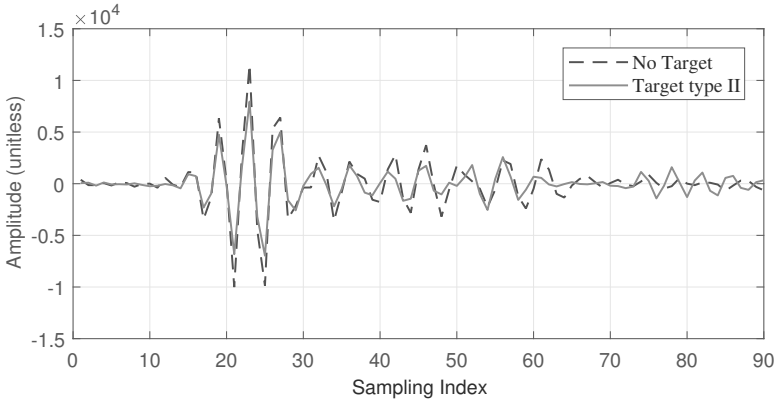

(b)

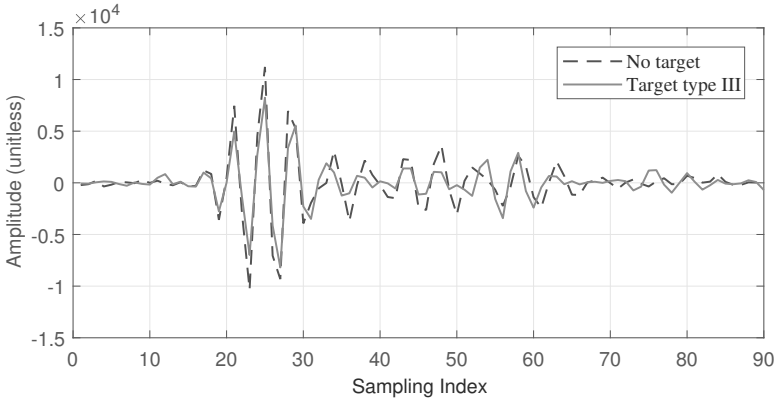

(c)

Figure 5.3: Measured waveform with the different types of target under snowy conditions: (a) no target vs target type I, (b) no target vs target type II, (c) no target vs target type III

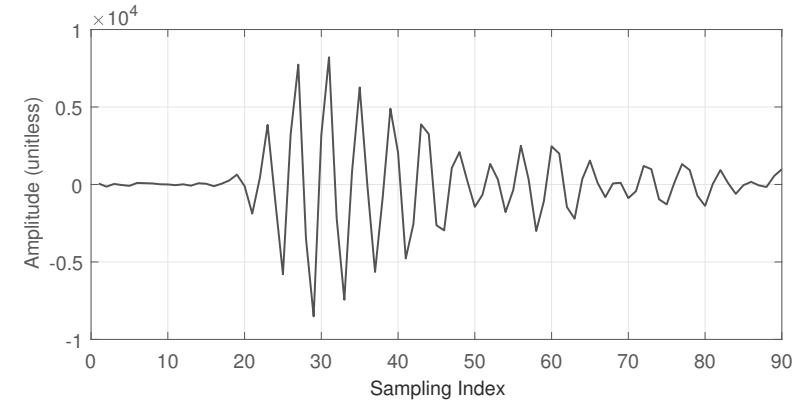
×10^4
1
0.5
0
-0.5
-1
Amplitude (unitless)
0
10
20
30
40
50
60
70
80
90
Sampling Index

(a)

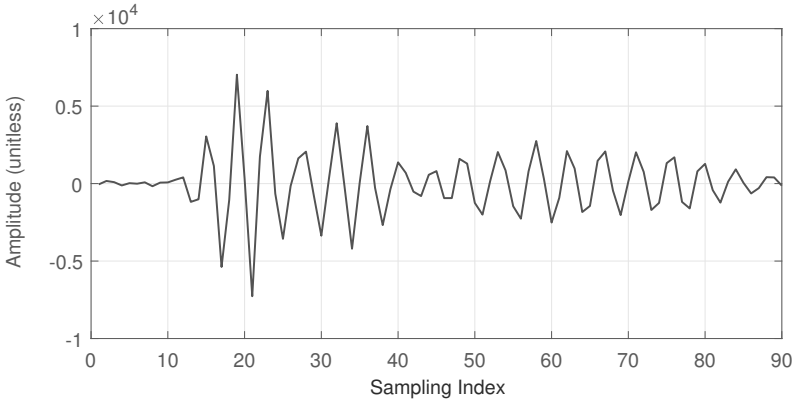
×10^4
1
0.5
0
-0.5
-1
Amplitude (unitless)
0
10
20
30
40
50
60
70
80
90
Sampling Index

(b)

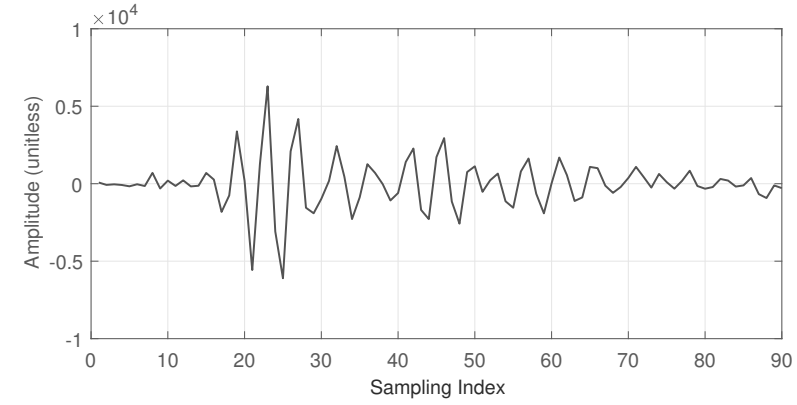
×10^4
1
0.5
0
-0.5
-1
Amplitude (unitless)
0
10
20
30
40
50
60
70
80
90
Sampling Index

(c)

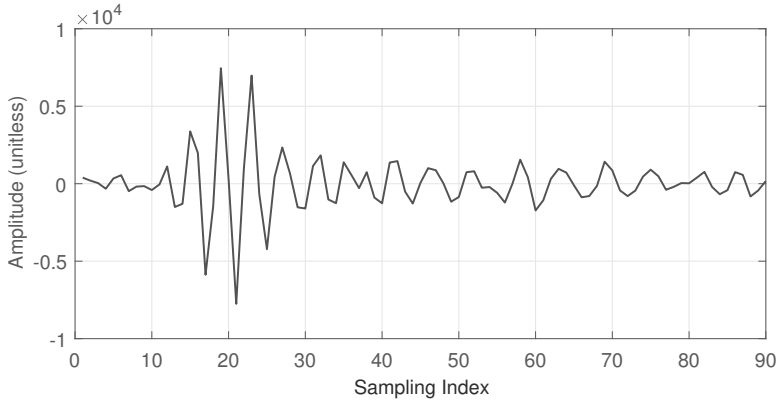

(d)

Figure 5.4: Measured waveform with a human target under different weather conditions: (a) sunny, (b) rainy, (c) snowy and (d) foggy

the Structural Risk Minimization (SRM) principle (Gunn et al. 1998), which has been shown to be superior to traditional Empirical Risk Minimization (ERM) principle (Cortes & Vapnik 1995), SVM can successfully overcome the classification problems of over-fitting, failing local minimum and low-convergence rate existing in the network and does well in the case of small sample size and high dimension.

SVM is a learning machine originally for solving linearly separable cases by finding an optimal separating hyperplane that separates two different classes which can be extended for solving linearly non-separable cases. If two classes are linearly separable, using the following function, an optimal hyperplane can be found to separate them.

$$f(x) = \langle w \cdot x \rangle + b = 0 \tag{5.1}$$

where w, x and b denote the weight vector, input vector and bias term, respectively. The terms w and b are used to define the location of the optimal hyperplane which can be found by solving the following constrained

optimization problem:

$$\begin{aligned} &Minimize \quad \tfrac{1}{2}\|w\|^2 \\ &Subject\ to \quad y_i \langle w \cdot x_i + b \rangle \geq 1, i = 1, 2, \cdots, N \end{aligned} \tag{5.2}$$

where $y_i \in \{-1, +1\}$ is the set of class labels, if $\{x_i, y_i\}^N{}_{i=1}$ is the set of training datasets. However, the classes involved in most practical problems are not separable. In this case, the SVM classifier is obtained by solving the following optimization problem:

$$\begin{aligned} &Minimize \quad \tfrac{1}{2}\|w\|^2 + C\sum_{i=1}^{N}\xi_i \\ &Subject\ to \begin{cases} y_i \langle w \cdot x_i + b \rangle \geq 1 - \xi_i, i = 1, 2, \cdots, N \\ \xi_i \geq 0, i = 1, 2, \cdots, N \end{cases} \end{aligned} \tag{5.3}$$

where ξ_i are slack variables that allow the SVM to tolerate mis-classifications and C is the penalization parameter which is used to control the trade-off between minimized training errors and model complexity. Using the Lagrangian multipliers algorithm, the aforementioned optimization problem can be transformed into a dual quadratic optimization problem, that is:

$$\begin{aligned} &Maximize \quad \sum_{i=1}^{N}\alpha_i - \tfrac{1}{2}\sum_{i,j=1}^{N}\alpha_i\alpha_j y_i y_j (x_i \cdot x_j) \\ &Subject\ to \quad \sum_{i=1}^{N}\alpha_i y_i = 0, C \geq \alpha_i \geq 0, i = 1, 2, \cdots, N \end{aligned} \tag{5.4}$$

By solving the dual optimization problem, the linear decision function can be created as:

$$f(x) = sign\left(\sum_{i=1}^{N}\alpha_i y_i (x_i, x) + b\right) \tag{5.5}$$

In order to use an SVM in a non-linear classification, the kernel function $K(x_i, x)$ needs to be determined. The value of $K(x_i, x)$ equals $\varphi(x_i) \cdot \varphi(x)$, where $\varphi(\cdot)$ is the transformation function which takes the input data into high-dimensional feature space. Then, the non-linear decision function is

described as below:

$$f(x) = sign\left(\sum_{i=1}^{N} \alpha_i y_i K(x_i, x) + b\right) \tag{5.6}$$

In SVM, the kernel function plays a significant role because it is used to map the input data into a higher dimensional feature space to make the classification problem becomes linearly separable. There are many kinds of SVM kernels such as the radial basis function kernel, linear kernel, the polynomial kernel and so on. Since radial basis function kernel has excellent non-linear classification ability, in this chapter, the radial basis function (RBF) kernel function $K(x_i,\ x) = exp\left(-\|x_i - x\|^2/2\sigma^2\right)$ is selected to construct the SVM, where σ denotes the width of the RBF kernel function. Note that both the width of the RBF kernel function σ and the penalization parameter C are user-determined parameters.

As previously described, the SVM is an intrinsically binary classifier. However, in practice, most cases are multi-class. Several unique approaches have been presented in the literature to solve multi-class problems using a binary classifier (Melgani & Bruzzone 2004) (Hsu & Lin 2002*a*) (Madzarov, Gjorgjevikj & Chorbev 2009), such as the one-against-all (OAA), the one-against-one (OAO) and binary tree architecture (BTA) strategy. In the OAA strategy, K two-class SVM classifiers are generated for a problem with K-class where each one is trained to distinguish a class from the remaining classes. The OAO strategy generates $K(K-1)/2$ two-class SVM classifiers to construct N-class classifiers where each one is trained on data from two classes only. The BTA strategy uses multiple SVM classifiers arranged in a binary tree structure where each node makes a binary decision by an SVM classifier. As a result, it only needs $K-1$ SVM classifiers for K-class classification problem. For this reason, a BTA-based approach is adopted to construct the recognition model of target types.

5.3.2 Parameters Optimization of SVM

Nowadays, SVM has been successfully applied to numerous pattern recognition problems such as fault diagnosis (Chenglin, Xuebin, Songlin & Ting 2011), electrocardiogram signal classification (Melgani & Bruzzone 2004), face detection (Khan, Ksantini, Ahmad & Boufama 2012) and human action recognition (Zhang & Tao 2012). However, in those applications, the selection of some critical parameters could have a great influence on the performance of SVM but it is very difficult to select due to the lack of the corresponding theoretical basis. Therefore, the selection of the optimal parameters is an important issue to obtain good performance for solving pattern recognition problems with SVM.

In the past several years, the parameters optimization of SVM has drawn great attention. The simplest method for the selection of the SVM parameters is Grid algorithm (Hsu & Lin 2002*b*) which finds the optimal parameters values that produce the highest classification accuracy rate by setting the upper and lower limits (search interval) for parameters and the jumping interval in the search. But the performance of grid search is sensitive to the setting of the search interval for each parameter. Too large a search interval is time-consuming while too small a search interval might render a satisfactory outcome impossible. In addition to the commonly adopted grid search technique, many other optimization approaches have been proposed in the literature (Keerthi 2002) (Duan, Keerthi & Poo 2003) (Gold & Sollich 2003) (Adankon & Cheriet 2007) (Li & Tan 2010). However, owing to the non-convexity of the generalization bounds, these methods may be prone to local optimality and cause instabilities. Additionally, these methods are sensitive to the initial point and require that the kernel functions and the bounds of generalization error have to be differentiable with respect to the SVM parameters. To overcome these limitations, some intelligent evolutionary algorithms (EA) such as genetic algorithm (GA) (Cohen, Hilario & Geissbuhler 2004), artificial immunization algorithm (AIA) (Aydin, Karakose & Akin 2011), particle swarm optimization (PSO) (Lin, Ying, Chen & Lee 2008), covariance matrix adap-

tation evolution strategy (CMA-ES) (Friedrichs & Igel 2005) and ant colony optimization algorithm (ACO) (Huang 2009) have been used in SVM to improve the global search ability of the choice of parameter values. Although EAs are generally good at finding near-optimal solutions to problems, they are not well suited to perform finely tuned search and thus not guaranteed to find the global optimum solution to a problem.

From the aforementioned literature review, it can be seen that methods for obtaining the optimal parameters in the SVM still remains a challenging task. In view of this, a novel SVM parameter optimization algorithm is given in the next section.

5.4 DEFPA-SVM Classifier

This section presents the parameters optimization of SVM by proposed hybrid DEFPA. Section 5.4.1 and Section 5.4.2 present a brief introduction of the flower pollination algorithm and differential evolution algorithm respectively. Section 5.4.3 introduces the proposed DEFPA algorithm to optimize the SVM parameters. Finally, Section 5.4.4 provides the target recognition model in foliage under different weather conditions.

5.4.1 Flower Pollination Algorithm

Pollination is a phenomenon which plays an extremely significant role in the sexual reproduction of plants. It can be achieved by both self-pollination and cross-pollination. The latter means pollination can occur from different plants while the former is the fertilization of one flower, from either the same flower or different flowers of the same plant that often occurs when there is no reliable pollinator available. This process of transfer can occur by both abiotic and biotic agents. Depending on the distance that pollen is transferred, pollination can be considered as either global or local one. Pollinators like birds, insects, and bats that fly over these long distances with varying distance steps and this phenomenon can be simulated by using

Lévy flight patterns (Yang, Karamanoglu & He 2013) .

Approximately 10% of all plants are subject to pollination by abiotic means and it depends on the movement of non-living natural elements like wind and water. The rest of the plants are dependent on biological agents to accomplish pollination. Examples of such agents include insects (like honeybees), birds (like hummingbirds) and mammals (like fruit bats). In pollinating insects, flower constancy can be observed, in which a certain species of pollinators develops a trait to only collect nectar from a specific species of plants. These pollinators tend to visit exclusive certain flower species while bypassing other flower species. Such flower constancy may have evolutionary advantages because this will maximize the transfer of flower pollen to the same or specific plants, and thus maximizing the reproduction of the same flower species. Such flower constancy may be advantageous for pollinators as well because they can be sure that nectar supply is available with their limited memory and minimum cost of learning or exploring. Rather than focusing on some unpredictable but potentially more rewarding new flower species, flower constancy may require minimum investment cost and more likely guaranteed intake of nectar.

Inspired by this flower pollination phenomenon, the FPA was first presented in (Yang, Karamanoglu & He 2014) . A distinct advantage of this algorithm is that it very well balances the defined goals between local and global optimization. The behavior of pollination can be summarized using the following four rules:

Rule 1: Biotic cross-pollination can be considered as a process of global pollination and pollen-carrying pollinators move in a way that obeys *Lévy* flights.

Rule 2: Abiotic and self-pollination can be considered as a process of local pollination.

Rule 3: Pollinators, such as insects, can develop flower constancy which is equivalent to a reproduction probability that is proportional to the similarity of the two flowers involved.

Rule 4: The interaction or switching between local and global pollination can be controlled by a switch probability $p \in [0, 1]$ with a slight bias towards local pollination.

To model these rules, the following equations are developed. In the step of global pollination, gametes of flowers can travel over a long distance, if they are carried biotically. Therefore, Rules 1 and 3 can be represented mathematically as:

$$x_i^{t+1} = x_i^t + \gamma L\left(\lambda\right)\left(x_i^t - g_*\right) \tag{5.7}$$

where x_i^t is the pollen i or solution vector x_i at generation t, and g_* is the current best solution found among all solutions for the current generation. Here, γ is a scaling factor to control step size. In addition, $L\left(\lambda\right)$ is the parameter that corresponds to the strength of the pollination, which also essentially affects the step size. Since insects may move over a long distance with various distance steps, a *Lévy* flight can be used to mimic this characteristic efficiently. That is, we draw $L > 0$ from a *Lévy* distribution.

$$L \sim \frac{\lambda\Gamma\left(\lambda\right)\sin\left(\pi\lambda/2\right)}{\pi}\,\frac{1}{s^{1+\lambda}},\ \left(s \geq s_0 > 0\right) \tag{5.8}$$

where $\Gamma\left(\lambda\right)$ is the standard gamma function. Its distribution is valid for large steps $s > 0$. In order to model local pollination, both rules 2 and 3 can be represented as:

$$x_i^{t+1} = x_i^t + \epsilon\left(x_j^t - x_k^t\right) \tag{5.9}$$

where x_j^t and x_k^t are pollen of the same plant species but from different flowers, which represent ower constancy with local pollination. Mathematically, if x_j^t and x_k^t come from the same species or are selected from the same population, this would become a local random pollination if ϵ is drawn from a uniform distribution in [0, 1]. Though pollination activities can occur at all scales, both local and global, adjacent flower patches or nearby flowers are more likely to be pollinated by local flower pollen than those far away. In order

to mimic this, Rule 4 or the proximity probability p can be used to switch between common global pollination and intensive local pollination.

5.4.2 Differential Evolution

Differential Evolution (DE) algorithm has been introduced by Storn and Price in (Storn & Price 1997). DE algorithm is a simple yet powerful stochastic population-based search method successfully applied in global optimization problems and uses vector differences for perturbing the vector population. This algorithm includes three important operations: mutation, crossover and selection, and it utilizes the three operators to evolve from randomly generated initial population to final individual solution. Mutation and crossover are used to generate new vectors (trial vectors) and selection is then used to determine whether the new generated vectors can survive the next generation. In short, the procedure of the DE works as follows:

- **Initialization**

DE starts with a population consisting of N D-dimensional vectors which can be represented as:

$$X_{i,G} = x^1_{i,G}, \ldots, x^D_{i,G}, i = 1, \ldots, N \tag{5.10}$$

where i index denotes the population and G denotes the generation of population. These vectors are randomly selected on the intervals $[x_{j,L}, x_{j,U}]$. During the evolution, each of the N vectors undergoes mutation, crossover and selection operations.

- **Mutation Operation**

The mutation operator can not only enhance the diversity of solution vectors but also improve the exploration capability of solution space for the DE algorithm. For each target vector $X_{i,G}$ at the generation G, its associated

mutant vector $V_{(i,G)} = v^1_{(i,G)}, \ldots, v^D_{(i,G)}$ can be generated according to the following equation:

$$V_{i,G} = X_{best,G} + F \cdot (X_{r^i_1,G} - X_{r^i_2,G}) \tag{5.11}$$

where F is the mutant factor for scaling the difference vector and the indicates $r^i_1, r^i_2 \in [1, 2, \ldots, N]$ are randomly selected integers that must be different from each other and also different from the running index i. Here, $X_{best,G}$ is the best individual vector with the best fitness value in the population at generation G.

- **Crossover Operation**

After the mutation phase, crossover operation is applied to each pair of the target vector $X_{i,G}$. For each mutant vector $V_{i,G}$, a trial vector $U_{i,G} = \left\{u^1_{i,G}, \ldots, u^D_{i,G}\right\}$ is obtained via the following equation:

$$u^j_{i,G} = \begin{cases} v^j_{i,G}, & if\ \ (rand_j\,[0,1) \leq CR)\ \ or\ \ (j = j_{rand}) \\ x^j_{i,G}, & otherwise \end{cases} \tag{5.12}$$

where $i = 1, 2, \ldots, N$ and $j = 1, 2, \ldots, D$. Here, the crossover rate CR is a user-specified constant within the range $[0, 1)$ and the index j_{rand} is a randomly chosen integer in the range $[1, D]$.

- **Selection Operation**

The selection operation selects the better individual from the target vector $X_{i,G}$ and the trial vector $U_{i,G}$ in terms of their cost value calculated by the objective function $f(\cdot)$. In the case of minimization problems, the selected vector can be created as:

$$X_{i,G+1} = \begin{cases} U_{i,G}, & if\ f(U_{i,G}) \leq f(X_{i,G}) \\ X_{i,G}, & otherwise \end{cases} \tag{5.13}$$

The above three operations mutation, crossover and selection are repeated over the course of evolution until some specific termination criteria are satisfied. In addition, there are four control parameters in DE, i.e., the population size N, the mutation factor F, crossover rate CR and the maximum number of generation.

5.4.3 Parameters Optimization using DEFPA-SVM

In this work, we employ an RBF kernel function in the SVM to discover the optimal solution. Two significant parameters of the RBF applied in SVM, C and σ, have to be set appropriately. Parameter C is the cost of the penalty which determines the classification outcome. For example, if C is too large, then the classification accuracy rate is very high in the training stage but very low in the testing stage; if C is too small, then the classification accuracy rate is unsatisfactory, making the model useless. Parameter σ controls the width of the RBF kernel function which influences the partitioning outcome in the feature space. An excessive value for parameter σ leads to over-fitting, while a disproportionately small value results in under-fitting.

Since the selection of both C and σ-values could have a great influence on the performance of SVM, it is important to find an optimized solution for these parameters in an effective way. FPA is able to deal with an optimization issue on a large scale with relatively fast convergence but the method has a low convergence rate and sometimes is easy to trap into local optimum because of pollen diversity loss. DE algorithm improves the population diversity of candidate solutions over several generations in order to reach an optimal solution. To exploit the advantages of the high speed of FPA and the exploration ability of DE, a hybrid differential evolution and Flower pollination algorithm (DEFPA) is proposed to select the parameters of SVM. The basic steps used to determine the parameters of the SVM by means of DEFPA are explained below and the flow chart of this algorithm is shown in Figure 5.5.

Step 1: Initialization. In this step, a population of pollen with random solutions (C and σ-parameters for SVM) is initialized first. Then, original values for other important parameters such as the size of the initialized population N, switch probability p, the mutation factor CR and the maximum generation number $G_{\max}$ are defined.

Step 2: Evaluation of fitness function. The fitness function is used to evaluate the quality of every solution. It is based on the classification error of an SVM classifier which is defined as follows:

$$fitness = 1 - \frac{N_t}{N_t + N_f} \tag{5.14}$$

where N_t and N_f denote the number of true and false classifications, respectively.

Step 3: Global vs local optimization. Suppose $rand \in [0, 1]$ is a random number for each solution x_i and p is the switch probability. If $(rand < p)$, a new solution needs to be determined using Equation (5.7) and Equation (5.8) for global optimization; otherwise, the local optimization needs to be conducted using Equation (5.9). It is noted that each new solution generated in this step must be evaluated and if their fitness values are better than the initial ones, the results must be updated.

Step 4: Perform DE operators according to Equation (5.11) - (5.13) for all the updated solutions obtained by step 3.

Step 6: Update the global best solution of the entire population.

Step 7: Step 3 keeps executing until the predetermined maximum number of generations $G_{\max}$ is reached. Finally, the global optimal values of C and σ can be obtained for the SVM classifier.

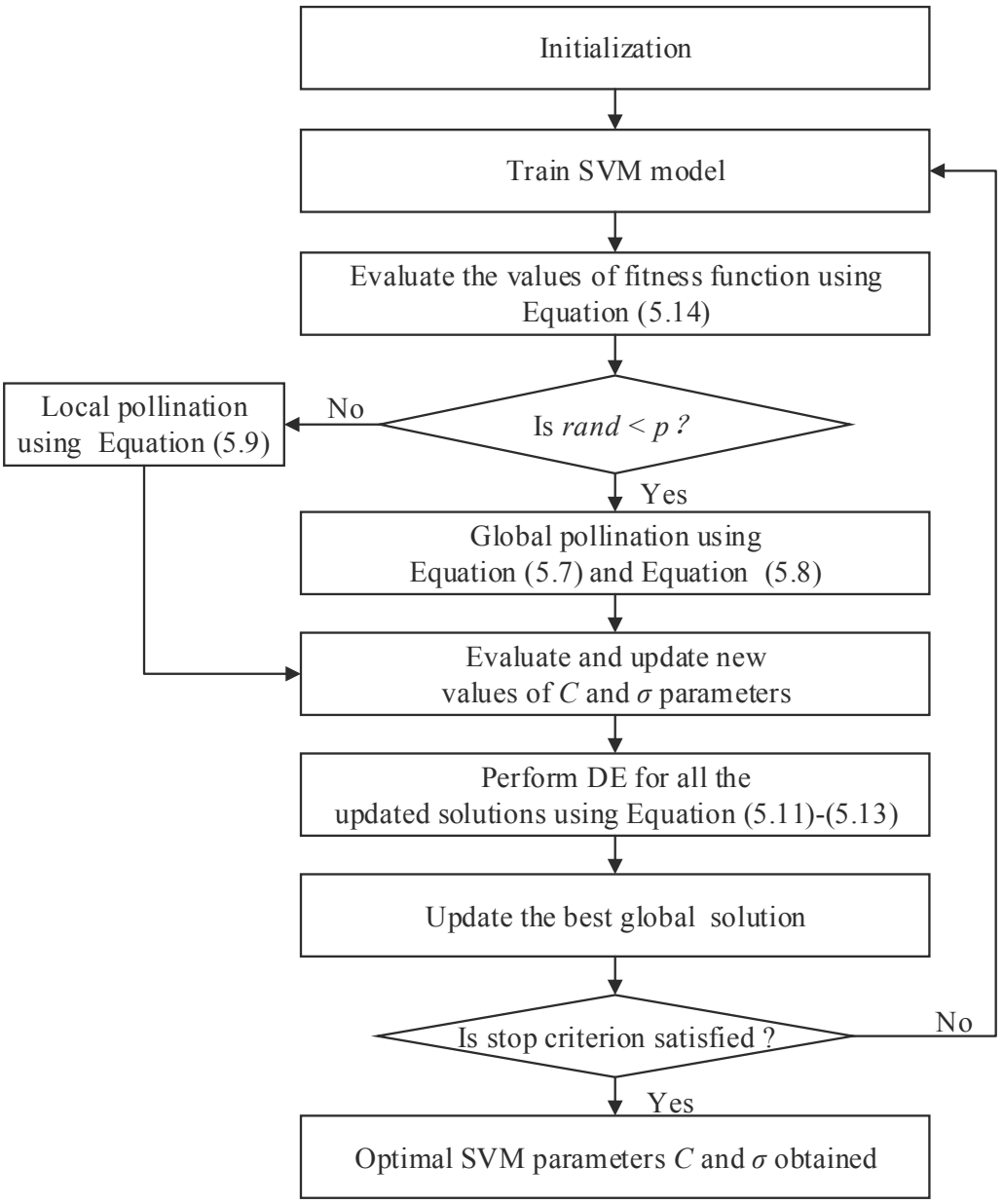

Figure 5.5: The flow chart of parameters optimization using the presented DEFPA-SVM

5.4.4 Target Classification using the Presented Model

The different types of targets can be treated as different classification labels. The presented model used in this work is shown in Figure 5.6.

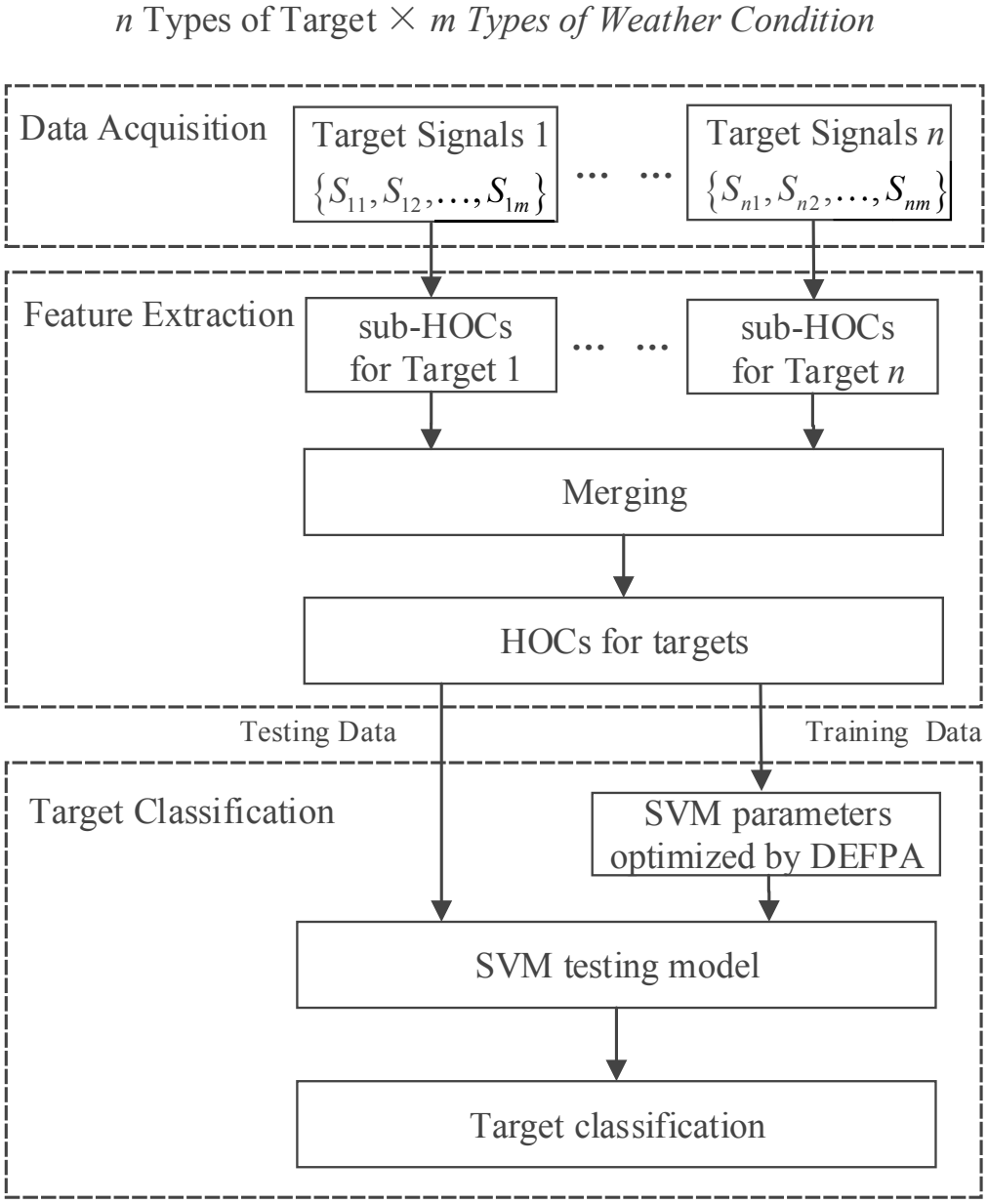

Figure 5.6: The presented classification model

As can be seen, this model is divided into three stages: data acquisition, feature extraction and parameters optimization plus target classification. The design flow of this model is briefly given in this section. If n types of target need to be classified under m types of weather condition, the size of the overall scenarios needing to be considered is $n \times m$. In our case, 16 different scenarios need to be taken into consideration. In the data acquisition stage, identical numbers of data samples are collected for each scenario. Based on these collected samples, the distinctive features from each scenario are extracted using the HOC-based algorithm. Once sufficient features are gained for each scenario, these features are then merged to form databases that can be used for target classification. As four types of targets need to be classified, four databases are required. It is noted that an identical number of features is used for each merged database. In the target classification stage, using the randomly selected training data from the merged databases, the parameters of the SVM classifier are optimized by means of the presented DEFPA. Once the optimization of these parameters is accomplished, the classifier should be able to recognize different types of targets using the previously created test data. As will be shown in the next section, using this model the type of detected target can be classified with good accuracy even under different weather conditions.

5.5 Experimental Results and Discussions

In this section, we make extensive experiments to show the effectiveness of proposed DEFPA-SVM target recognition model. Section 5.5.1 presents the classification results and fitness performance of our proposed method. In Section 5.5.2 and Section 5.5.3, we discuss the results of our algorithm by comparing it with reference methods.

5.5.1 Performance Analysis for the Proposed Model

In this section, we evaluate the performance of the previously proposed method for sense-through-foliage target detection and recognition. In this work, the features of the received signals are extracted using the HOC-based algorithm according to Equation (4.13), so that the impact on detection accuracy due to unwanted clutters can be minimized. To illustrate the effectiveness of using the HOC-based method for feature extraction, the two scenarios that are previously used for waveform generation in Figure 5.3 and Figure 5.4 are used again, in Figure 5.7 and Figure 5.8. As illustrated, there are 179 extracted features used in this project. Then, the proposed DEFPA-SVM classifier is used to classify and recognize the target types.

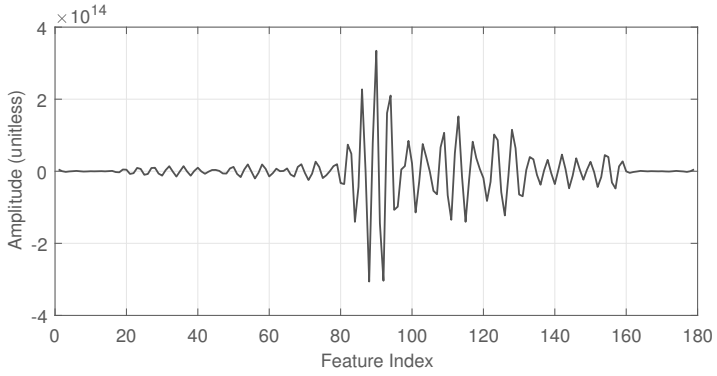

(a)

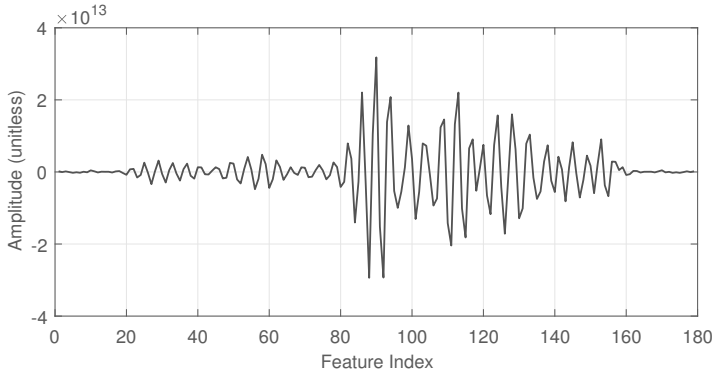

(b)

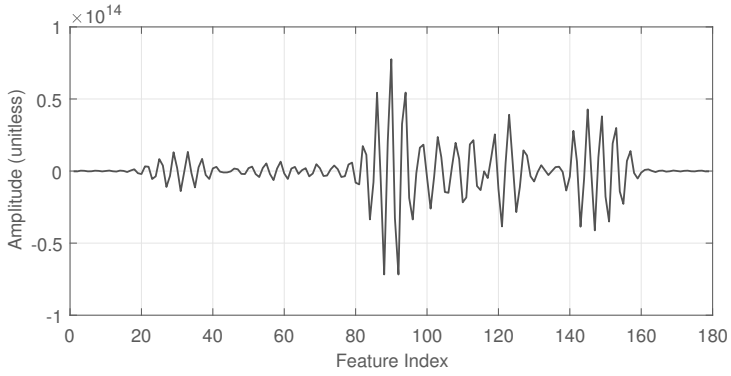

(c)

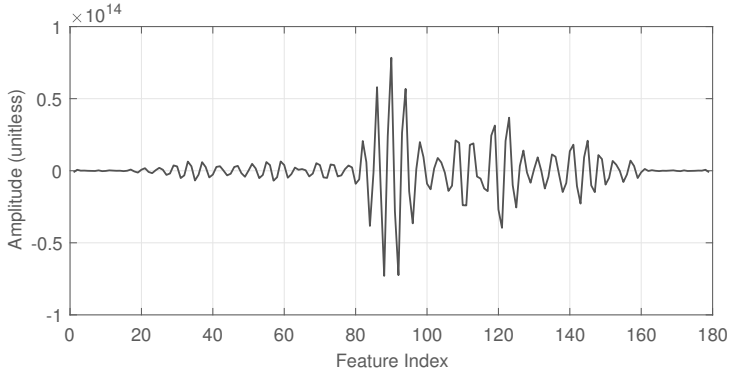

(d)

Figure 5.7: Extracted features using the presented approach under snowy weather: (a) no target, (b) target type I, (c) target type II and (d) target type III

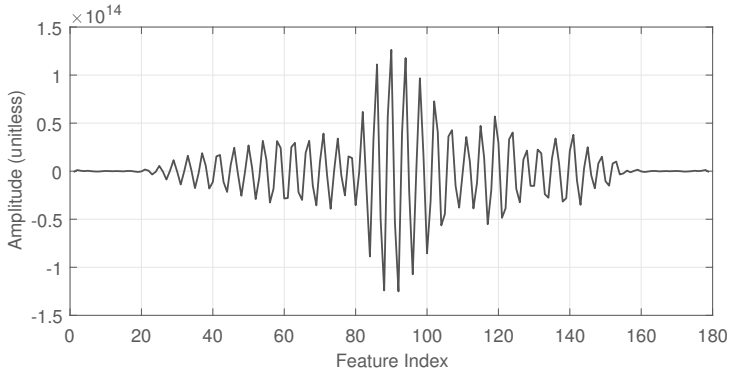

(a)

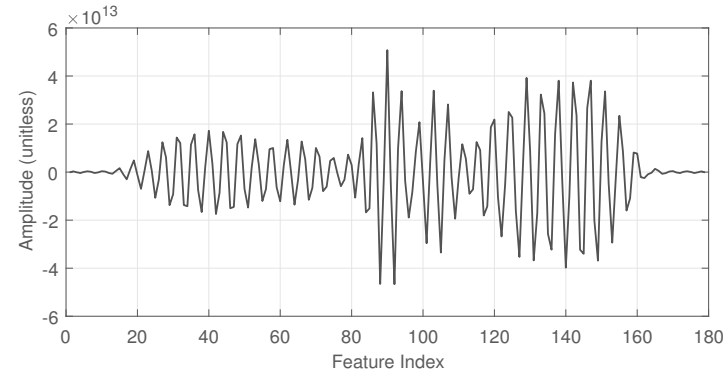

(b)

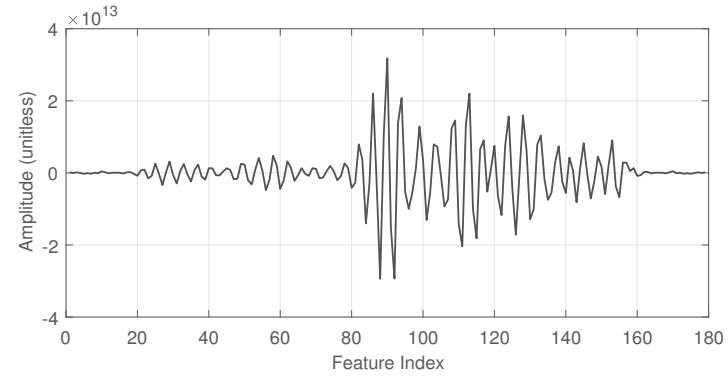

(c)

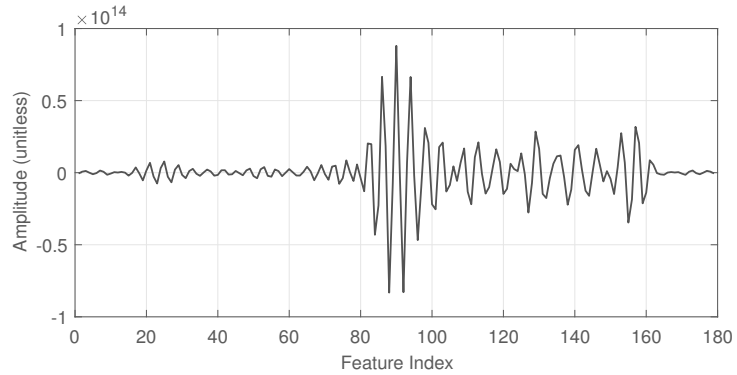

(d)

Figure 5.8: Extracted features of type I target with different weather conditions: (a) sunny, (b) rainy, (c) snowy and (d) foggy

The data obtained in Section 5.2 are divided into two categories: training and testing datasets, in which the training datasets are used to calculate the fitness function and train the DEFPA-SVM classifier while the testing datasets are mainly used to evaluate the performance of the classification model. Under every weather condition, from the created dataset 120 data samples are randomly selected for each target type which indicates that a total of 1920 data samples are used, as four types of target need to be classified under four different weather conditions. It is worthwhile to mention that, once data samples are used for training, they are then removed from the overall database. Consequently, it is ensured that no same data samples are used for both training and testing purposes which makes the evaluation results more meaningful. To form the required testing dataset, 160 data samples are randomly selected from each target type for the same weather condition. Consequently, overall 640 data samples are used to test each target type with different weather conditions.

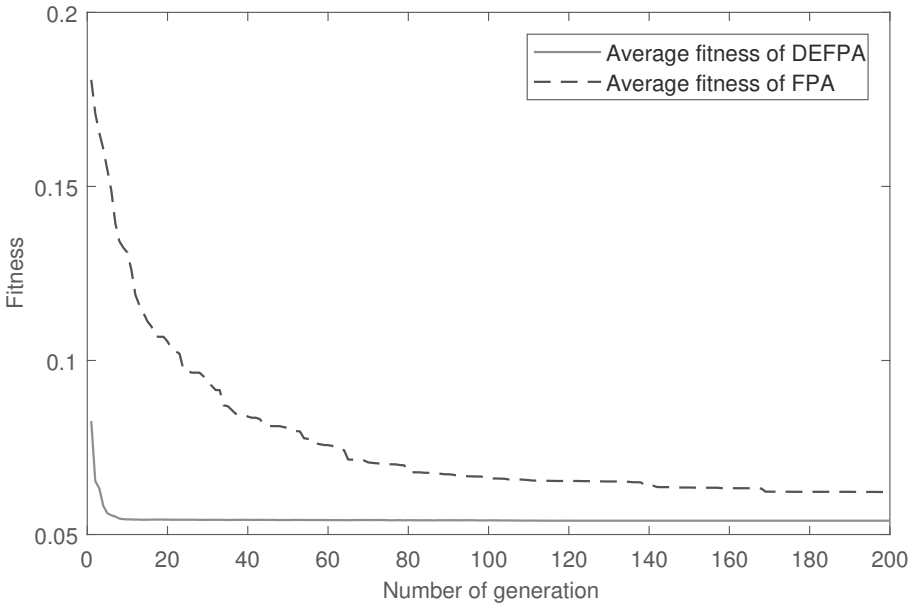

Figure 5.9: Fitness performance for the proposed hybrid DEFPA and classical FPA algorithm.

In the context of optimization of the parameters of SVM, in this experiment, we first provide the performance comparison between the hybrid DEFPA and classical FPA. The population size N for both DEFPA and FPA is 20 and the maximum evolution generation is set to 200. According to the preliminary parametric studies, the following values are used for the key parameters of FPA, the switch probability $p = 0.8$, the controlling parameters for step size $\lambda = 1.5$ and the scaling factor $\gamma = 0.1$. In DEFPA, the mutation factor F and the crossover rate CR are both 0.8. Figure 5.9 shows the fitness curve of DEFPA and FPA for finding the optimal parameters of SVM. From the fitness performances that are shown in Figure 5.9, it is clearly seen that FPA may either fall into a local minimum easily or have a rather slow evolution speed while DEFPA is built with good global search capability and fast convergence. It indicates that DEFPA is superior to FPA in SVM parameters optimization.

All experimentally gained data samples are adopted to verify the performance of the presented approach in terms of classification accuracy. In the optimized DEFPA-SVM classifier, penalty parameter C and the width of RBF kernel function σ adjusted with minimal classification error are selected as the most appropriate parameters. Then, the optimal parameters are utilized to train the SVM model. In the canonical SVM model, the parameter C and σ-parameters are randomly selected to construct the classification model. The experimental results of DEFPA-SVM are shown in Table 5.1.

Table 5.1: Test Results of the DEFPA-SVM Approach

Target type of samples	Test results			
	No target	Target type I	Target type II	Target type III
No target	627	7	2	4
Target type I	9	590	29	12
Target type II	7	16	598	19
Target type III	4	4	24	608

5.5.2 Performance Comparison with Other Approaches

In order to demonstrate the performance improvement by using the DEFPA-SVM classifier, other classical classifiers are also used as benchmarks, including the FPA-SVM, the conventional SVM, the BPNN, and the KNN models. The comparison results are shown in Table 5.2. For the KNN classifier, the Euclidean distance is used as a similarity measure and the number of neighbors is selected to be 10. For the BPNN classifier, three layers are applied to the target classification. The number of input nodes is determined according to the dimensions of the features. The output layer contains four nodes which is the number of target types in this work. The optimal parameters of the nodes for the hidden layer, the target error, the training rate, and the momentum were determined to be 25, 0.005, 0.1 and 0.01, respectively. As can be seen, the presented approach outperforms all others in target classification in a foliage environment, even with different weather conditions.

Table 5.2: Summary of Classification Accuracy (%) using Different Classifiers

Target type	Classification rate (%)				
	DEFPA-SVM	FPA-SVM	SVM	BPNN	KNN
No target	97.97	97.34	96.72	96.25	95.16
Target type I	92.18	91.09	86.56	81.09	80.78
Target type II	93.44	92.34	88.44	87.03	86.41
Target type III	95.08	94.78	90.31	88.91	87.34
Average	94.65	93.78	90.51	88.32	87.42

To further investigate the performance improvement from using the HOC-based algorithm for feature extraction, the previous RSS-based algorithm listed in Table 4.1 is used as a benchmark. The comparison results are shown in Table 5.3. As can be seen, it is evident that DEFPA-SVM, FPA-SVM and SVM classifier with the HOC-based feature extraction algorithm offers an inherently improved accuracy over the RSS-based one. On the other hand, using either the HOC- or RSS-based algorithm for feature extraction,

any approach that adopts the DEFPA-SVM classifier always provides better performance than its SVM-based counterpart. It therefore once again proves that the presented approach is superior to the conventional ones.

Table 5.3: Summary of Classification Accuracy (%) using Different Feature Extraction Methods

Target type	DEFPA-SVM		FPA-SVM		SVM	
	HOC	RSS	HOC	RSS	HOC	RSS
No target (%)	97.97	92.66	97.34	91.41	96.72	90.31
Target type I (%)	92.18	71.09	91.09	69.84	86.56	64.22
Target type II (%)	93.44	76.25	92.34	75.16	88.44	72.50
Target type III (%)	95.08	76.88	94.78	75.47	90.31	6375
Average (%)	94.65	79.22	93.78	77.97	90.51	72.69

5.5.3 Reliability Analysis

To further evaluate the performance of the presented approach in terms of reliability, the impact on the accuracy of different sizes of training dataset is investigated. The number of training samples for each target type is varied from 160 to 480 with a step of 40. The obtained results are shown in Figure 5.10. As illustrated, using the DEFPA-SVM classifier, the classification accuracy is inherently improved compared with that of PFA-SVM and SVM classifiers, even when the size of the training dataset is reduced. It can be seen that the proposed DEFPA-SVM model not only has higher classification accuracy but also does well in the case of small sample size.

As RF signals can be easily attenuated due to environmental variations, evaluating the impact of SNR variation on classification accuracy is also very critical. To do so, additional Gaussian white noise is added to the original collected data so that the SNR can be effectively varied. In the simulation, the noise level is varied from 5 dB to 30 dB with a step of 5 dB. The average

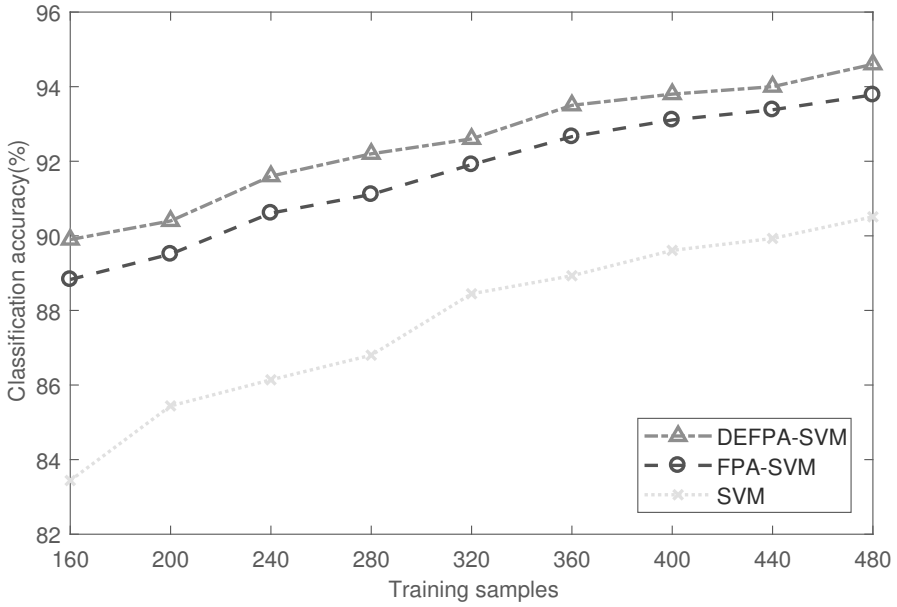

Figure 5.10: The impact on average classification accuracy due to different numbers of training samples

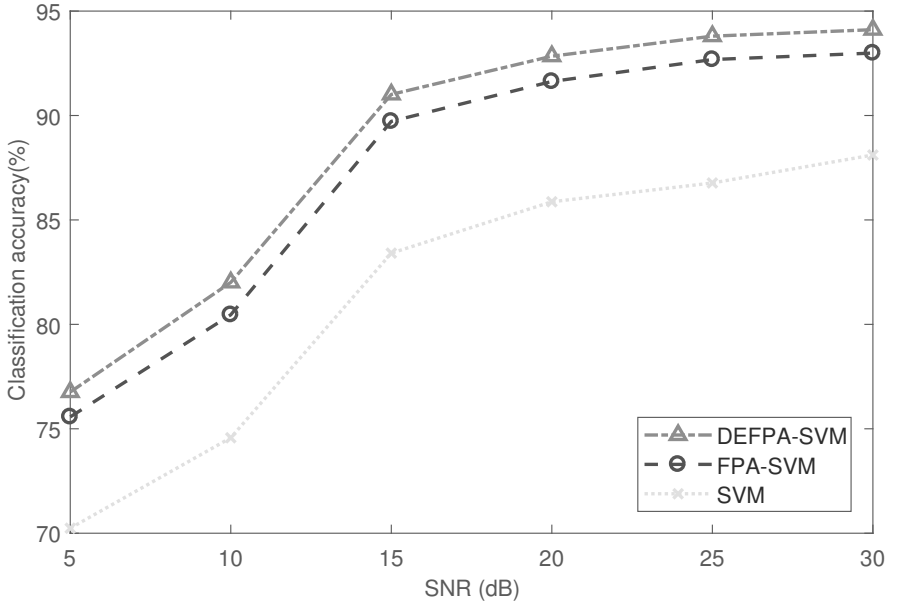

Figure 5.11: The impact on average classification accuracy due to SNR variations

accuracy obtained from these tests is shown in Figure 5.11. As illustrated, the presented approach has not only higher classification accuracy but also excellent immunity against noise, compared with the that of FPA-SVM and classical SVM-based classifier. Although the original target echo signal is distorted by some noise in simulation recognition, it still can be recognized by this method with high accuracy.

Therefore, the experimental results indicate that the proposed DEFPA-SVM model has the stronger robustness of data analysis and better generalization ability than conventional recognition model for target recognition.

5.6 Summary

In this chapter, the performance analysis of using the presented DFS approach for FOPEN in all seasons is investigated. To ensure reliable performance in all seasons with different weather conditions in terms of classification accuracy, a DEFPA-SVM based classifier is used in conjunction with HOC-based feature extraction. As a result, the adverse effect on accuracy due to seasonal variations such as different weather conditions can be mitigated. To demonstrate the feasibility of using this approach for FOPEN, a variety of data samples have been taken under 16 different scenarios, including four different types of target and four different weather conditions, in a foliage environment. Using these data samples, the robustness of the prototype is extensively verified, the impact on classification accuracy due to the number of training samples and SNR variations are analyzed. Without using any sensing devices other than RF transceivers, the average accuracy is greater than 94%, while the classical SVM classifier using the conventional RSS-based approach can only achieve an accuracy of 73% under the same scenario. Therefore, we can firmly conclude that the presented approach is feasible for FOPEN related applications in all seasons such as intelligent border control and smart search-and-rescue.

Chapter 6

Foliage Penetrating Target Classification under Severe Weather Conditions based on Auto-ED

In Chapter 5 we evaluated the detection performance of using the DFS approach for target detection beneath foliage in all seasons. Although the feasibility of using this technology under different weather conditions has been explored to some extent, we observe that it still cannot perform promisingly under adverse weather conditions such as rain, fog, and snow. In this chapter, experiments are conducted under severe weather conditions based on a proposed deep learning approach. We present an Auto-Encoder/Decoder (Auto-ED) deep neural network that can learn the deep representation and conduct classification task concurrently. As we pursue the signal-based mission, two components are involved in the proposed Auto-ED approach. First, an encoder is utilized that encode signal-based inputs into higher dimensional tensors by fractionally-strided convolution operations. Then, a decoder is leveraged with convolution operations to extract deep representations and learn the classifier simultaneously. To verify the effectiveness of the proposed

approach, we compare it with several machine learning approaches under different weather conditions. Also, a simulation experiment is conducted by adding additive White Gaussian noise to the original target signals with different SNRs. Experimental results demonstrate that the proposed approach can best tackle the challenge of target detection under severe weather conditions in the high-clutter foliage environment.

6.1 Introduction

Vegetation plays a significant role in the fading phenomena in wireless communications (Tamir 1967) (Meeks 1983) (Rogers, Seville, Richter, Ndzi, Savage, Caldeirinha, Shukla, Al-Nuaimi, Craig, Vilar et al. 2002) (Hashim & Stavrou 2006). Many efforts have been put into path loss modeling and measurement of communication channel within foliage areas such as outdoor propagation channel modeling in foliage environment (Liang & Liang 2010*a*), electromagnetic scattering from foliage camouflaged targets (Dehmollaian & Sarabandi 2006), and RF propagation measurements in forest (Rao, Balachander, Kiran & Oscar 2012). Different influences on the path loss in a foliage channel have been discussed such as species of the vegetation, density of the forest, geometries of the path, height of the antenna, etc. In particular, the study of weather-induced effects on RSS has gained extensive attention for RF propagation in foliage environments. The seasonal variation of temperature and humidity is studied in (Low 1988) (Luomala & Hakala 2015) and the wind-induced temporal variation is investigated in (Dal Bello, Siqueira & Bertoni 2000) (Pelet, Salt & Wells 2004) (Hashim & Stavrou 2006). Hence, weather conditions particularly can significantly affect the performance of wireless communication and therefore cannot be ignored (Anastasi, Falchi, Passarella, Conti & Gregori 2004) (Capsuto & Frolik 2006) (Bannister, Giorgetti & Gupta 2008).

In previous chapters, the DFS technology which only uses RF signals as sensing devices, has demonstrated its capability for target classification in fo-

liage environments. As fas as DFS is concerned, the location of transceivers may be fixed and their surroundings might remain almost static, but the weather will change and fluctuate due to both diurnal and seasonal variation. Though changes in weather conditions are inevitable, they are usually measurable and could be mitigated based on experimental measurements. Therefore, in order to ensure reasonable detection accuracy with seasonal variations, in Chapter 5 we conducted an experiment under four different weather conditions and propose a DEFPA algorithm to optimize the parameters of the SVM classifier. However, this approach still cannot perform promisingly under some severe weather conditions such as rain, fog and snow. This is because the RSS may reduce by the changes in temperature and humidity under such weather conditions (Luomala & Hakala 2015). Consequently, a severe degradation in detection performance inevitable takes place.

The emergence of deep learning approaches allows compelling performance in enormous recognition tasks (Krizhevsky, Sutskever & Hinton 2012) (Szegedy, Liu, Jia, Sermanet, Reed, Anguelov, Erhan, Vanhoucke & Rabinovich 2015) (He, Zhang, Ren & Sun 2016). In this chapter, we propose an end-to-end Auto-Encoder and Decoder deep neural network (Auto-ED) to tackle the challenge of severe weather conditions for target detection under high-clutter foliage environment. Unlike traditional learning approaches that extract target representations first and then conduct a metric learning algorithm (Dalal & Triggs 2005) (Zhu, Yeh, Cheng & Avidan 2006) (Tuzel, Porikli & Meer 2007), the proposed Auto-ED method can learn a deep feature to represent each target and classify different targets simultaneously. Compared with the traditional learning method, our proposed Auto-ED approach can establish automatic interaction among two modules in the training process. This is crucial for the overall system performance since if useful information is lost in previous steps (*e.g.*, feature extraction), it cannot be recovered later (*e.g.*, in metric learning) (Li, Zhao, Xiao & Wang 2014), in case, the signals received by transmitters already suffering from degradation caused by the severe weather conditions. Hence, directly extracting features from

these singles may not well handle such undesirable characteristics potentially embedded in the raw data. As an alternative, deep learning approach, *i.e.*, the proposed Auto-ED approach can mitigate the disturbance produced by the weather conditions through an automatic interaction scheme between the feature extraction and metric learning modules.

Overall, the contributions of this chapter can be summarized in three-folds:

1. First, we observe existing attempts by using DFS sensing to achieve target detection in the high-clutter foliage environment cannot well handle the impact of severe weather conditions, *e.g.*, fog, rain, and snow due to the changes of humidity and temperature. This chapter attempts to solve this problem under such conditions.

2. Second, we propose an Auto-ED deep neural network to tackle the challenge of adverse weather conditions for target detection using DFS sensing. Compared with previous attempts, our proposed approach can simultaneously extract deep representation for each target and classify them in an end-to-end fashion by leveraging the proposed deep learning architecture.

3. Third, comprehensive experiments are carried out to verify the effectiveness of the proposed method. Experimental results demonstrate that the proposed Auto-ED approach can well handle the new challenge presented in this chapter.

This chapter is organized as follows. We first review related works in Section 6.2. The proposed Auto-ED neural network approach is presented in Section 6.3. The DFS-based dataset for target detection in foliage environment and experiments are shown in Section 6.4. Summary is in Section 6.5.

6.2 Related Works

In this section, we first review the previous studies of DFS-based technologies for foliage penetration target classification in Section 6.2.1, and then we report some deep learning approaches related to our work in Section 6.2.2.

6.2.1 DFS-based Technologies for Foliage Penetration Target Classification

The DFS-based technology has been widely used in many applications such as localization, intrusion detection, and activity recognition. Amongst them, no attempt has been made to transfer the technology to applications that are operated in cluttered outdoor environments. In order to fill this void, the feasibility of using the DFS approach for target classification in foliage environment is investigated in our studies. In Chapter 3, we first demonstrated the possibility of using this approach for human and animal target classification in a low-clutter outdoor environment. To further evaluate the performance of the presented approach in terms of reliability, the impact on detection accuracy of high-clutters was investigated in Chapter 4. In Chapter 5, an experiment conducted in four weather conditions is intensively explored in order to mitigate the effects of seasonal variations. Although the effect of weather variations is addressed, these approaches still cannot produce relatively modest performance under severe weather conditions which makes them unfeasible to attain and sustain realistic missions.

Therefore, to make our research tackle well severe weather conditions, we propose to use the deep learning method in this chapter. Although the previous approaches have attempted to use traditional learning methods in target detection with DFS-based technology, unfortunately, deep learning related approaches which demonstrate its promising performance in many recognition and classification tasks, have not been fully explored.

6.2.2 Deep Learning Technologies

Since the emergence of deep learning technology, many approaches have been proposed to tackle various kinds of recognition and classification tasks, *e.g.*, human detection (Girshick 2015) (Ren, He, Girshick & Sun 2015) (Girshick, Donahue, Darrell & Malik 2014), tracking (Wang & Yeung 2013), and re-identification (Huang, Sheng, Zheng & Xiong 2017). However, most of them are image-based methods which may not be suitable for our scenario. To bridge the gap between the image-based deep learning method and RF signals for target detection, in this chapter, we first try to encode an input signal into a higher dimensional distinguishable tensor. Then the traditional convolutional neural network employed by the decoder can be easily adopted after encoding. Our approach is motivated by the architectures of Deep Convolutional GANs (DCGAN) for image generation (Radford, Metz & Chintala 2015). But unlike DCGAN, our inputs have practical significance instead of randomly generated Gaussian noise. To make an improvement in the performance of our proposed Auto-ED approach, several boosting methods are utilized. Amongst them, the batch normalization (BN) is proposed to address the internal covariate shift caused by the fact of different distributions of layer's inputs (Ioffe & Szegedy 2015). By using BN, we can use a higher learning rate to accelerate the training speed and be less careful about initialization of parameters concurrently. In addition, we use the Rectified Linear Unit (ReLU) as our activation function because of its sparsity and a reduced likelihood of vanishing gradient in training deep neural networks (Nair & Hinton 2010). Finally, the dropout layer is utilized to prevent the neural network from over-fitting (Srivastava, Hinton, Krizhevsky, Sutskever & Salakhutdinov 2014). It is also worthwhile to mention that since our input data is signal instead of images, we change part of the parameters to make Auto-ED suitable for our task. In addition, we verify the effectiveness of some important hyper-parameters in experiments such as the dropout rate, the number of learnable parameters, etc.

In general, by leveraging the proposed Auto-ED deep learning approach

that can establish automatic interaction between the feature extraction and metric learning, we achieve an extremely competitive performance in tackling severe weather conditions for target detection even though the strength of signals are degraded significantly in such situations.

6.3 Auto-Encoder/Decoder Deep Neural Network

6.3.1 Higher-Order Cumulant Feature for Encoding

We use the Higher-Order Cumulant (HOC) as the input vector to the encoder in our proposed Auto-ED neural network. We choose HOC as our inputs since it has the capability of classifying non-Gaussian signals and immunizing to high disturbances in applications where the original signals are corrupted by the noise. Also, both of the amplitude and phase information is involved in HOC, making it particularly suitable for targets classification. Typically, the number crunching of HOC is high since it requires higher order cumulants to depress the influence of noise. To simplify this process, we utilize the one-dimensional slice of fourth-order cumulants in HOC because it already involves the characteristic of multi-order cumulants. Given k-dim signal source $\{x_1, x_2, ..., x_k\}$ its corresponding fourth-order cumulant can be calculated by Equation (4.13). More details of the HOC features can be found in Section 4.3.2. In this chapter, we extract 179-dimensional HOC slice as shown in Figure 5.7 and Figure 5.8 as the input to the Auto-ED network we proposed.

6.3.2 Auto-Encoder/Decoder Deep Neural Network

After extracting the one-dimensional slice of the fourth-order HOC from the original signals, we propose an Auto-ED deep neural network to simultaneously learn deep representations with high discriminability and optimize a

deep classifier for target classification (distinguish human from other interference targets) in a high-clutter foliage environment. The architecture of the proposed Auto-ED network is shown in Figure 6.1. The main components including an encoder and a decoder are involved in the deep architecture. In training, given a one-dimensional HOC slice (1×179) input, the Encoder will automatically map it to a high dimensional tensor by using four continuous Fractionally-Strided Convolution (FS-Conv) layers. Then, a sequence of Convolution (Conv) layers is followed after the Encoder to learn deep representations for classifying different targets. Finally, a softmax loss function is used to calculate the bias between the predicted probability of an input and its ground-truth label. During the training process, the network will execute a forward propagation (calculating the deep representation from input→Encoder→Decoder→softmax loss) and a backward propagation (updating the learnable parameters of the Encoder and the Decoder according to the bias: softmax loss→Decoder→Encoder→input) iteratively when different inputs are fed into the network. The following part will introduce all the operations we used in our Auto-ED network including FS-Conv, Conv, softmax loss, and other boosting layers.

- **Encoder**

The encoder is used to map the one-dimensional HOC slice (1×179) input to a higher dimensional tensor ($32 \times 32 \times 16$) through four fractionally-strided convolution operations. Given:

- input map $x^{fs-conv} \in R^{H \times W \times D}$,
- convolution filter $f^{fs-conv} \in R^{H^{'} \times W^{'} \times D \times D^{''}}$,
- output map $y^{fs-conv} \in R^{H^{''} \times W^{''} \times D^{''}}$,

between two adjacent layers, where $H(H^{'}$ or $H^{''})$, $W(W^{'}$ or $W^{''})$ and $D(D^{''})$ respectively represent the height, width and depth. Formally, the output

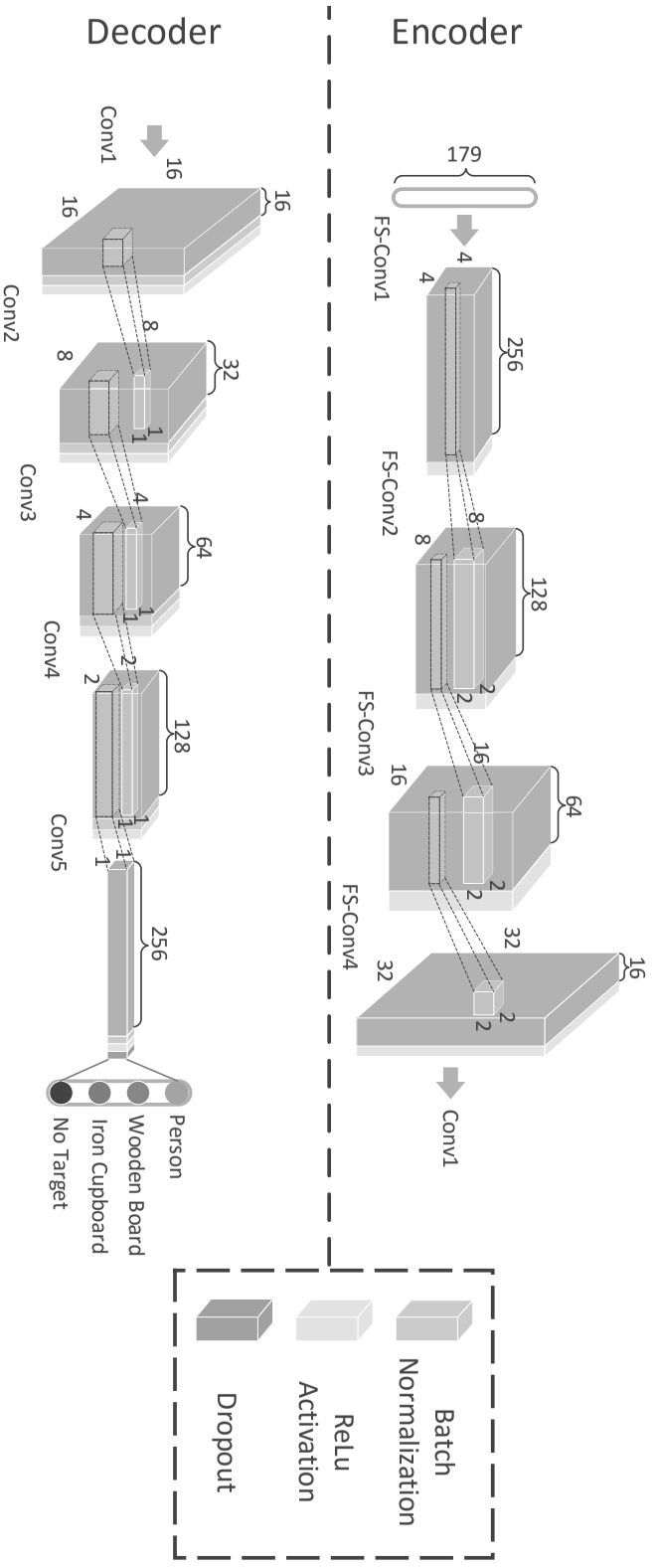

Figure 6.1: Four different targets (*e.g.*, human, wooden board, iron cupboard, and no target) and weather conditions (*e.g.*, sunshine, rain, snow, and fog) we used for data acquisition in realistic scenarios

$y^{fs-conv}$ is given by:

$$\begin{aligned} y^{fs-conv}_{i''j''d''} &= b_{d''} + \sum_{d=1}^{D} \sum_{i'=0}^{q(H',S_h)} \sum_{j'=0}^{q(W',S_w)} \\ & f^{fs-conv}_{1+S_h i'+m(i''+P_h^-,S_h),1+S_w j'+m(j''+P_w^-,S_w),d,d''} \times \\ & x^{fs-conv}_{1-i'+q(i''+P_h^-,S_h),1-j'+q(j''+P_w^-,S_w),d} \end{aligned} \tag{6.1}$$

where $d'' \in \left[1, D''\right]$, $b_{d''}$ is the bias term, (S_h, S_w) are the vertical and horizontal input up-sampling factors, $(P_h^-, P_h^+, P_w^-, P_w^+)$ represent crops of output in vertical (h) and horizontal (w) directions. The $+$ and $-$ respectively represents the top-left and bottom-right of the output map y. $m(k,S) = (k-1)\, mod\, S$ and $q(k,n) = \left\lfloor \frac{k-1}{S} \right\rfloor$ which is a quotient operation. The height (H'') and width (W'') of the output map y are given by:

$$\begin{aligned} H'' &= S_h(H-1) + H' - (P_h^- + P_h^+) \\ W'' &= S_w(W-1) + W' - (P_w^- + P_w^+) \end{aligned} \tag{6.2}$$

In our encoder component, we use four FS-Convs to learn efficient representations by mapping the raw inputs to a higher dimensional distinguishable tensor. The output of the encoder will be directly connected to our decoder to process it and make a decision (target classification).

- **Decoder**

The decoder is utilized to process the output of the encoder and make a decision for the target classification task by five Conv layers. The input of the decoder is the output of the encoder with the size of $32 \times 32 \times 16$. Given:

- input map $x^{conv} \in R^{H \times W \times D}$,
- convolution filter $f^{conv} \in R^{H' \times W' \times D \times D''}$,
- output map $y^{conv} \in R^{H'' \times W'' \times D''}$,

between two adjacent layers, y^{conv} is given by:

$$y^{conv}_{i''j''d''} = b_{d''} + \sum_{i'=1}^{H'} \sum_{j'=1}^{W'} \sum_{d=1}^{D} f^{conv}_{i',j',d,d''} \times \tag{6.3}$$

$$x_{S_h(i''-1)+i'-P_h^-, S_w(j''-1)+j'-P_w^-, d},$$

We use the same notations as for the FS-Conv layers in our decoder since they share the same meaning except for the $(P_h^-, P_h^+, P_w^-, P_w^+)$. In the decoder, it represents paddings instead of crops. Unlike the FS-Conv, the height $(H^{''})$ and the width $(W^{''})$ of the output map y are given by:

$$\begin{aligned} H^{''} &= 1 + \left\lfloor \frac{H - H^{'} + P_h^- + P_h^+}{S_h} \right\rfloor \\ W^{''} &= 1 + \left\lfloor \frac{W - W^{'} + P_w^- + P_w^+}{S_w} \right\rfloor \end{aligned} \tag{6.4}$$

Finally, after five continuous convolution operations (*i.e.*, Conv1 to Conv5). A 256-dimensional feature representation is learned by the Auto-ED deep neural network. This feature will be fed into the softmax loss to classify different targets during the training process (details can be found in Equation 6.9). Table 6.1 lists the parameters settings for the encoder and decoder components.

- **Boosting Layers**

To boost the performance of our proposed Auto-ED deep neural network, three boosting layers are utilized in our network architecture, including Batch Normalization, ReLu Activation, and Dropout. These layers are followed after each FS-Conv and Conv layers according to the sequence shown in Figure 6.1.

- **BN.** BN (Ioffe & Szegedy 2015) is designed for addressing the problem of internal covariate shift caused by the discrepancy between different distributions of the input layers (Ioffe & Szegedy 2015). By utilizing

Table 6.1: Parameters Setting for the Proposed Auto-ED neural network including four FS-Conv layers and five Conv layers.

Layer name	output size $(H'' \times W'')$	output depth (D'')	input size $(H \times W)$	input depth (D)	kernel size $(H' \times W')$	stride (S_h, S_w)	padding $(P_h^-, P_h^+, P_w^-, P_w^+)$	has bias $b_{d''}$
Four Fractionally-Strided Convolution Encoder Layers								
FS-Conv1	4×4	256	1×1	179	4×4	(4,4)	(0,0,0,0)	yes
FS-Conv2	8×8	128	4×4	256	2×2	(2,2)	(0,0,0,0)	yes
FS-Conv3	16×16	64	8×8	128	2×2	(2,2)	(0,0,0,0)	yes
FS-Conv4	32×32	16	16×16	64	2×2	(2,2)	(0,0,0,0)	yes
Five Convolution Decoder Layers								
Conv1	16×16	16	32×32	16	2×2	(2,2)	(0,0,0,0)	yes
Conv2	8×8	32	16×16	16	2×2	(2,2)	(0,0,0,0)	yes
Conv3	4×4	64	8×8	32	2×2	(2,2)	(0,0,0,0)	yes
Conv4	2×2	128	4×4	64	2×2	(2,2)	(0,0,0,0)	yes
Conv5	1×1	256	2×2	128	2×2	(2,2)	(0,0,0,0)	yes

BN, a higher training rate can be leveraged to accelerate the training speed of our proposed Auto-ED network. We only use it after each Conv layer before the ReLU activation. Let T be the mini-batch size we used in each training iteration, $x^{BN} \in R^{H\times W\times D\times T}$ and $y^{BN} \in R^{H\times W\times D\times T}$ respectively represent the input and output of the BN layer with height H, weight W, and depth D. The output feature map of BN is given by:

$$y_{ijdt} = w_d \frac{x_{ijdt} - \mu_d}{\sqrt{\sigma_d^2 + \varepsilon}} + b_d, \tag{6.5}$$

where μ_d is the mean value across the dimensionality of depth (D) in x:

$$\mu_d = \frac{1}{HWT} \sum_{i=1}^{H} \sum_{j=1}^{W} \sum_{t=1}^{T} x_{ijdt}, \tag{6.6}$$

σ_d^2 is the variance corresponding to the μ_d:

$$\sigma_d^2 = \frac{1}{HWT} \sum_{i=1}^{H} \sum_{j=1}^{W} \sum_{t=1}^{T} (x_{ijdt} - \mu_d)^2, \tag{6.7}$$

w_d and b_d define as component-wise multiplicative and additive constants respectively.

- **ReLU.** We use ReLU (Nair & Hinton 2010) as our activation function of each output map in both of the encoder and decoder components because of its sparsity and a reduced likelihood of vanishing gradient in training our proposed Auto-ED network. Given an output tensor $y \in R^{H,W,D,T}$, its activation result $y^{relu} \in R^{H,W,D,T}$ is given by:

$$\begin{aligned} &y_{ijdt}^{relu} = max(0, y_{ijdt}), \\ &i \in [1, H], j \in [1, W], d \in [1, D], t \in [1, T], \end{aligned} \tag{6.8}$$

- **Dropout.** Normally, over-fitting is a severe problem in training deep neural networks since many parameters are optimized to fit the training set which may fail to achieve a desirable performance on the testing set because there is no a certain overlap between them. Therefore, we use

dropout (Srivastava et al. 2014) to prevent over-fitting. Given an input, dropout will randomly set values of a part of input neurons to zero according to the preset dropout rate. For instance, if the dropout rate set to 0.9, 10% values in the feature representation will be randomly set to zero in training. Notably, this trick is only utilized in training, when testing, the dropout layer will be removed (see Figure 6.1). The dropout can be interpreted as a way to add noise in training to regularize the quality of generalization of the neural network.

Figure 6.1 shows the architecture of the proposed Auto-ED network, the three kinds of boosting layers are followed after each FS-Conv1-4 and Conv1-5 layers. Finally, a fully connected layer with four neurons which respectively represents the person, wooden board, iron cupboard and no target, is followed after dropout. We use the softmax loss function to make the final decision and optimize the whole network (encoder + decoder) through the backward propagation algorithm. The softmax loss is given by:

$$L = -\sum_{c=1}^{C} y_c log \frac{e^{a_c}}{\sum_{c'=1}^{C} e^{a_{c'}}}, \tag{6.9}$$

where C is the total number of target classes. a is a $1 \times C$ vector which is given by the output of the final fully connected layer (specifically the output of the dropout layer). Each value in a represents the prediction that belongs to different target classes. y is a $1 \times C$ 'one-hot' label vector that only the corresponding class of sample is set to one; others are set to zero.

In training, each input data will be fed into the Auto-ED network to get a high dimensional tensor after encoding. Followed by the encoder, the decoder will deal with the output of the encoder and make a decision (prediction) to the softmax loss function. Hence, Equation 6.9 is used to calculate the bias between the ground-truth label and the prediction value. Then, the background propagation algorithm is utilized to update all the parameters belonging to the Auto-ED system. After iteratively updating the network using the data in the training set, the loss (defined in Equation (6.9)) tends

to converge in a small value close to zero. It means the network so far can perform well in classifying different targets in the training set.

In testing, feeding an input data from the testing set into the proposed Auto-ED network, the probabilities of the data belonging to different classes will be calculated after the encoder and decoder processes. More specifically, the outputs of the final fully connected layer are used to calculate the prediction value as follows:

$$P = \frac{e^{a_c}}{\sum_{c'=1}^{C} e^{a_{c'}}}, \tag{6.10}$$

Notably, the dropout layer is removed from the system since it is just used to prevent the network from over-fitting in training and not be used in testing. Therefore, a_c represents the output of the last ReLU layer (see Figure 6.1) in Equation (6.10).

6.4 Experimental Results and Discussion

In this section, Section 6.4.1 first introduces the dataset for target detection in our experiment. Then, an experimental setup is given for the proposed Auto-ED neural network in Section 6.4.2. After that, a study is presented to verify the effectiveness of the proposed approach in Section 6.4.3. A brief comparison between our and other approaches is given in Section 6.4.4. In addition, we will verify the accuracy of the proposed method under different weather conditions in Section 6.4.5. Finally, we attempt to add additional white Gaussian noise on the original signals to further verify the anti-noise capability of the proposed Auto-ED approach in Section 6.4.6.

6.4.1 Dataset for Target Detection

To verify the accuracy of the proposed Auto-ED approach in distinguishing different targets under severe weather conditions, we use a Foliage Penetration Target Detection (FPHD) dataset introduced in Chapter 5. This dataset consists of four weather conditions with four different targets in the

high-clutter foliage environment. In our experiment, an IR-UWB transceiver with operating frequency from 3.1 to 5.3 GHz and a center frequency of 4.2 GHz is used for data acquisition. All the data collected in FPHD is from a park with a mixture of hardwood trees and low-lying underground. Four targets are included such as human, wooden board, iron cupboard and no target. In addition, each target is measured under four weather conditions, including sunshine, rain, fog and snow. Figure 6.2 shows the experimental topology in foliage environment under four weather conditions in the realistic scenario. In our experiments, we randomly select 400 samples for each target in eight locations. Thus, there are totally 400 (samples) $\times$ 8 (locations) $\times$ 4 (weather conditions) = 12,800 samples for each target class used in our experiment dataset. More detailed information about the FPHD dataset can be found in Section 5.2.

For the training set, we randomly select 615 samples under each weather conditions for each target. Thus 2460 samples constitute one training class. Overall 9,840 samples are included in the training set. We also randomly select 100 samples for each target to constitute our validation set, on average, 25 samples are selected under each weather condition. There are 2,560 samples left as our testing set, 640 samples for each target. On average, there are 160 samples under each weather condition. Notably, there is no overlapped samples amongst the three sets, *i.e.*, if a sample is used in training set, it will not be involved in both of the validation and testing sets and vice versa. Table 6.2 lists the result of data split for training, validation and testing. As mentioned in Section 3.3.1, we use the last 90 dimensions of each original signal since it covers the most meaningful information.

6.4.2 Experimental Setup

We train the encoder and the decoder of the proposed Auto-ED neural network as a whole. Given the original signal samples, HOC features are extracted as inputs of the Auto-ED model. The total number of layers is 25. The initial learning rate is set to 5e-2 and decays to 5e-3 after 30 training

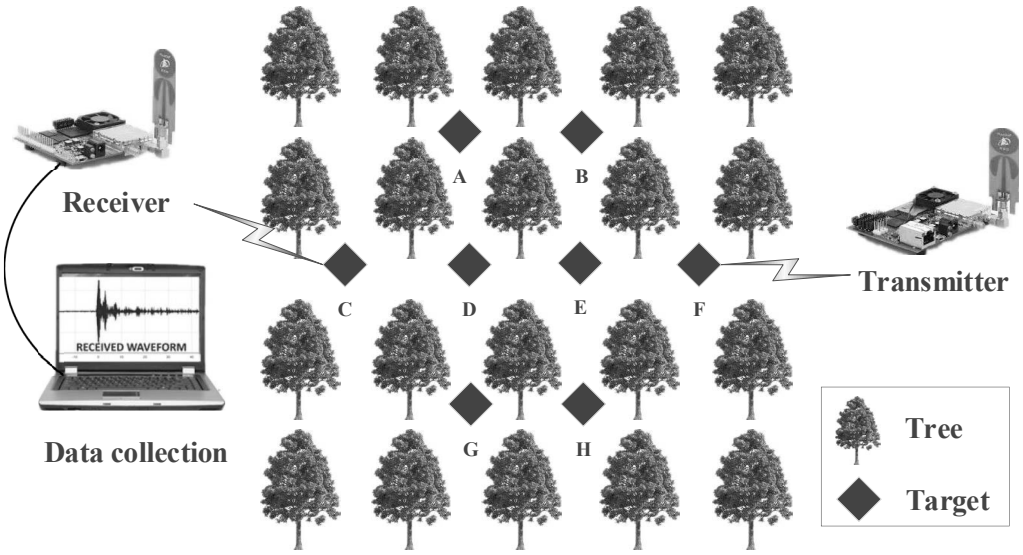

(a)

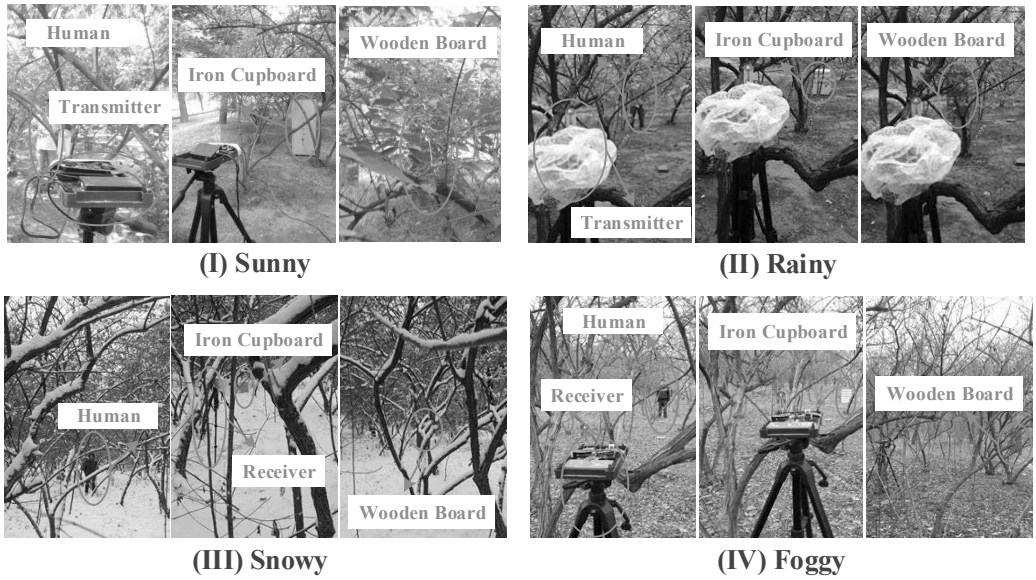

(b)

Figure 6.2: (a) The experimental topology in foliage environment for FPHD data acquisition. (b) Four different targets (*e.g.*, human, wooden board, iron cupboard and no target) and weather conditions (*e.g.*, sunshine, rain, snow, and fog) we used for data acquisition in realistic scenarios.

Table 6.2: Split of the experiment dataset

Split	Training		Testing
Subsets	Training	Validation	Testing
Person	2460	100	640
Wooden Board	2460	100	640
Iron Cupboard	2460	100	640
No Target	2460	100	640

epochs. Finally, after 50 training epochs, we use 5e-4 for the last 10 epochs to establish a convergent result. The number of the overall training epochs is 60. We cannot load all the training samples once in each training iteration because of the limited storage of memory. We use the mini-batch Stochastic Gradient Descent (SGD) to optimize the overall learnable parameters in training. We set the batchsize to 1024. As we use dropout to prevent overfitting in training, we set the dropout rate to 0.75. Other settings of the hyper-parameters such as momentum and weight decay can be found in Table 6.3. Before starting training, the initial learnable parameters are given randomly.

6.4.3 Study of the Proposed Auto-DE Approach

In this section, two studies are presented of the proposed Auto-ED network.

- **First**

We try to change the dropout rate to observe the classification accuracy. We use the data split shown in Table 6.2. Figure 6.3 shows the result by changing the dropout rate from 0.5 to 1; the step size is 0.05. It can be observed that when the dropout rate is set to 0.75, our proposed Auto-ED network achieves the best classification accuracy (98.23%). As the dropout rate gets close to 1 (there is no neuron set to zero), the likelihood of overfitting is increased that influences the testing performance. Also, it does not

Table 6.3: The Parameters Setup for Training the Proposed Auto-ED Neural Network.

Settings	Values
Number of Layer	25
Learning Rate	5e-2(30), 5e-3(20), 5e-4(10)
Number of Training Epoch	60
Batchsize	1024
Momentum	0.9
Weight Decay	1e-4
Optimization Algorithm	mini-batch SGD
Dropout Rate	0.75
Parameter Initialization	random

mean we can blindly reduce the dropout rate. As shown in Figure 6.3, the classification accuracy (from 98.23% to 97.95%) is depressed as we reduce the dropout rate from 0.75 to 0.5. Notably, the performance change is pretty small when we set the dropout rate from 0.5 to 0.55. This indicates that the network is hard to learn a robust representation if it is too sparse in training by using dropout to prevent the network from over-fitting (*i.e.*, nearly half values in the feature representation are set to zero.). As we continuously increase the dropout rate (*i.e.*, 0.6, which means only 40% values of feature representation will be randomly set to zero in training), this phenomenon can be mitigated, and the performance can be improved to some extent.

- **Second**

We attempt to change the number of learnable parameters in our Auto-ED model by reducing or increasing the number of channel of the convolution filters on each FS-Conv and Conv layers exponentially. There are 9 convolution filters involved in the four FS-Conv and five Conv layers. We denote the number of the overall learnable parameters of the proposed Auto-ED network as #P. Table 6.4 lists the results of the classification accuracy by

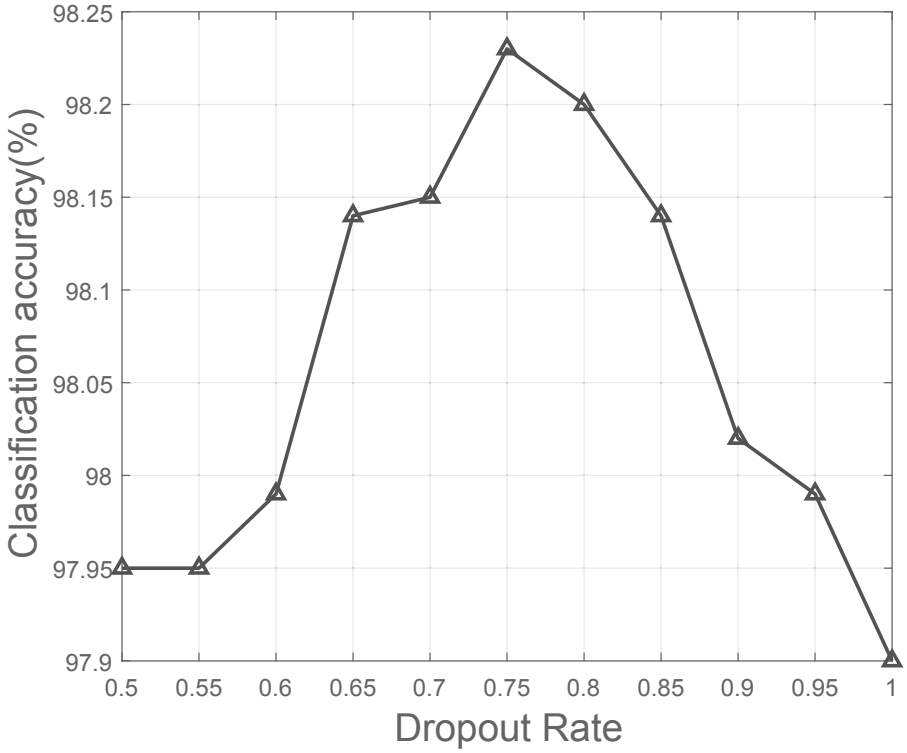

Figure 6.3: The classification accuracy by using different dropout rate (from 0.5 to 1, the step size is 0.05). The whole training set is used.

utilizing a different number of learnable parameters in the proposed Auto-ED network. We can observe that the number of parameters we used achieving the best performance compared with other attempts. The Auto-ED achieves the lowest classification accuracy (95.97%) when the number of the learnable parameters is increased by 16 times. This is because with more learnable parameters, the network tends to converge to the training set (*i.e.*, over-fitting) which affects the generalization performance in testing.

6.4.4 Comparison with Other Approaches

To verify the performance of the proposed Auto-ED approach, we also try to use several machine learning methods including DEFPA-SVM, SVM, BPNN and KNN on the FPHD dataset. We use the data split shown in Table 6.2.

Table 6.4: Comparison between the different number of learning parameters. #P represents the number of parameters. All the training samples are used.

Number of Parameters	#P/16	#P/8	#P/4	#P/2	#P
Classification Rate (%)	96.43%	96.95%	97.86%	98.10%	**98.23%**
Number of Parameters	#P*2	#P*4	#P*8	#P*16	
Classification Rate (%)	97.60%	96.85%	96.02%	95.97%	

The classification accuracy on different targets is shown in Table 6.5. It can be observed that the proposed Auto-ED method achieves the best classification accuracy. It also outperforms the second-best approach DEFPA-SVM 3.77% on average (98.23% vs. 94.46%) which demonstrates the effectiveness and superiority of our proposed method. Compared with our Auto-ED deep neural network, the BPNN approach can be regarded as a benchmark method which only uses an input layer, a hidden layer and an output layer. We use the same experimental setting in Section 3.4 to train BPNN. Specifically, the input layer shares the same dimension with the feature; then it passes through 25 hidden nodes to learn a deep representation; finally, four output nodes are followed after the hidden nodes using a fully connected fashion to classify different targets (*e.g.*, wooden board, iron cupboard, human, and no target) in our task. Compared with just using three layers in BPNN, the proposed Auto-ED method with a deeper neural network architecture and more learnable parameters can significantly outperform the BPNN method by a large margin (98.23% *vs.* 88.29% on average).

In Table 6.2, we can observe that the proposed Auto-ED can achieve the best performance compared with other machine learning methods such as DEFPA-SVM, SVM, and KNN. This is because by utilizing a deep architecture, the proposed Auto-ED approach can further explore information with higher discriminative power from the inputs, *i.e.*, the HOC-based features. More importantly, compared with the other machine learning methods we used, the Auto-ED neural network is an end-to-end system which can learn more distinguishable information between different targets and classify them

Table 6.5: Comparison between the proposed Auto-ED and other approaches.

Methods	**Classification Rate (%)**				
	No Target	Person	Wood	Iron	Average
Auto-ED	**99.73**	**97.47**	**96.78**	**98.95**	**98.23**
DEFPA-SVM	97.82	92.32	92.59	95.12	94.46
SVM	96.72	85.57	89.61	89.89	90.45
BPNN	96.42	80.02	86.98	89.75	88.29
KNN	95.98	81.25	88.17	86.12	87.88

simultaneously. However, the traditional machine learning method usually uses two separate processes, *i.e.*, extracting robust features firstly and then training a metric model to classify different targets according to the learning task. Since our task is to recognize targets in a high-clutter foliage environment, the impact of noise is extremely large compared with the normal environment. Under such conditions, if some effective information is lost during the process of feature extraction, it is irreversible if we still intend to utilize these missing parts to train a classifier (metric model). To address this problem, the Auto-ED neural network can integrate the two processes together that implicitly ensure the full usage of the information in an end-to-end learning fashion.

6.4.5 Comparison in Different Weather Conditions

Since severe weather conditions such as rain, fog and snow often involve disturbances that may reduce the strength of radio signals due to the changes of temperature and humidity, the classification task on FPHD becomes extremely challenging under such situations. Figure 6.4 shows the original signals received by the transmitter. It can be observed that on sunny days (see Figure 6.4 (a)), signals belonging to different targets are more distinguishable than in other three weather conditions. Meanwhile, other three weather conditions (*i.e.*, rain, fog, and snow) make the task more difficult

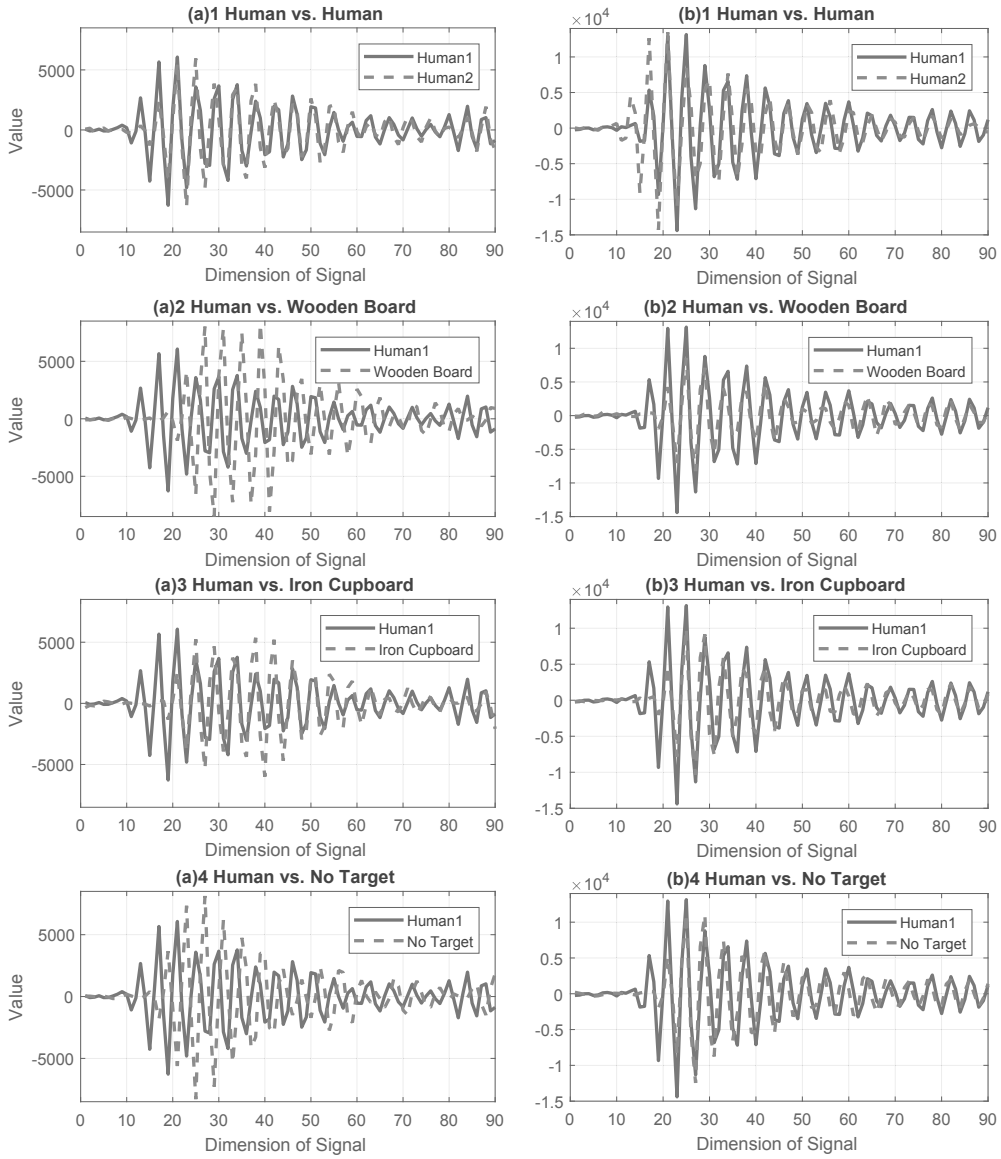

(a) Sunny (b) Rainy

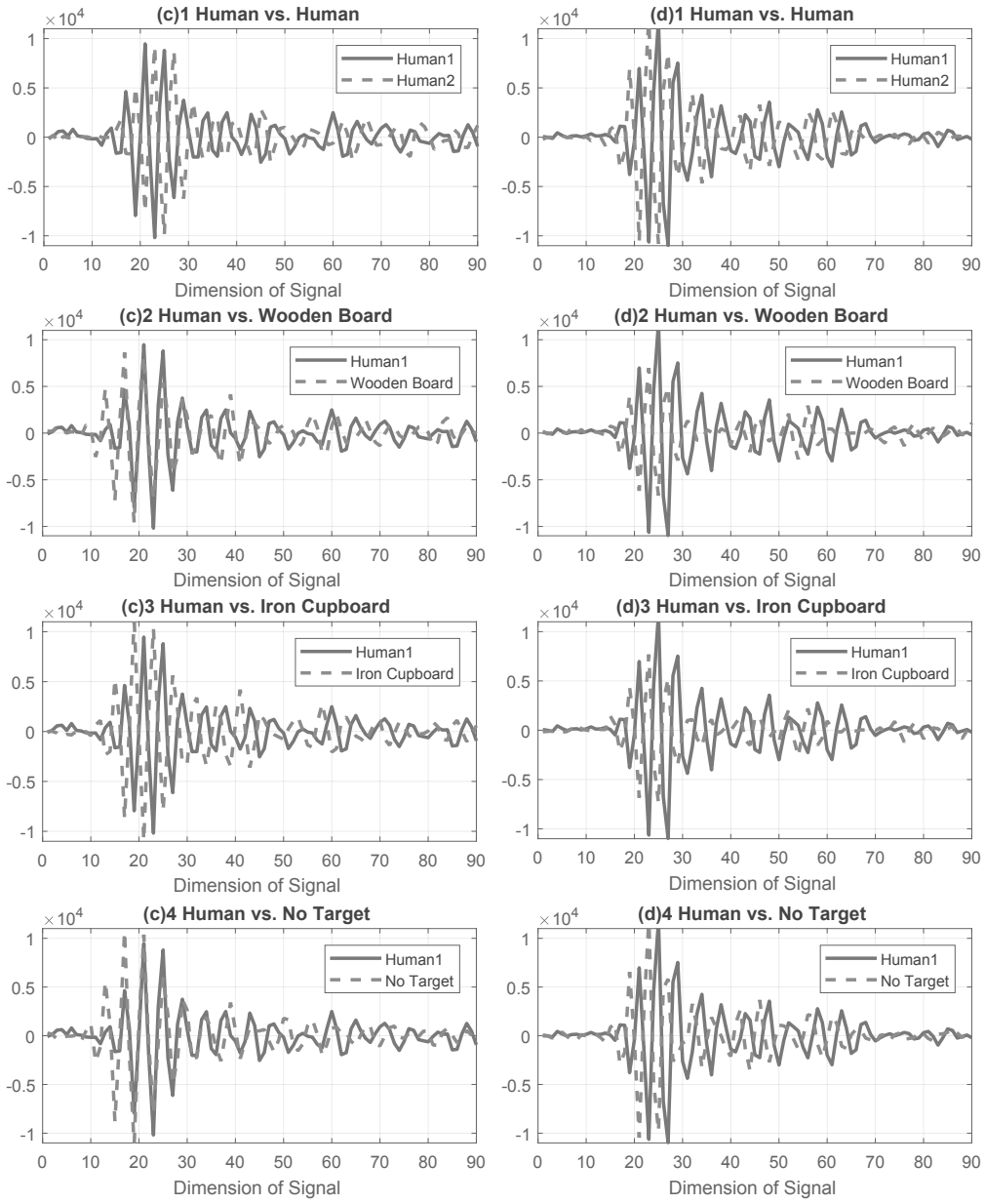

(c) Foggy (d) Snowy

Figure 6.4: Original signals received by a receiver (transmitter). (a)-(d) represent comparisons between human and different targets (*e.g.*, human vs. human, human vs. wooden board, human vs. iron cupboard, and human vs. no target) under four different weather conditions (*e.g.*, (a) sunny, (b) rainy, (c) foggy and (d) snowy) respectively. Notably, Human1 and Human2 respectively represent different data samples belonging to the same person.

since signals belonging to different targets are difficult to classify Figure 6.4 (b), Figure 6.4 (c), and Figure 6.4 (d). Unlike the data split in Table 6.2, to verify the effectiveness of the proposed Auto-ED approach under different weather conditions, we try to respectively split the training, validation and testing sets into four groups according to the different weather conditions. Specifically, for each weather condition, there are 2460 training samples; 615 samples for each target. We train the proposed Auto-ED models under four different weather conditions separately and then test the classification accuracy for each of them using their corresponding testing samples (*e.g.*, when the model trained on 2460 samples in rainy days, the testing samples we used also in the same weather condition). In this experiment, we use the proposed Auto-ED approach and the second-best method DEFPA-SVM as the comparison study. Table 6.6 lists the results. Our method outperforms DEFPA-SVM under all the weather conditions. On average, we outperform DEFPA-SVM by $\sim$6% in the classification accuracy on rainy, foggy, and snowy days which demonstrates the effectiveness of the proposed Auto-ED approach under severe weather conditions.

It can be clearly observed that the performance is the worst on snowy days (*e.g.*, 86.99% classification accuracy using the DEFPA-SVM approach). Our Auto-ED approach still achieves 93.53% classification accuracy under such conditions. Actually, under severe weather conditions, the effective information can be easily submerged by the noise. Therefore, using traditional machine learning methods, the impacts of embedded noise is hard to be mitigated in the feature extraction process which can result in inferior performance when they further participate in metric learning. On the contrary, the proposed Auto-ED method can effectively integrate these two processes which is a better solution for our case.

6.4.6 Comparison on Different Noise Levels

In the end, to verify the robustness of the proposed Auto-ED approach under different SNRs, we try to add additional white Gaussian noise to the original

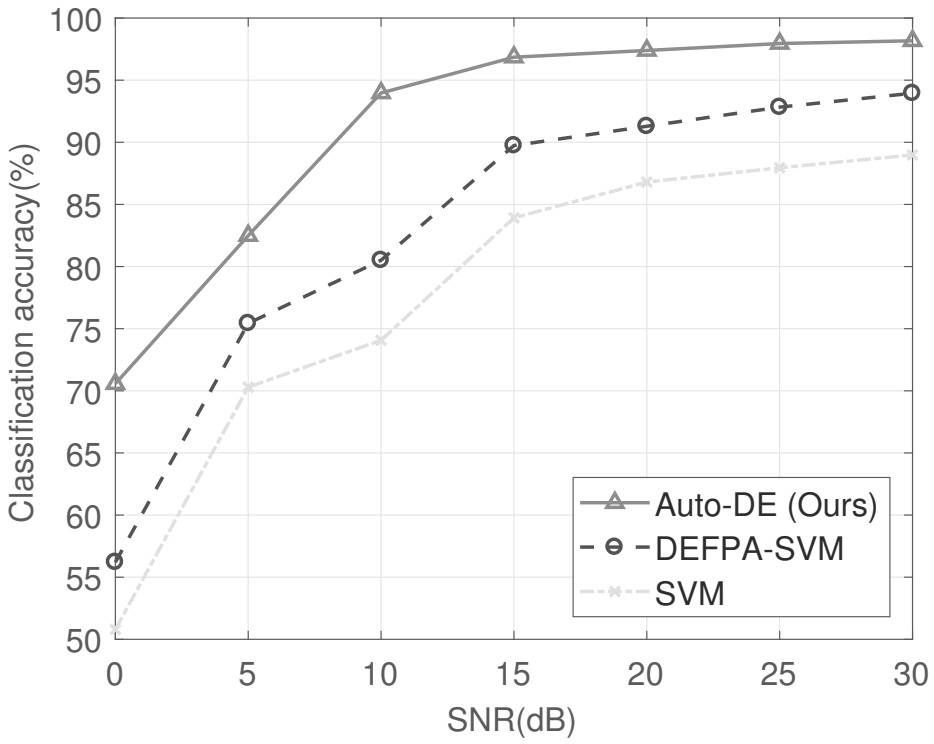

Figure 6.5: Comparisons between Auto-ED and SVM-based methods under different SNRs.

signals to train and test the FPHD dataset (using the data split in Table 6.2). We compare our method with the DEFPA-SVM and SVM methods. Figure 6.5 shows the experiment results. It can be observed that the proposed Auto-ED method achieves the best classification accuracy under all the SNR settings. Although DEFAP-SVM shows its superiority compared with the original SVM algorithm in Chapter 5, it is still inferior compared with our method under the low SNR conditions.

Table 6.6: Comparisons between the proposed Auto-ED method and DEFPA-SVM under different weather conditions.

Weathers	**Classification Rate (%)**				
	No Target	Person	Wood	Iron	Average
The proposed Auto-ED					
Sunny	99.65	95.48	94.96	97.29	**96.85**
Foggy	98.22	94.36	94.75	96.62	**95.99**
Rainy	96.59	92.19	94.28	97.18	**95.04**
Snowy	95.35	89.95	92.85	95.98	**93.53**
DEFPA-SVM					
Sunny	96.09	87.34	89.06	91.88	*91.09*
Foggy	95.47	86.25	87.03	90.31	*89.77*
Rainy	93.75	84.53	86.88	89.38	*88.64*
Snowy	92.19	82.03	85.16	88.59	*86.99*

6.5 Summary

In this chapter, the performance analysis of using the presented DFS approach for high-clutter foliage environment target detection under severe weather conditions is investigated. To ensure reliable performance under severe weather conditions in terms of classification accuracy, a deep learning approach named "Auto-ED" is proposed that can concurrently learn deep representations and the classifier. As a result, the adverse effect which are

produced by changes in humidity and temperature due to the severe weather conditions can be mitigated. To demonstrate the feasibility of utilizing the proposed approach, the FPHD dataset is used which includes four different types of targets and four different weather conditions, in a high-clutter foliage environment. Using these data, the robustness of the proposed approach is extensively verified by comparison with other approaches which are suitable for our task. In addition, a comprehensive evaluation is carried out to demonstrate the performance of our approach under severe weather conditions. Without using any sensing devices other than RF transceivers, the average accuracy under severe weather conditions is greater than 93%, while the previous attempt can only achieve an accuracy of 86%+ under the same scenario. Further, to verify the robustness of the proposed Auto-ED approach, we also discuss the classification accuracy with different SNRs. Therefore, we can conclude that the presented approach is feasible for target detection under high-clutter foliage environment and it is robust to severe weather conditions.

Chapter 7

Conclusions and Future Work

This thesis focuses on using DFS technology to provide a cost-effective sensing solution for target detection and classification in a foliage environment. Using this solution, the Internet of Mission-Critical Things may be advanced into a new domain by enabling several applications, ranging from purposes of military and surveillance to search-and-rescue operations such as intelligent border control, smart cities, and autonomous sensing. Due to the limited time, this thesis still leaves some valuable research topics for future work. In this chapter, we summarize the innovations of this thesis in Section 7.1, and then we point out the directions for future work in Section 7.2.

7.1 Conclusions

In conclusion, this thesis presents several techniques to address DFS-based approach for target detection and classification.

As one of the most critical issues for target detection and classification is to correctly distinguish between human and animal targets, in Chapter 3 we present a low-cost but robust approach that uses a combination of IR-UWB and machine-learning technologies to tackle this issue. To verify the performance of the developed approach, we carry out the measurements in a cornfield to obtain the real datasets. We then employ a probability density

function to analyze several typical statistical properties of the received RF signals. In this way, the computational cost can be minimized without compromising the accuracy. Consequently, we have found that two distinguishing features appear to be sufficient for human and animal classification, namely standard deviation and root mean square delay spread. Using them, we evaluate the impact on the classification accuracy due to different classifiers, the number of training samples and different values of SNR which indicates that the presented approach has excellent performance to be deployed in a cluttered outdoor environment for human and animal classification.

In Chapter 4 we extend the basic idea of the DFS-based approach in Chapter 3 to the target classification problem in a high-clutter environment. To solve this problem, we propose a HOC-based algorithm using 1-D slices of fourth-order cumulants to extract target features from the received RF signals. The main reasons for the HOC-based feature extraction method are two folds: first, it can extract distinct features from a higher-order domain which contains both amplitude and phase information of a signal; second, it can be used to separate additive mixtures of independent non-Gaussian signals and Gaussian noise, so we utilize it to enhance the immunity of the system against the noise generated by clutters. In order to validate the feasibility of the proposed method, we take the measurements with three types of targets in a medium-sized foliage environment. Applying these data along with SVM, the proposed HOC-based method improves the performance compared with the RSS-based algorithm introduced in Chapter 3.

Then we start to take the seasonal variations into consideration for the task of foliage penetration target detection and classification in Chapter 5. To address this concern, we develop a new recognition method using an optimization-based SVM in conjunction with HOC-based feature extraction introduced in Chapter 4. In the proposed method, to exploit the advantages of the high speed of FPA and the exploration ability of DE, we develop a DEFPA algorithm to optimize SVM parameters accommodated to datasets of all seasons. In order to demonstrate the feasibility of using the proposed

approach, we conduct an experiment in four seasons with four types of targets in a foliage environment. The experiment results indicate that the adverse effect on accuracy due to seasonal variations can be mitigated by using the proposed method.

Chapter 6 further investigates the effects of seasonal variations on the task of foliage penetration target detection, to improve the classification accuracy under adverse weather conditions such as rain, fog, and snow. We present an Auto-ED deep neural network that can concurrently learn deep representations and the classifier. As we pursue the signal-based mission, we adopt two components in the proposed approach. First, an encoder is utilized to encode signal-based inputs into higher dimensional tensors by fractionally-strided convolution operations. Then, a decoder is leveraged with convolution operations to extract deep representations and learn the classifier simultaneously. Compared with several traditional learning methods, the proposed deep learning method achieves the highest performance which makes it feasible to tackle severe weather conditions.

Each chapter (i.e. from Chapter 3 to Chapter 6) of this thesis is supported by the conference or journal papers listed in **List of Publications**.

7.2 Future Work

This thesis still leaves some fundamental issues to be tackled because not only target recognition in foliage environments is challenging but also device-free sensing is still young. In the future, we will continue to explore new potential directions. Some of the important and interesting research directions are pointed out as follows.

1. **Moving targets classification and detection**: This thesis focuses on the research issues in terms of static targets. However, the targets of the real world may be static or moving. Since motion will affect the prorogation of an RF signal for each target type, it would be quite difficult to ensure good detection accuracy for moving targets. For example, the

received RF signals of two types of targets in different motions maybe look nearly identical in a certain instant. For this reason, the detection of a moving target is essentially a problem of recognizing target behavior. In the future, we can develop an improved algorithm to detect moving targets by analyzing the existing approaches for DFS-based target activity detection and classification.

2. **Target detection and classification based on wireless communication network**: Due to experimental limitations, the work in this thesis is dependent on a single-input and single-output (SISO) system which has practical limitations from an engineering point of view. In order to ensure good practical applications value, it is a natural choice to introduce wireless communication networks to extend our current studies. In this way, not only the target detection range can be expanded but also the recognition performance can be improved. In the future, we can apply multiple-input and multiple-output (MIMO) systems to take actual measurements and investigate the impact of targets on multi-link transmission which makes it possible to achieve the aim of target detection, localization and tracking in foliage environments.

3. **Multimodal pattern recognition**: We have proposed the DFS-based approach for target detection and classification in foliage environments. However, it is only a supplement to the existing approaches. As shown in our studies, no single detection method can perform well in different situations and circumstances because each method has its shortcomings and limitations. Therefore, it is inevitable to combine the different approaches to tackle this issue. In this context, the traditional pattern recognition approach often makes recognition at each modality which results in ineffective detection, localization, or tracking. Therefore, how to process and integrate information from a large amount of multimodal data (e.g., optical, EO/IR, acoustic/seismic, RF, electromagnetic, mechanical, thermal, electrical, etc.) has become a critical

task.

Bibliography

Abdelnasser, H., Youssef, M. & Harras, K. A. (2015), Wigest: A ubiquitous wifi-based gesture recognition system, *in* 'Computer Communications (INFOCOM), 2015 IEEE Conference on', IEEE, pp. 1472–1480.

Acharya, U. R., Sree, S. V. & Suri, J. S. (2011), 'Automatic detection of epileptic eeg signals using higher order cumulant features', *International Journal of Neural Systems* **21**(05), 403–414.

Adankon, M. M. & Cheriet, M. (2007), 'Optimizing resources in model selection for support vector machine', *Pattern Recognition* **40**(3), 953–963.

Ali, K., Liu, A. X., Wang, W. & Shahzad, M. (2015), Keystroke recognition using wifi signals, *in* 'Proceedings of the 21st Annual International Conference on Mobile Computing and Networking', ACM, pp. 90–102.

Allen, M. R. (1996), Efficient approach to physics-based fopen-sar atd/r, *in* 'Algorithms for Synthetic Aperture Radar Imagery III', Vol. 2757, International Society for Optics and Photonics, pp. 163–173.

Anastasi, G., Falchi, A., Passarella, A., Conti, M. & Gregori, E. (2004), Performance measurements of motes sensor networks, *in* 'Proceedings of the 7th ACM International Symposium on Modeling, Analysis and Simulation of Wireless and Mobile Systems', ACM, pp. 174–181.

Aydin, I., Karakose, M. & Akin, E. (2011), 'A multi-objective artificial immune algorithm for parameter optimization in support vector machine', *Applied Soft Computing* **11**(1), 120–129.

Aziz, N. A., Abdullah, R. & Yusof, A. M. (2017), 'Human detection and recognition system using passive forward scattering radar', *Science International* **29**(1), 69–73.

Bahrampour, S., Ray, A., Sarkar, S., Damarla, T. & Nasrabadi, N. M. (2013), 'Performance comparison of feature extraction algorithms for target detection and classification', *Pattern Recognition Letters* **34**(16), 2126–2134.

Balanis, C. A. (1989), 'Advanced engineering electromagnetics, john willey & sons', *Inc., New York* .

Bannister, K., Giorgetti, G. & Gupta, S. (2008), Wireless sensor networking for hot applications: Effects of temperature on signal strength, data collection and localization, *in* 'Proceedings of the 5th Workshop on Embedded Networked Sensors (HotEmNets 08)', Citeseer.

Benbouzid, M. E. H. (2000), 'A review of induction motors signature analysis as a medium for faults detection', *IEEE Transactions on Industrial Electronics* **47**(5), 984–993.

Bessette, L., Crooks, S. & Ayasli, S. (1999), P-3 ultra-wideband sar, grayling, michigan, target and clutter phenomenology, *in* 'Radar Conference, 1999. The Record of the 1999 IEEE', IEEE, pp. 125–129.

Binder, B., Toups, M., Ayasli, S. & Adams, E. (1995), Sar foliage penetration phenomenology of tropical rain forest and northern us forest, *in* 'Radar Conference, 1995., Record of the IEEE 1995 International', IEEE, pp. 158–163.

Capsuto, B. & Frolik, J. (2006), A system to monitor signal fade due to weather phenomena for outdoor sensor systems, *in* 'Fifth International Conference on Information Processing in Sensor Networks (IPSN 2006)'.

Centenaro, M., Vangelista, L., Zanella, A. & Zorzi, M. (2016), 'Long-range communications in unlicensed bands: The rising stars in the iot and smart city scenarios', *IEEE Wireless Communications* **23**(5), 60–67.

Chan, T.-K., Kuga, Y. & Ishimaru, A. (1999), 'Experimental studies on circular sar imaging in clutter using angular correlation function technique', *IEEE Transactions on Geoscience and Remote Sensing* **37**(5), 2192–2197.

Chandran, V., Carswell, B., Boashash, B. & Elgar, S. (1997), 'Pattern recognition using invariants defined from higher order spectra: 2-d image inputs', *IEEE Transactions on Image Processing* **6**(5), 703–712.

Chandran, V. & Elgar, S. L. (1991), 'Mean and variance of estimates of the bispectrum of a harmonic random process-an analysis including leakage effects', *IEEE Transactions on Signal Processing* **39**(12), 2640–2651.

Chen, H.-K., Zhao, X.-G., Sun, S.-Y. & Tan, M. (2017), 'Pls-cca heterogeneous features fusion-based low-resolution human detection method for outdoor video surveillance', *International Journal of Automation and Computing* **14**(2), 136–146.

Chen, X., Edelstein, A., Li, Y., Coates, M., Rabbat, M. & Men, A. (2011), Sequential monte carlo for simultaneous passive device-free tracking and sensor localization using received signal strength measurements, *in* 'Information Processing in Sensor Networks (IPSN), 2011 10th International Conference on', IEEE, pp. 342–353.

Chenglin, Z., Xuebin, S., Songlin, S. & Ting, J. (2011), 'Fault diagnosis of sensor by chaos particle swarm optimization algorithm and support vector machine', *Expert Systems with Applications* **38**(8), 9908–9912.

Chow, T. W. & Tan, H.-Z. (2000), 'Hos-based nonparametric and parametric methodologies for machine fault detection', *IEEE Transactions on Industrial Electronics* **47**(5), 1051–1059.

Cohen, G., Hilario, M. & Geissbuhler, A. (2004), Model selection for support vector classifiers via genetic algorithms. an application to medical decision support, *in* 'International Symposium on Biological and Medical Data Analysis', Springer, pp. 200–211.

Cortes, C. & Vapnik, V. (1995), 'Support-vector networks', *Machine learning* **20**(3), 273–297.

Dal Bello, J. C. R., Siqueira, G. L. & Bertoni, H. L. (2000), 'Theoretical analysis and measurement results of vegetation effects on path loss for mobile cellular communication systems', *IEEE Transactions on Vehicular Technology* **49**(4), 1285–1293.

Dalal, N. & Triggs, B. (2005), Histograms of oriented gradients for human detection, *in* 'Computer Vision and Pattern Recognition, 2005. CVPR 2005. IEEE Computer Society Conference on', Vol. 1, IEEE, pp. 886–893.

Damarla, R. & Ufford, D. (2007), Personnel detection using ground sensors, *in* 'Unattended Ground, Sea, and Air Sensor Technologies and Applications IX', Vol. 6562, International Society for Optics and Photonics, p. 656205.

Damarla, T., Bradley, M., Mehmood, A. & Sabatier, J. M. (2013), 'Classification of animals and people ultrasonic signatures', *IEEE Sensors Journal* **13**(5), 1464–1472.

Damarla, T., Mehmood, A. & Sabatier, J. (2011), Detection of people and animals using non-imaging sensors, *in* 'Information Fusion (FUSION), 2011 Proceedings of the 14th International Conference on', IEEE, pp. 1–8.

Davis, M. E., Tomlinson, P. G. & Maloney, R. P. (1999), Technical challenges in ultra-wideband radar development for target detection and terrain

mapping, *in* 'Radar Conference, 1999. The Record of the 1999 IEEE', IEEE, pp. 1–6.

Dehmollaian, M. & Sarabandi, K. (2006), 'Electromagnetic scattering from foliage camouflaged complex targets', *IEEE Transactions on Geoscience and Remote Sensing* **44**(10), 2698–2709.

Dias, J. B. & Marques, P. A. (2003), 'Multiple moving target detection and trajectory estimation using a single sar sensor', *IEEE Transactions on Aerospace and Electronic Systems* **39**(2), 604–624.

Ding, Y. & Tang, J. (2014), 'Micro-doppler trajectory estimation of pedestrians using a continuous-wave radar', *IEEE Transactions on Geoscience and Remote Sensing* **52**(9), 5807–5819.

Domingo, M. C. (2012), 'An overview of the internet of things for people with disabilities', *Journal of Network and Computer Applications* **35**(2), 584–596.

Du, L., Ma, Y., Wang, B. & Liu, H. (2014), 'Noise-robust classification of ground moving targets based on time-frequency feature from micro-doppler signature', *IEEE Sensors Journal* **14**(8), 2672–2682.

Duan, K., Keerthi, S. S. & Poo, A. N. (2003), 'Evaluation of simple performance measures for tuning svm hyperparameters', *Neurocomputing* **51**, 41–59.

Durden, S. L., Klein, J. D. & Zebker, H. A. (1991), 'Radar measurement of l-band signal fluctuations caused by propagation through trees', *IEEE Transactions on Antennas and Propagation* **39**(10), 1537–1539.

Durden, S. L., Klein, J. D. & Zebker, H. A. (1993), 'Measurement and simulation of signal fluctuations caused by propagation through trees', *Radio Science* **28**(6), 1049–1051.

Fan, Y. J., Yin, Y. H., Da Xu, L., Zeng, Y. & Wu, F. (2014), 'Iot-based smart rehabilitation system', *IEEE Transactions on Industrial Informatics* **10**(2), 1568–1577.

Fioranelli, F., Ritchie, M. & Griffiths, H. (2016), 'Performance analysis of centroid and svd features for personnel recognition using multistatic micro-doppler', *IEEE Geoscience and Remote Sensing Letters* **13**(5), 725–729.

Fleischman, J., Ayasli, S., Adams, E. t. & Gosselin, D. (1996), 'Foliage attenuation and backscatter analysis of sar imagery', *IEEE Transactions on Aerospace and Electronic Systems* **32**(1), 135–144.

Foster, T. (1995), Application of pattern recognition techniques for early warning radar, Technical report, SENCOM CORP BEDFORD MA.

Friedrichs, F. & Igel, C. (2005), 'Evolutionary tuning of multiple svm parameters', *Neurocomputing* **64**, 107–117.

Frolind, P.-O., Gustavsson, A., Lundberg, M. & Ulander, L. M. (2012), 'Circular-aperture vhf-band synthetic aperture radar for detection of vehicles in forest concealment', *IEEE Transactions on Geoscience and Remote Sensing* **50**(4), 1329–1339.

Gallagher, K. A. & Narayanan, R. M. (2013), Human detection and ranging at long range and through light foliage using a w-band noise radar with an embedded tone, *in* 'Radar Sensor Technology XVII', Vol. 8714, International Society for Optics and Photonics, p. 871402.

Geng, Y., Chen, J., Fu, R., Bao, G. & Pahlavan, K. (2016), 'Enlighten wearable physiological monitoring systems: On-body rf characteristics based human motion classification using a support vector machine', *IEEE Transactions on Mobile Computing* **15**(3), 656–671.

Girshick, R. (2015), Fast r-cnn, *in* 'Proceedings of the IEEE International Conference on Computer Vision', pp. 1440–1448.

Girshick, R., Donahue, J., Darrell, T. & Malik, J. (2014), Rich feature hierarchies for accurate object detection and semantic segmentation, *in* 'Proceedings of the IEEE Conference on Computer Vision and Pattern Recognition', pp. 580–587.

Gold, C. & Sollich, P. (2003), 'Model selection for support vector machine classification', *Neurocomputing* **55**(1-2), 221–249.

Guan, Q., Yin, X., Guo, X. & Wang, G. (2016), 'A novel infrared motion sensing system for compressive classification of physical activity', *IEEE Sensors Journal* **16**(8), 2251–2259.

Gunn, S. R. et al. (1998), 'Support vector machines for classification and regression', *ISIS technical report* **14**(1), 5–16.

Guo, C. & Zhou, H. (2018), Synthetic aperture radar target identification based on incremental kernel extreme learning machine, *in* 'Tenth International Conference on Digital Image Processing (ICDIP 2018)', Vol. 10806, International Society for Optics and Photonics, p. 108060L.

Halversen, S. D., Nanis, J. G., Owirka, G. J. & Novak, L. M. (1994), Comparison of ultrawideband sar target detection algorithms, *in* 'Algorithms for Synthetic Aperture Radar Imagery', Vol. 2230, International Society for Optics and Photonics, pp. 230–244.

Hashim, M. H. & Stavrou, S. (2006), 'Measurements and modelling of wind influence on radiowave propagation through vegetation', *IEEE Transactions on Wireless Communications* **5**(5), 1055–1064.

He, K., Zhang, X., Ren, S. & Sun, J. (2016), Deep residual learning for image recognition, *in* 'Proceedings of the IEEE Conference on Computer Vision and Pattern Recognition', pp. 770–778.

Houston, K. M. & McGaffigan, D. P. (2003), Spectrum analysis techniques for personnel detection using seismic sensors, *in* 'Unattended Ground

Sensor Technologies and Applications V', Vol. 5090, International Society for Optics and Photonics, pp. 162–174.

Howard, D., Roberts, S. & Brankin, R. (1999), 'Target detection in sar imagery by genetic programming', *Advances in Engineering Software* **30**(5), 303–311.

Hsu, C.-W. & Lin, C.-J. (2002*a*), 'A comparison of methods for multiclass support vector machines', *IEEE Transactions on Neural Networks* **13**(2), 415–425.

Hsu, C.-W. & Lin, C.-J. (2002*b*), 'A simple decomposition method for support vector machines', *Machine Learning* **46**(1-3), 291–314.

Huang, C.-L. (2009), 'Aco-based hybrid classification system with feature subset selection and model parameters optimization', *Neurocomputing* **73**(1-3), 438–448.

Huang, P.-S., Damarla, T. & Hasegawa-Johnson, M. (2011), Multi-sensory features for personnel detection at border crossings, *in* 'Information Fusion (FUSION), 2011 Proceedings of the 14th International Conference on', IEEE, pp. 1–8.

Huang, Y., Sheng, H., Zheng, Y. & Xiong, Z. (2017), 'Deepdiff: learning deep difference features on human body parts for person re-identification', *Neurocomputing* **241**, 191–203.

Ioffe, S. & Szegedy, C. (2015), 'Batch normalization: Accelerating deep network training by reducing internal covariate shift', *arXiv preprint arXiv:1502.03167* .

Ivashov, S., Razevig, V., Sheyko, A. & Vasilyev, I. (2004), Detection of human breathing and heartbeat by remote radar, *in* 'Progress in Electromagnetic Research Symposium', pp. 663–666.

Iyengar, S. G., Varshney, P. K. & Damarla, T. (2007), On the detection of footsteps based on acoustic and seismic sensing, *in* 'Signals, Systems and Computers, 2007. ACSSC 2007. Conference Record of the Forty-First Asilomar Conference on', IEEE, pp. 2248–2252.

Iyengar, S. G., Varshney, P. K. & Damarla, T. (2011), 'A parametric copula-based framework for hypothesis testing using heterogeneous data', *IEEE Transactions on Signal Processing* **59**(5), 2308–2319.

Javier, R. J. & Kim, Y. (2014), 'Application of linear predictive coding for human activity classification based on micro-doppler signatures', *IEEE Geoscience and Remote Sensing Letters* **11**(10), 1831–1834.

Jin, X., Gupta, S., Ray, A. & Damarla, T. (2011), Multimodal sensor fusion for personnel detection, *in* 'Information Fusion (FUSION), 2011 Proceedings of the 14th International Conference on', IEEE, pp. 1–8.

Jin, X., Sarkar, S., Ray, A., Gupta, S. & Damarla, T. (2012), 'Target detection and classification using seismic and pir sensors', *IEEE Sensors Journal* **12**(6), 1709–1718.

Kalgaonkar, K. & Raj, B. (2007), Acoustic doppler sonar for gait recoginationtion, *in* 'Advanced Video and Signal Based Surveillance, 2007. AVSS 2007. IEEE Conference on', IEEE, pp. 27–32.

Kaltiokallio, O., Bocca, M. & Patwari, N. (2012), Enhancing the accuracy of radio tomographic imaging using channel diversity, *in* 'Mobile Adhoc and Sensor Systems (MASS), 2012 IEEE 9th International Conference on', IEEE, pp. 254–262.

Kapoor, R., Tsihrintzis, G. & Nandhakumar, N. (1996), Detection of obscured targets in heavy-tailed radar clutter using an ultra-wideband (uwb) radar and alpha-stable clutter models, *in* 'Signals, Systems and Computers, 1996. Conference Record of the Thirtieth Asilomar Conference on', IEEE, pp. 863–867.

Keerthi, S. S. (2002), 'Efficient tuning of svm hyperparameters using radius/margin bound and iterative algorithms', *IEEE Transactions on Neural Networks* **13**(5), 1225–1229.

Khadra, L., Al-Fahoum, A. S. & Binajjaj, S. (2005), 'A quantitative analysis approach for cardiac arrhythmia classification using higher order spectral techniques', *IEEE Transactions on Biomedical Engineering* **52**(11), 1840–1845.

Khan, N. M., Ksantini, R., Ahmad, I. S. & Boufama, B. (2012), 'A novel svm+ nda model for classification with an application to face recognition', *Pattern Recognition* **45**(1), 66–79.

Kim, Y., Ha, S. & Kwon, J. (2015), 'Human detection using doppler radar based on physical characteristics of targets', *IEEE Geoscience and Remote Sensing Letters* **12**(2), 289–293.

Kim, Y. & Moon, T. (2016), 'Human detection and activity classification based on micro-doppler signatures using deep convolutional neural networks', *IEEE Geoscience and Remote Sensing Letters* **13**(1), 8–12.

Kortuem, G., Kawsar, F., Sundramoorthy, V. & Fitton, D. (2010), 'Smart objects as building blocks for the internet of things', *IEEE Internet Computing* **14**(1), 44–51.

Krizhevsky, A., Sutskever, I. & Hinton, G. E. (2012), Imagenet classification with deep convolutional neural networks, *in* 'Advances in Neural Information Processing Systems', pp. 1097–1105.

Kumar, A., Li, Z., Liang, Q., Zhang, B. & Wu, X. (2014), 'Experimental study of through-wall human detection using ultra wideband radar sensors', *Measurement* **47**, 869–879.

Lee, Y. & Meng, Y. (2007), 'Tropical weather effects on foliage propagation'.

Li, B., Zhao, C., Zhang, H., Sun, X. & Zhou, Z. (2013), 'Characterization on clustered propagations of uwb sensors in vehicle cabin: measurement, modeling and evaluation', *IEEE Sensors Journal* **13**(4), 1288–1300.

Li, S. & Tan, M. (2010), 'Tuning svm parameters by using a hybrid clpso–bfgs algorithm', *Neurocomputing* **73**(10-12), 2089–2096.

Li, W., Zhao, R., Xiao, T. & Wang, X. (2014), Deepreid: Deep filter pairing neural network for person re-identification, *in* 'Proceedings of the IEEE Conference on Computer Vision and Pattern Recognition', pp. 152–159.

Li, Y., Chen, X., Coates, M. & Yang, B. (2011), Sequential monte carlo radio-frequency tomographic tracking, *in* 'Acoustics, Speech and Signal Processing (ICASSP), 2011 IEEE International Conference on', IEEE, pp. 3976–3979.

Liang, B., Iwnicki, S. & Zhao, Y. (2013), 'Application of power spectrum, cepstrum, higher order spectrum and neural network analyses for induction motor fault diagnosis', *Mechanical Systems and Signal Processing* **39**(1-2), 342–360.

Liang, J. & Liang, Q. (2010*a*), 'Outdoor propagation channel modeling in foliage environment', *IEEE Transactions on Vehicular Technology* **59**(5), 2243–2252.

Liang, J. & Liang, Q. (2010*b*), 'Sense-through-foliage target detection using uwb radar sensor networks', *Pattern Recognition Letters* **31**(11), 1412–1421.

Liang, J., Liang, Q. & Samn, S. W. (2008), Foliage clutter modeling using the uwb radar, *in* 'Communications, 2008. ICC'08. IEEE International Conference on', IEEE, pp. 1937–1941.

Liang, Q. (2011), 'Radar sensor wireless channel modeling in foliage environment: Uwb versus narrowband', *IEEE Sensors Journal* **11**(6), 1448–1457.

Lin, K., Chen, M., Deng, J., Hassan, M. M. & Fortino, G. (2016), 'Enhanced fingerprinting and trajectory prediction for iot localization in smart buildings', *IEEE Transactions on Automation Science and Engineering* **13**(3), 1294–1307.

Lin, S.-W., Ying, K.-C., Chen, S.-C. & Lee, Z.-J. (2008), 'Particle swarm optimization for parameter determination and feature selection of support vector machines', *Expert systems with applications* **35**(4), 1817–1824.

Liu, K., Liu, B., Blasch, E., Shen, D., Wang, Z., Ling, H. & Chen, G. (2015), A cloud infrastructure for target detection and tracking using audio and video fusion, *in* 'Proceedings of the IEEE Conference on Computer Vision and Pattern Recognition Workshops', pp. 74–81.

Low, K. (1988), 'Uhf measurement of seasonal field-strength variations in forests', *IEEE Transactions on Vehicular Technology* **37**(3), 121–124.

Luomala, J. & Hakala, I. (2015), Effects of temperature and humidity on radio signal strength in outdoor wireless sensor networks, *in* 'Computer Science and Information Systems (FedCSIS), 2015 Federated Conference on', IEEE, pp. 1247–1255.

MacDonald, D., Isenman, J. & Roman, J. (1997), Radar detection of hidden targets, *in* 'Aerospace and Electronics Conference, 1997. NAECON 1997., Proceedings of the IEEE 1997 National', Vol. 2, IEEE, pp. 846–855.

Madzarov, G., Gjorgjevikj, D. & Chorbev, I. (2009), 'A multi-class svm classifier utilizing binary decision tree', *Informatica* **33**(2).

Martis, R. J., Acharya, U. R., Lim, C. M., Mandana, K., Ray, A. K. & Chakraborty, C. (2013), 'Application of higher order cumulant features for cardiac health diagnosis using ecg signals', *International Journal of Neural Systems* **23**(04), 1350014.

Meeks, M. (1983), 'Vhf propagation over hilly, forested terrain', *IEEE Transactions on Antennas and Propagation* **31**(3), 483–489.

Melgani, F. & Bruzzone, L. (2004), 'Classification of hyperspectral remote sensing images with support vector machines', *IEEE Transactions on Geoscience and Remote Sensing* **42**(8), 1778–1790.

Mendel, J. M. (1991), 'Tutorial on higher-order statistics (spectra) in signal processing and system theory: Theoretical results and some applications', *Proceedings of the IEEE* **79**(3), 278–305.

Minaeian, S., Liu, J. & Son, Y.-J. (2016), 'Vision-based target detection and localization via a team of cooperative uav and ugvs', *IEEE Transactions on Systems, Man, and Cybernetics: Systems* **46**(7), 1005–1016.

Moussa, M. & Youssef, M. (2009), Smart cevices for smart environments: Device-free passive detection in real environments, *in* 'Pervasive Computing and Communications, 2009. PerCom 2009. IEEE International Conference on', IEEE, pp. 1–6.

Muñoz-Marí, J., Bovolo, F., Gómez-Chova, L., Bruzzone, L. & Camp-Valls, G. (2010), 'Semisupervised one-class support vector machines for classification of remote sensing data', *IEEE Transactions on Geoscience and Remote Sensing* **48**(8), 3188–3197.

Mustapha, H. & Dimitrakopoulos, R. (2010), 'A new approach for geological pattern recognition using high-order spatial cumulants', *Computers & Geosciences* **36**(3), 313–334.

Muthuswamy, J., Sherman, D. L. & Thakor, N. V. (1999), 'Higher-order spectral analysis of burst patterns in eeg', *IEEE Transactions on Biomedical Engineering* **46**(1), 92–99.

Nair, V. & Hinton, G. E. (2010), Rectified linear units improve restricted boltzmann machines, *in* 'Proceedings of the 27th International Conference on Machine Learning (ICML-10)', pp. 807–814.

Nandakumar, R., Kellogg, B. & Gollakota, S. (2014), 'Wi-fi gesture recognition on existing devices', *arXiv preprint arXiv:1411.5394* .

Nannuru, S., Li, Y., Coates, M., Yang, B. et al. (2011), Multi-target device-free tracking using radio frequency tomography, *in* 'Seventh IEEE International Conference on Intelligent Sensors, Sensor Networks and Information Processing (ISSNIP)', pp. 508–513.

Nannuru, S., Li, Y., Zeng, Y., Coates, M. & Yang, B. (2013), 'Radio-frequency tomography for passive indoor multitarget tracking', *IEEE Transactions on Mobile Computing* **12**(12), 2322–2333.

Nashashibi, A. Y., Sarabandi, K., Oveisgharan, S., Dobson, M. C., Walker, W. S. & Burke, E. (2004), 'Millimeter-wave measurements of foliage attenuation and ground reflectivity of tree stands at nadir incidence', *IEEE Transactions on Antennas and Propagation* **52**(5), 1211–1222.

Nashashibi, A. Y. & Ulaby, F. T. (2005), 'Detection of stationary foliage-obscured targets by polarimetric millimeter-wave radar', *IEEE Transactions on Geoscience and Remote Sensing* **43**(1), 13–23.

Nikias, C. L. & Mendel, J. M. (1993), 'Signal processing with higher-order spectra', *IEEE Signal Processing Magazine* **10**(3), 10–37.

Nohara, T. J. & Haykin, S. (1991), Canadian east coast radar trials and the k-distribution, *in* 'IEE Proceedings F (Radar and Signal Processing)', Vol. 138, IET, pp. 80–88.

Orlic, V. D. & Dukic, M. L. (2009), 'Automatic modulation classification algorithm using higher-order cumulants under real-world channel conditions', *IEEE Communications Letters* **13**(12).

Park, H. O., Dibazar, A. A. & Berger, T. W. (2009), Cadence analysis of temporal gait patterns for seismic discrimination between human and quadruped footsteps, *in* 'Acoustics, Speech and Signal Processing, 2009. ICASSP 2009. IEEE International Conference on', IEEE, pp. 1749–1752.

Patwari, N. & Wilson, J. (2010), 'Rf sensor networks for device-free localization: Measurements, models, and algorithms', *Proceedings of the IEEE* **98**(11), 1961–1973.

Pelet, E. R., Salt, J. E. & Wells, G. (2004), 'Effect of wind on foliage obstructed line-of-sight channel at 2.5 ghz', *IEEE Transactions on Broadcasting* **50**(3), 224–232.

Radford, A., Metz, L. & Chintala, S. (2015), 'Unsupervised representation learning with deep convolutional generative adversarial networks', *arXiv preprint arXiv:1511.06434* .

Rao, T. R., Balachander, D., Kiran, A. N. & Oscar, S. (2012), Rf propagation measurements in forest & plantation environments for wireless sensor networks, *in* 'Recent Trends In Information Technology (ICRTIT), 2012 International Conference on', IEEE, pp. 308–313.

Rau, R. & McClellan, J. H. (1998), A directional image decomposition for ultra-wideband sar, *in* 'Acoustics, Speech and Signal Processing, 1998. Proceedings of the 1998 IEEE International Conference on', Vol. 5, IEEE, pp. 2877–2880.

Ren, S., He, K., Girshick, R. & Sun, J. (2015), Faster r-cnn: Towards real-time object detection with region proposal networks, *in* 'Advances in Neural Information Processing Systems', pp. 91–99.

Rogers, N. C., Seville, A., Richter, J., Ndzi, D., Savage, N., Caldeirinha, R., Shukla, A., Al-Nuaimi, M., Craig, K., Vilar, E. et al. (2002), 'A generic model of 1-60 ghz radio propagation through vegetation-final report', *Radio Agency, UK* .

Runkle, P., Nguyen, L. H., McClellan, J. H. & Carin, L. (2001), 'Multi-aspect target detection for sar imagery using hidden markov models', *IEEE Transactions on Geoscience and Remote Sensing* **39**(1), 46–55.

Sabatier, J. M. & Ekimov, A. E. (2008), Range limitation for seismic footstep detection, *in* 'Unattended Ground, Sea, and Air Sensor Technologies and Applications X', Vol. 6963, International Society for Optics and Photonics, p. 69630V.

Sakaino, H. (2013), 'Video-based tracking, learning, and recognition method for multiple moving objects', *IEEE Transactions on Circuits and Systems for Video Technology* **23**(10), 1661–1674.

Savazzi, S., Nicoli, M., Carminati, F. & Riva, M. (2014), 'A bayesian approach to device-free localization: modeling and experimental assessment', *IEEE Journal of Selected Topics in Signal Processing* **8**(1), 16–29.

Seifeldin, M., Saeed, A., Kosba, A. E., El-Keyi, A. & Youssef, M. (2013), 'Nuzzer: A large-scale device-free passive localization system for wireless environments', *IEEE Transactions on Mobile Computing* **12**(7), 1321–1334.

Sheen, D. R., Malinas, N. P., Kletzli, D. W., Lewis, T. B. & Roman, J. F. (1994), 'Foliage transmission measurements using a ground-based ultrawide band (300-1300 mhz) sar system', *IEEE Transactions on Geoscience and Remote Sensing* **32**(1), 118–130.

Sigg, S., Scholz, M., Shi, S., Ji, Y. & Beigl, M. (2014), 'Rf-sensing of activities from non-cooperative subjects in device-free recognition systems using ambient and local signals', *IEEE Transactions on Mobile Computing* **13**(4), 907–920.

Srivastava, N., Hinton, G., Krizhevsky, A., Sutskever, I. & Salakhutdinov, R. (2014), 'Dropout: a simple way to prevent neural networks from overfitting', *The Journal of Machine Learning Research* **15**(1), 1929–1958.

Storn, R. & Price, K. (1997), 'Differential evolution–a simple and efficient heuristic for global optimization over continuous spaces', *Journal of Global Optimization* **11**(4), 341–359.

Sun, Z., Wang, P., Vuran, M. C., Al-Rodhaan, M. A., Al-Dhelaan, A. M. & Akyildiz, I. F. (2011), 'Bordersense: Border patrol through advanced wireless sensor networks', *Ad Hoc Networks* **9**(3), 468–477.

Sundaresan, A., Subramanian, A., Varshney, P. K. & Damarla, T. (2010), A copula-based semi-parametric approach for footstep detection using seismic sensor networks, *in* 'Multisensor, Multisource Information Fusion: Architectures, Algorithms, and Applications 2010', Vol. 7710, International Society for Optics and Photonics, p. 77100C.

Szegedy, C., Liu, W., Jia, Y., Sermanet, P., Reed, S., Anguelov, D., Erhan, D., Vanhoucke, V. & Rabinovich, A. (2015), Going deeper with convolutions, *in* 'Proceedings of the IEEE Conference on Computer Vision and Pattern Recognition', pp. 1–9.

Tamir, T. (1967), 'On radio-wave propagation in forest environments', *IEEE Transactions on Antennas and Propagation* **15**(6), 806–817.

Tang, Y., Zhang, Y.-Q., Chawla, N. V. & Krasser, S. (2009), 'Svms modeling for highly imbalanced classification', *IEEE Transactions on Systems, Man, and Cybernetics, Part B (Cybernetics)* **39**(1), 281–288.

Thouin, F., Nannuru, S. & Coates, M. (2011), Multi-target tracking for measurement models with additive contributions, *in* 'Information Fusion (FUSION), 2011 Proceedings of the 14th International Conference on', IEEE, pp. 1–8.

Toups, M., Ayasli, S. & Fleischman, J. (1996), 'Analysis of foliage-induced synthetic pattern distortions', *IEEE Transactions on Aerospace and Electronic Systems* **32**(1), 145–155.

Tuzel, O., Porikli, F. & Meer, P. (2007), Human detection via classification on riemannian manifolds, *in* 'Computer Vision and Pattern Recognition, 2007. CVPR'07. IEEE Conference on', IEEE, pp. 1–8.

Vapnik, V. (1998), *Statistical learning theory. 1998*, Vol. 3, Wiley, New York.

Vapnik, V. (2013), *The nature of statistical learning theory*, Springer Science & Business Media.

Wang, G., Zou, Y., Zhou, Z., Wu, K. & Ni, L. M. (2016), 'We can hear you with wi-fi!', *IEEE Transactions on Mobile Computing* **15**(11), 2907–2920.

Wang, J., Gao, Q., Yu, Y., Cheng, P., Wu, L. & Wang, H. (2013), 'Robust device-free wireless localization based on differential rss measurements', *IEEE Transactions on Industrial Electronics* **60**(12), 5943–5952.

Wang, N. & Yeung, D.-Y. (2013), Learning a deep compact image representation for visual tracking, *in* 'Advances in Neural Information Processing Systems', pp. 809–817.

Wang, Y. & Fathy, A. E. (2012), 'Advanced system level simulation platform for three-dimensional uwb through-wall imaging sar using time-domain approach', *IEEE Transactions on Geoscience and Remote Sensing* **50**(5), 1986–2000.

Wang, Y., Liu, J., Chen, Y., Gruteser, M., Yang, J. & Liu, H. (2014), E-eyes: device-free location-oriented activity identification using fine-grained wifi signatures, *in* 'Proceedings of the 20th Annual International Conference on Mobile Computing and Networking', ACM, pp. 617–628.

Wang, Y., Liu, Q. & Fathy, A. E. (2013), 'Cw and pulse–doppler radar processing based on fpga for human sensing applications', *IEEE Transactions on Geoscience and Remote Sensing* **51**(5), 3097–3107.

Wang, Y., Wu, K. & Ni, L. M. (2017), 'Wifall: Device-free fall detection by wireless networks', *IEEE Transactions on Mobile Computing* **16**(2), 581–594.

Watts, S. (1987), 'Radar detection prediction in k-distributed sea clutter and thermal noise', *IEEE Transactions on Aerospace and Electronic Systems* (1), 40–45.

Wei, B., Hu, W., Yang, M. & Chou, C. T. (2015), Radio-based device-free activity recognition with radio frequency interference, *in* 'Proceedings of the 14th International Conference on Information Processing in Sensor Networks', ACM, pp. 154–165.

Wilson, J. & Patwari, N. (2010), 'Radio tomographic imaging with wireless networks', *IEEE Transactions on Mobile Computing* **9**(5), 621–632.

Wilson, J. & Patwari, N. (2011), 'See-through walls: Motion tracking using variance-based radio tomography networks', *IEEE Transactions on Mobile Computing* **10**(5), 612–621.

Wilson, J. & Patwari, N. (2012), 'A fade-level skew-laplace signal strength model for device-free localization with wireless networks.', *IEEE Trans. Mob. Comput.* **11**(6), 947–958.

Xiao, J., Wu, K., Yi, Y., Wang, L. & Ni, L. M. (2013), Pilot: Passive device-free indoor localization using channel state information, *in* 'Distributed Computing Systems (ICDCS), 2013 IEEE 33rd International Conference on', IEEE, pp. 236–245.

Yang, J., Ge, Y., Xiong, H., Chen, Y. & Liu, H. (2010), Performing joint learning for passive intrusion detection in pervasive wireless environments, *in* 'INFOCOM, 2010 Proceedings IEEE', IEEE, pp. 1–9.

Yang, X.-S., Karamanoglu, M. & He, X. (2013), 'Multi-objective flower algorithm for optimization', *Procedia Computer Science* **18**, 861–868.

Yang, X.-S., Karamanoglu, M. & He, X. (2014), 'Flower pollination algorithm: a novel approach for multiobjective optimization', *Engineering Optimization* **46**(9), 1222–1237.

Youssef, M., Mah, M. & Agrawala, A. (2007), Challenges: device-free passive localization for wireless environments, *in* 'Proceedings of the 13th annual ACM international conference on Mobile computing and networking', ACM, pp. 222–229.

Yu, W., Wang, Y., Liu, H. & He, J. (2016), 'Superpixel-based cfar target detection for high-resolution sar images', *IEEE Geoscience and Remote Sensing Letters* **13**(5), 730–734.

Zanella, A., Bui, N., Castellani, A., Vangelista, L. & Zorzi, M. (2014), 'Internet of things for smart cities', *IEEE Internet of Things journal* **1**(1), 22–32.

Zhang, D., Liu, Y., Guo, X. & Ni, L. M. (2013), 'Rass: A real-time, accurate, and scalable system for tracking transceiver-free objects', *IEEE Transactions on Parallel and Distributed Systems* **24**(5), 996–1008.

Zhang, D., Ma, J., Chen, Q. & Ni, L. M. (2007), An rf-based system for tracking transceiver-free objects, *in* 'Pervasive Computing and Communications, 2007. PerCom'07. Fifth Annual IEEE International Conference on', IEEE, pp. 135–144.

Zhang, D. & Ni, L. M. (2009), Dynamic clustering for tracking multiple transceiver-free objects, *in* 'Pervasive Computing and Communications, 2009. PerCom 2009. IEEE International Conference on', IEEE, pp. 1–8.

Zhang, Z., Pouliquen, P., Waxman, A. & Andreou, A. G. (2007), Acoustic micro-doppler gait signatures of humans and animals, *in* 'Information Sciences and Systems, 2007. CISS'07. 41st Annual Conference on', IEEE, pp. 627–630.

Zhang, Z. & Tao, D. (2012), 'Slow feature analysis for human action recognition', *IEEE Transactions on Pattern Analysis and Machine Intelligence* **34**(3), 436–450.

Zhao, Q. & Principe, J. C. (2001), 'Support vector machines for sar automatic target recognition', *IEEE Transactions on Aerospace and Electronic Systems* **37**(2), 643–654.

Zhu, Q., Yeh, M.-C., Cheng, K.-T. & Avidan, S. (2006), Fast human detection using a cascade of histograms of oriented gradients, *in* 'Computer Vision and Pattern Recognition, 2006 IEEE Computer Society Conference on', Vol. 2, IEEE, pp. 1491–1498.